

The chikungunya disease: Modeling, vector and transmission global dynamics

D. Moulay ^{*}, M.A. Aziz-Alaoui, M. Cadivel

Laboratoire de Mathématiques Appliquées, Université du Havre, 25 rue Philippe Lebon, B.P. 540, 76058 Le Havre Cedex, France

ARTICLE INFO

Article history:

Received 16 March 2010

Received in revised form 23 October 2010

Accepted 29 October 2010

Available online 9 November 2010

Keywords:

Chikungunya

Modeling

Competitive systems

Global stability

ABSTRACT

Models for the transmission of the chikungunya virus to human population are discussed. The chikungunya virus is an alpha arbovirus, first identified in 1953. It is transmitted by *Aedes* mosquitoes and is responsible for a little documented uncommon acute tropical disease. Models describing the mosquito population dynamics and the virus transmission to the human population are discussed. Global analysis of equilibria are given, which use on the one hand Lyapunov functions and on the other hand results of the theory of competitive systems and stability of periodic orbits.

© 2010 Elsevier Inc. All rights reserved.

1. Introduction

An unprecedented chikungunya epidemic has appeared on the Reunion Island (775,000 inhabitants) with over 244,000 reported and 205 deaths (directly or indirectly linked) as of April 2006. *Aedes albopictus* [1], long present on the island, is the main vector of this disease. *Aedes aegypti* [2], which is also known to transmit dengue fever, is the other vector of chikungunya. After the Grande Comore Island epidemic, first cases were reported in the Reunion Island in March 2005. It was the first time that a chikungunya epidemic was described in this part of the world.

The Asian tiger mosquito or forest day mosquito (*Aedes albopictus*), from the mosquito family Culicidae, is characterized by its black and white striped legs, small black and white body. It is native of the tropical and subtropical areas of Southeast Asia. In the past couple of decades this species has invaded many countries throughout the world, through the increasing transport of goods and international travels. It has recently appeared in Europe, like in France [3], in the USA and in Australia.

The chikungunya is an arthropod-borne viral disease (arbovirus). The name is derived from the Makonde word meaning “that which bends up” in reference to the stooped posture developed as a result of the arthritic symptoms of the disease. It was first described by Marion Robinson and Lumsden [4,5], following an outbreak in 1952 on the Makonde Plateau, in Tanzania [5].

Some arboviruses are able to cause emergent diseases and transmit the virus upon biting, allowing it to enter the bloodstream which

can cause viremia. The dynamics of arboviral diseases like dengue or chikungunya are influenced by many factors such as humans, the mosquito vector, the virus itself, as well as the environment which affects all the present mechanisms directly or indirectly.

Through the 20th century, mathematical models have been established as major tools for epidemiological models (see [6–8] and references therein), and in particular the study of vector-borne infections [9–12].

In [13,14], the authors study a SI-SIR model in which the total human population size is constant. Models with a variable human population are studied in [15,16]. In [15] the authors use a non classical contact rate among humans that depend on the total vector population size. Such models do not take into account the dynamics of the vector.

In [17,18], mathematical models describing the dynamics of vector-borne diseases taking into account the controlling mechanisms applied on the vector population are developed. In [17], the human population is supposed to be constant and the incidence rate among humans depends on the total vector population size. Moreover, only the local stability of equilibria was studied analytically.

This paper deals with two models involving differential equations for the mosquito population and virus transmission to the human population. Following [15], we consider a model which takes into account the dynamics of the vector with a non-constant population size and a contact rate that depends on the vector population size.

The local and global stability of equilibria are studied. This work can be seen as a complement to the study of [17,18]. The conclusion discusses the use of a contact rate among humans that depends on the vector population size.

This paper is organized as follows. In the second section we give the biological explanation of the problem and address the vector

* Corresponding author. Address: LMAH, Université du Havre, 25 rue Philippe Lebon, BP540, 76058 Le Havre Cedex, France.

E-mail address: djamila.moulay@univ-lehavre.fr (D. Moulay).

life cycle (embryonic, larvae, pupae and adult stages), the reproduction and oviposition habitat selection, and finally the transmission of the virus phenomenon.

The third section deals with the formulation of dynamical models, first of all for the population growth that is the *Aedes albopictus* mosquito, and secondly for the virus transmission to the human population. The first model uses a stage structure model; the second uses SI and SIR type models.

The fourth section is devoted to the mathematical analysis of both models, focusing on the boundedness and the positivity of the solutions, and on local or global stability of equilibria.

For the first system we use the Lyapunov theory to establish the global stability of the endemic equilibrium, while for the second we use the general theory of competitive systems and compound matrices. As usual in mathematical epidemiological studies, we also found two thresholds parameters that determine the global dynamical behavior.

2. Biological problem

2.1. Vector life cycle

The life of the vector, consists of four stages: embryonic stage (eggs), larvae stage, pupae stage and adult stage. The first three stages need water for their development while the last one needs only air. In this paper we will not distinguish the larvae stage and the pupae stage: these two stages are called the immature stage. The lifespan of each stage depends on several factors, such as temperature or the availability of food and water [19].

2.2. Oviposition habitat selection

Mosquitoes have developed various approaches to avoid predation. Many species breed in areas where predators are rare or absent. The oviposition habitat selection is made to make sure that the mosquito larvae can develop relatively unmolested. That is the case of the Asian tiger mosquito or *Aedes albopictus* mosquito which is a container-inhabiting species and which lays its eggs in any water-containing receptacle in urban, suburban, rural and forest areas. The primary immature habitats of this species are artificial containers [20,21].

These habitats are largely devoid of predators, thus offering a relatively secure refuge for larval development. Most female can lay their eggs not only on moist substrate but on dry substrate that is subject to flooding with rains or tides. They breed in small, often ephemeral, pools such as those in tree holes, bamboo pots and leaf axils. This strategy does have a negative side for mosquito: the development depends on the availability of water and they must be able to develop quickly before the water dries. Mosquitoes lay their eggs on the water or any moist surface, but they can also breed in natural habitats like vegetation or near rivers ...

2.3. The embryonic stage

The eggs need 48–72 hours to become mature [22]. They need water to hatch, but they are desiccation-resistant and cold-resistant and they have the capacity to cling to the inner side of any potential containers. Moreover, eggs are capable of winter diapause and mature eggs can wait until two years to hatch if the hydration conditions are not sufficient for the development of larvae [23,24].

2.4. The larvae and pupae stages

Depending on temperature and availability of food, *Aedes albopictus* can complete larval development (four stages) between five to

ten days; the pupae stage needs two days to develop [25]. An increase in larval density or a decrease in food (for example, a decrease in water due to evaporation) can cause more mortality and reduction in the number of adult subjects. Though limited food is the primary cause of death, parasites and predators may exert substantial influence on the population size. The amount of water in the containers also plays an important role in determining mosquito density. Although the overall population in containers appears greater, it is actually decreasing as resources decline and intra-specific competition increases [26,27], resulting in greater larval mortality and the production of small-sized adults. Moreover, it has been observed that the larvae of *Aedes albopictus* are cannibal, they are able to eat earlier-stage larva under certain conditions.

2.5. The adult stage

The exit of the pupae stage normally happens very early in the morning, perhaps in order to escape numerous predators whose main activity takes place during daytime [21,28]. Before any activity, male and female need to have a meal of sugar and water [29]. The flight range of adults is limited (from one to two hundred meters), they have not been observed to fly in strong winds [30,31]. Its major means of dispersal is through the transport of used and waste tires. The move of other water-holding containers could also play a role in expanding its range. The life expectancy for males is fifteen days whereas it is from two to four weeks for females [22] and can reach ten weeks under lab conditions.

2.6. Reproduction

Aedes albopictus is very aggressive during the daytime [32] with biting generally occurring during early morning and late afternoon [30]. Females require blood to produce their eggs. They feed on a number of hosts including human (indoors and outdoors), domestic and wild animals and birds. Their generalized feeding behavior contributes to their being potential vectors.

Females lay eggs one by one above the water level or on the sides of a variety of containers which serve as breeding habitat. They rely on rainfalls to raise water level in containers and inundate the eggs for hatching. Females lay from one hundred to three hundred eggs per oviposition and have from one to four ovipositions during their life.

2.7. Transmission of the virus

A vector is infected after biting an infected human. There is a delay (from seven to twelve days) or incubation period when mosquitoes are incurring the disease but still unable to transmit it. Recent research have shown, that a genetic mutation in the chikungunya virus identified in Réunion Island, has facilitated the transmission by *Aedes albopictus*. Indeed, the extrinsic incubation period was reduced to two days [33]. Mosquitoes remain infective until death. Vertical transmission in the vector has not yet been observed until today.

A human is infected after being bitten by an infected vector, after a delay of four to seven days (incubation period), the human is able to transmit the virus. This period, which can go on five to seven days, is the viraemia period. After this time, human recovers.

3. Vector population and virus transmission modeling

3.1. Formulation of a dynamical model for vector population growth

To describe the *Aedes albopictus* population dynamics we use a stage structured model, which consists of three main stages (see

Fig. 1: embryonic (E), larvae (L, which consists here of the larvae and pupae populations) and adult (A, which consists only of adults females). Even if eggs and immature stages are both aquatic, we dissociate them because these two populations respond differently to control measures. Indeed, eggs can cling and are desiccation-resistant and hence, drying the breeding sites does not kill eggs, but only larvae and pupae. Moreover, chemical interventions on the breeding sites has impact on the larvae population, but not on the eggs.

We assume that the number of laid eggs is proportional to the number of females.

The above hypotheses lead to the following equations.

$$\begin{cases} \frac{dE}{dt}(t) = bA(t) - sE(t) - dE(t), \\ \frac{dL}{dt}(t) = sE(t) - s_L L(t) - d_L L(t), \\ \frac{dA}{dt}(t) = s_L L(t) - d_m A(t). \end{cases} \quad (1)$$

Moreover, as we said in Sections 2.2 and 2.4, it has been observed that mosquitoes are able to detect the best breeding site for the eggs development. Indeed if there are too much eggs in the oviposition habitat or too few nutrients and water resources, then females laid less eggs or choose another site. It seems reasonable to express this biological phenomenon with a mathematical model which explicitly incorporates the idea of limited carrying capacity resources. This model should take into account the availability of nutrients and the occupation by eggs or larvae of the available breeder sites. That is why we assume that,

- per capita oviposition rate is given by,

$$b\left(1 - \frac{E(t)}{K_E}\right)A(t),$$

where K_E is the availability of nutrients and space, b represents the rate at which the population would grow if they were unencumbered by environmental degradation,

- the transition rate from class E to class L is s but when the availability of food is not sufficient for the class L, then the larvae can eat the young larvae to complete its development and we suppose that the death rate due to the lack of food is proportional to the young larvae sE and to the coefficient L/K_L that represent the availability of food for each larvae. At the end, the number of eggs that hatch and survive is given by,

$$s\left(1 - \frac{L(t)}{K_L}\right)E(t).$$

Then system (1) reads as follows,

$$\begin{cases} \frac{dE}{dt}(t) = b\left(1 - \frac{E(t)}{K_E}\right)A(t) - sE(t) - dE(t), \\ \frac{dL}{dt}(t) = s\left(1 - \frac{L(t)}{K_L}\right)E(t) - s_L L(t) - d_L L(t), \\ \frac{dA}{dt}(t) = s_L L(t) - d_m A(t). \end{cases} \quad (2)$$

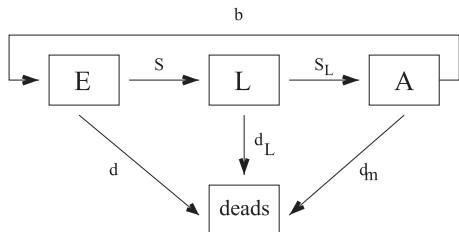


Fig. 1. A stage structured model for *Aedes albopictus* population dynamics. E states for eggs, L for larvae and pupae, A for female adult. s, s_L, b, d, d_L, d_m are nonnegative system parameters. In the diagram, b = eggs laying rate, s = E to L transfer rate, s_L = L to A transfer rates, d, d_L, d_m = mortality rates of eggs, larvae and adult population.

This system is mathematically well defined over the whole \mathbb{R}^3 . Nevertheless, the region of biological interest is Δ which is given by,

$$\Delta = \left\{ (E, L, A) \mid \begin{array}{l} 0 \leq E \leq K_E \\ 0 \leq L \leq K_L \\ 0 \leq A \leq \frac{s_L}{d_m} K_L \end{array} \right\}, \quad (3)$$

which its interior, denoted $int(\Delta)$, is given by

$$int(\Delta) = \left\{ (E, L, A) \mid \begin{array}{l} 0 < E < K_E \\ 0 < L < K_L \\ 0 < A < \frac{s_L}{d_m} K_L \end{array} \right\}. \quad (4)$$

We will see in Lemma 4.3 that Δ is a positive invariant set for system (2).

3.2. A compartmental model for the virus transmission to human population

Let us denote by N_H the human population size for which we assume an exponential growth. Then, its dynamics is described by,

$$\frac{dN_H}{dt}(t) = (b_H - d_H)N_H(t), \quad (5)$$

where b_H and d_H are, respectively, the human birth and natural death rates.

Let \bar{S}_H, \bar{I}_H and \bar{R}_H denote the total number of respectively susceptible, infective, and immune in the human population and \bar{S}_m, \bar{I}_m be the total number of susceptible and infective mosquitoes. The immune class in the vector population does not exist, since mosquitoes carry the infection throughout their life. The model is schematically represented in Fig. 2.

The effective contact rate β_H is the average number of contacts per day which would result in infection if the vector is infectious and, as in [15,34], we can assume that it is constant. The effective contact rate β_m is the average number of contacts per day that effectively transmit the infection to vectors. These hypotheses lead to the following equations,

$$\begin{cases} \frac{d\bar{S}_H}{dt}(t) = b_H(\bar{S}_H(t) + \bar{I}_H(t) + \bar{R}_H(t)) - \beta_H \frac{\bar{I}_m(t)}{A(t)} \bar{S}_H(t) - d_H \bar{S}_H(t), \\ \frac{d\bar{I}_H}{dt}(t) = \beta_H \frac{\bar{I}_m(t)}{A(t)} \bar{S}_H(t) - \gamma \bar{I}_H(t) - d_H \bar{I}_H(t), \\ \frac{d\bar{R}_H}{dt}(t) = \gamma \bar{I}_H(t) - d_H \bar{R}_H(t), \\ \frac{d\bar{S}_m}{dt}(t) = s_L \bar{L}(t) - d_m \bar{S}_m(t) - \beta_m \frac{\bar{I}_H(t)}{N_H(t)} \bar{S}_m(t), \\ \frac{d\bar{I}_m}{dt}(t) = \beta_m \frac{\bar{I}_H(t)}{N_H(t)} \bar{S}_m(t) - d_m \bar{I}_m(t). \end{cases} \quad (6)$$

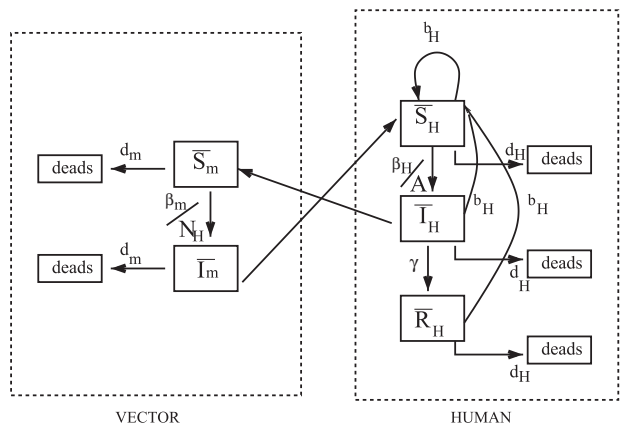


Fig. 2. A compartmental model for the chikungunya virus transmission with the nonnegative parameters: β_m = effective contact rate between susceptible vectors and humans, β_H = effective contact rate between susceptible humans and vectors, γ = recovery rate of infected humans, d_H = mortality rate of human population, d_m = mortality rate of vector population.

All parameters in this model are positive.

Introducing the proportions $S_H = \bar{S}_H/N_H$, $I_H = \bar{I}_H/N_H$, $R_H = \bar{R}_H/N_H$, $S_m = \bar{S}_m/A$, $I_m = \bar{I}_m/A$ in system (6) and by using relations $\bar{S}_H + \bar{I}_H + \bar{R}_H = N_H$ and $\bar{S}_m + \bar{I}_m = A$, the adult mosquito population is assumed to be described by the third equation of system (2), we obtain the following system that describes the dynamics of the proportion of individuals in each class, with the notation $u'(t) = \frac{du}{dt}(t)$,

$$\begin{cases} E'(t) = bA(t)\left(1 - \frac{E(t)}{K_E}\right) - (s + d)E(t), \\ L'(t) = sE(t)\left(1 - \frac{L(t)}{K_L}\right) - (s_L + d_L)L(t), \\ A'(t) = s_L L(t) - d_m A(t), \\ S'_H(t) = -(b_H + \beta_H I_m(t))S_H(t) + b_H, \\ I'_H(t) = \beta_H I_m(t)S_H(t) - (\gamma + b_H)I_H(t), \\ I'_m(t) = -\left(s_L \frac{L(t)}{A(t)} + \beta_m I_H(t)\right)I_m(t) + \beta_m I_H(t). \end{cases} \quad (7)$$

Remark 1. Obviously, this system has two different time scales, the one of mosquitoes of the order of weeks and the human lifespan of order of decades. Moreover, whether $b_H \neq d_H$ or $b_H = d_H$, when we consider the proportions, just above given, simple computations lead to the same system (7). Indeed, it suffices to note that $S'_H = (1/N_H^2)(\bar{S}'_H N_H - \bar{S}_H N'_H)$, $I'_H = (1/N_H^2)(\bar{I}'_H N_H - \bar{I}_H N'_H)$ and $S_H + I_H + R_H = 1$, similarly $I'_m = (1/A^2)(\bar{I}'_m A - \bar{I}_m A')$ and $S_m + I_m = 1$, where N'_H is given by (5) and $\bar{S}'_H, \bar{I}'_H, \bar{I}_m$ are given in system (6).

This system, as we will see in Section 5.2, is defined on the bounded subset of \mathbb{R}^6 , which is the region of biological interest, $\Delta \times \Omega$, where Δ is given by Eq. 3 and,

$$\Omega = \left\{ (S_H, I_H, I_m) \in \mathbb{R}_+^3 \mid \begin{array}{l} 0 \leq S_H + I_H \leq 1 \\ 0 \leq I_m \leq 1 \end{array} \right\} \quad (8)$$

and which its interior, denoted $\text{int}(\Omega)$, is given by

$$\text{int}(\Omega) = \left\{ (S_H, I_H, I_m) \in \mathbb{R}_+^3 \mid \begin{array}{l} 0 < S_H + I_H < 1 \\ 0 < I_m < 1 \end{array} \right\}. \quad (9)$$

Obviously, this model may be enhanced by taking into account the delay between the transfer to mosquitoes and the transmission to humans (from five to six days), see [35]. One can also use a SEI type model for the vector, see [12], although, if we consider a huge mosquito population, the number of mosquitoes in state E (exposed) can be neglected in comparison to the whole population.

4. Analysis of the population dynamics models

We investigate the asymptotic behavior of orbits starting in the non-negative cone,

$$\mathbb{R}_+^3 = \{(x, y, z) \in \mathbb{R}^3 \mid x \geq 0, y \geq 0, z \geq 0\}.$$

Let us also denote,

$$\mathbb{R}_+^{*3} = \{(x, y, z) \in \mathbb{R}^3 \mid x > 0, y > 0, z > 0\}.$$

Obviously, system (2) which is a C^∞ differential system, admits a unique maximal solution for any associated Cauchy problem. We shall use the following threshold parameter,

$$r = \left(\frac{b}{s+d}\right) \left(\frac{s}{s_L+d_L}\right) \left(\frac{s_L}{d_m}\right), \quad (10)$$

which arises in an obvious manner, when computing equilibria. It is easy to prove the following result.

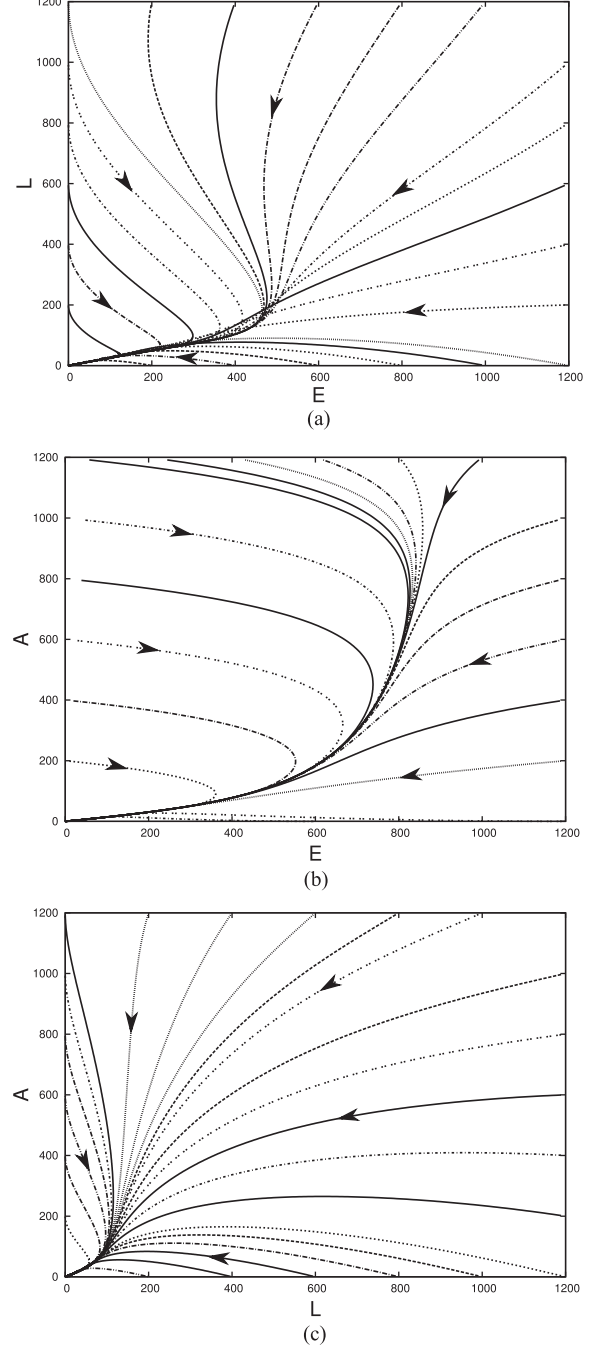


Fig. 3. Phase portraits of system (2) with parameters: $b = 5$, $s = 0.2$, $d = 0.6$, $K_E = 1000$, $s_L = 0.3$, $d_L = 0.6$, $K_L = 500$, $d_m = 0.7$. In this case $r = 0.595238$, then all trajectories tend to the mosquito-free equilibrium $X_0^* = (0, 0, 0)$.

Proposition 4.1. System (2) always has the mosquito-free equilibrium $X_0^* = (0, 0, 0)$.

- If $r \leq 1$, then system (2) has no other equilibrium.
- If $r > 1$, there is an unique endemic equilibrium,

$$X^* = \left(1 - \frac{1}{r}\right) \left(\frac{K_E}{\gamma_E}, \frac{K_L}{\gamma_L}, \frac{s_L}{d_m} \frac{K_L}{\gamma_L}\right) = (E^*, L^*, A^*),$$

where,

$$\gamma_E = 1 + \frac{(s+d)d_m K_E}{b s_L K_L} \quad \text{and} \quad \gamma_L = 1 + \frac{(s_L+d_L)K_L}{s K_E}.$$

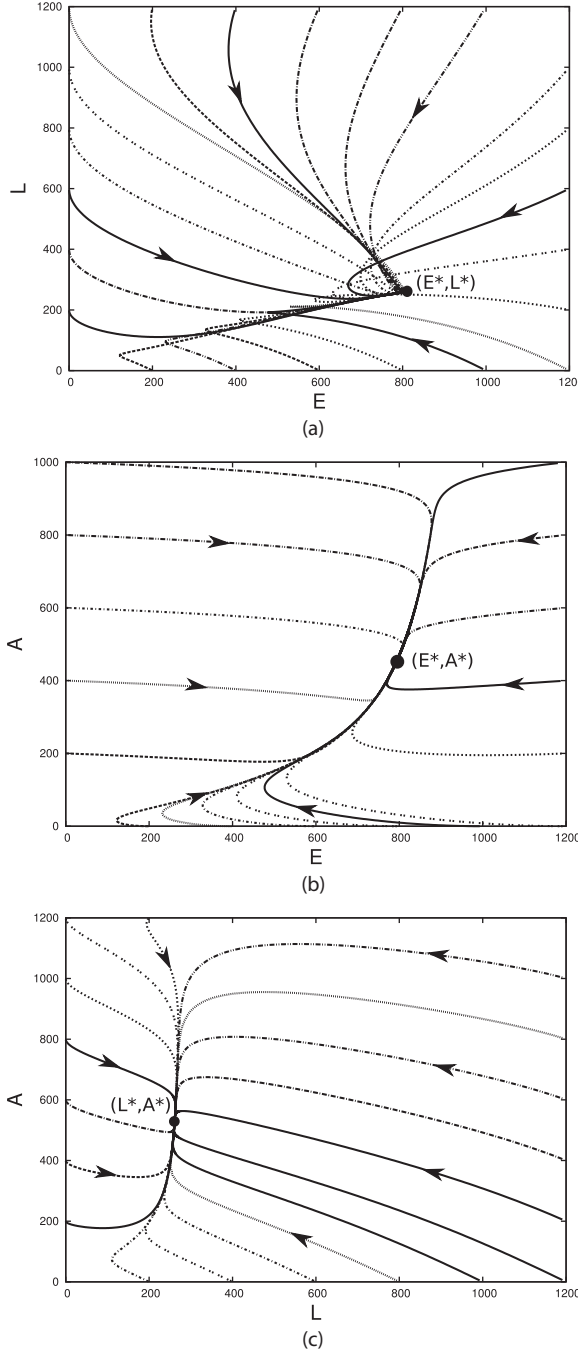


Fig. 4. Phase portraits of system (2) with parameters: $b = 6$, $s = 0.5$, $d = 0.2$, $K_E = 1000$, $s_L = 0.5$, $d_L = 0.25$, $K_L = 500$, $d_m = 0.25$. In this case $r = 11.428571$, then all trajectories tend to the endemic equilibrium X^* .

4.1. Non-negativity and boundedness of solutions

Lemma 4.2. Let $(t_0, X_0 = (E_0, L_0, A_0)) \in \mathbb{R}_+ \times \mathbb{R}_+^3$ and $([t_0, T], X = (E, L, A))$ be the maximal solution of the Cauchy problem associated to (2) with the initial condition (t_0, X_0) . Then,

$$\forall t \geq t_0, X(t) \in \mathbb{R}_+^3.$$

Proof. Let $(t_0, X_0 = (E_0, L_0, A_0)) \in \mathbb{R}_+ \times \mathbb{R}_+^3$ and $([t_0, T], X = (E, L, A))$ be the maximal solution of the Cauchy problem associated to (2) with the initial condition (t_0, X_0) . Let us assume that this solution becomes negative, i.e. $\tilde{t}_1 > t_0$ exists such that $X(\tilde{t}_1) \notin \mathbb{R}_+^3$. Let us define, $t_1 = \inf\{t, X(t) \notin \mathbb{R}_+^3\}$, i.e.

$$t_0 \leq t < t_1, X(t) \in \mathbb{R}_+^3$$

and $\varepsilon > 0$ exists such that

$$\forall t_1 < t \leq t_1 + \varepsilon, X(t) \notin \mathbb{R}_+^3. \quad (11)$$

Since $N_0^* = (0, 0, 0)$ is an equilibrium, the uniqueness of the solutions implies $X(t_1) \neq (0, 0, 0)$. For $t = t_1$, six cases are possible.

1. $X(t_1) = (0, L(t_1), A(t_1))$ with $(L(t_1), A(t_1)) \in (\mathbb{R}_+^*)^2$. Then, taking t_1 as an initial time, $E(t_1) = bA(t_1) > 0$. Since,

$$\begin{aligned} E(t) &= E'(t_1)(t - t_1) + \underset{t \rightarrow t_1}{\circ}(t - t_1) \\ &= bA(t_1)(t - t_1) + \underset{t \rightarrow t_1}{\circ}(t - t_1), \end{aligned}$$

thus, $\tilde{\varepsilon} > 0$ exists such that, $\forall t_1 < t \leq t_1 + \tilde{\varepsilon}$ we have $E(t) > 0$. Besides $L(t_1)$ and $A(t_1)$ are positive for all $t \in [t_1, t_1 + \tilde{\varepsilon}]$, therefore $\forall t \in [t_1, t_1 + \min\{\tilde{\varepsilon}, \tilde{\varepsilon}\}]$,

$$X(t) \in \mathbb{R}_+^3,$$

which is a contradiction.

2. Let $X(t_1) = (0, 0, A(t_1))$ with $A(t_1) > 0$. We can show as above that $\tilde{\varepsilon} > 0$ exists such that $\forall t_1 < t \leq t_1 + \tilde{\varepsilon}, E(t) > 0$. Now from the second equation of (2), since $L(t_1) = 0$, $L'(t_1) = 0$ and $L''(t_1) = sE(t_1) = sbA(t_1) > 0$, then

$$\begin{aligned} L(t) &= L''(t_1) \frac{(t - t_1)^2}{2} + \underset{t \rightarrow t_1}{\circ}((t - t_1)^2) \\ &= sbA(t_1) \frac{(t - t_1)^2}{2} + \underset{t \rightarrow t_1}{\circ}((t - t_1)^2), \end{aligned}$$

thus, $\tilde{\varepsilon} > 0$ exists such that $\forall t_1 < t \leq t_1 + \tilde{\varepsilon}$, we have $L(t) > 0$. Besides $A(t_1) > 0$, is positive for all $t \in [t_1, t_1 + \tilde{\varepsilon}]$, therefore $\forall t \in [t_1, t_1 + \min\{\tilde{\varepsilon}, \tilde{\varepsilon}\}]$

$$X(t) \in \mathbb{R}_+^3,$$

which is a contradiction.

Similar proof can easily be done for the other cases that are $X(t) = (E(t_1), 0, A(t_1))$ or $X(t) = (E(t_1), L(t_1), 0)$ or $X(t) = (E(t_1), 0, 0)$ or $X(t) = (0, L(t_1), 0)$. \square

Lemma 4.3. The set

$$\Delta = \left\{ (E, L, A) \mid \begin{array}{l} 0 \leq E \leq K_E \\ 0 \leq L \leq K_L \\ 0 \leq A \leq \frac{s_L}{d_m} K_L \end{array} \right\}$$

is an invariant region under the flow induced by (2).

Proof. Let $(t_0, X_0 = (E_0, L_0, A_0)) \in \mathbb{R}_+ \times \mathbb{R}_+^3$ and $([t_0, T], X = (E, L, A))$ be the maximal solution of the Cauchy problem associated to system (2) with the initial condition $(t_0, X_0), T \in [t_0, +\infty]$. Let $t_1 \in [t_0, T]$. We only have to show that,

1. if $E(t_1) \leq K_E$ then $\forall t_1 \leq t < T, E(t) \leq K_E$
2. if $L(t_1) \leq K_L$ then $\forall t_1 \leq t < T, L(t) \leq K_L$
3. if $A(t_1) \leq \frac{s_L}{d_m} K_L$ then $\forall t_1 \leq t < T, A(t) \leq \frac{s_L}{d_m} K_L$

since we have already shown that solutions are nonnegative, Lemma 4.2.

1. Assume that $\varepsilon_1 > 0$ exists such that $E(t_1 + \varepsilon_1) > K_E$. Let,

$$t_1^* = \inf\{t \geq t_1 \mid E(t) > K_E\}.$$

Since, $E(t_1^*) = K_E$, then,

$$E(t) = K_E + E'(t_1^*)(t - t_1^*) + \underset{t \rightarrow t_1^*}{\circ}(t - t_1^*).$$

Moreover, from the first equation of system (2), $E(t_1^*) = -(s+d)K_E < 0$, then there exists $\tilde{\varepsilon} > 0$ such that $\forall t_1^* \leq t < t_1^* + \tilde{\varepsilon}, E(t) < K_E$ which is a contradiction. As a result, $\forall t \in [t_0, T], E(t) \leq K_E$.

2. Assume that $\varepsilon_1 > 0$ exists such that $L(t_1 + \varepsilon_1) > K_L$. Let,

$$t_1^* = \inf\{t \geq t_1 \mid L(t) > K_L\}.$$

Since $L(t_1^*) = K_L$, then,

$$L(t) = K_L + L'(t_1^*)(t - t_1^*) + \underset{t \rightarrow t_1^*}{\circ}(t - t_1^*).$$

Moreover from the second equation of system (2), $L'(t_1^*) = -(s_L + d_L)K_L < 0, \tilde{\varepsilon} > 0$ exists such that $\forall t_1^* \leq t < t_1^* + \tilde{\varepsilon}, L(t) < K_L$ which is a contradiction. As a result, $\forall t \in [t_0, T], L(t) \leq K_L$.

3. Assume that $\varepsilon_1 > 0$ exists such that $A(t_1 + \varepsilon_1) > \frac{s_L}{d_m}K_L$. Let,

$$t_1^* = \inf\{t \geq t_1 \mid A(t) > \frac{s_L}{d_m}K_L\}.$$

Since $A(t_1^*) = \frac{s_L}{d_m}K_L$, then,

- If $L(t_1^*) < K_L$, then, $A'(t_1^*) < 0$.

$$A(t) = \frac{s_L}{d_m}K_L + A'(t_1^*)(t - t_1^*) + \underset{t \rightarrow t_1^*}{\circ}(t - t_1^*)$$

with

$$A'(t_1^*) = s_L(L(t_1^*) - K_L).$$

- If $L(t_1^*) = K_L$ then, $A'(t_1^*) = 0$ and

$$A(t) = \frac{s_L}{d_m}K_L + A''(t_1^*)\frac{(t - t_1^*)^2}{2} + \underset{t \rightarrow t_1^*}{\circ}\left((t - t_1^*)^2\right)$$

with $A''(t_1^*) = s_L L'(t_1^*) = -s_L(s_L + d_L)K_L < 0$.

In both cases, there exists $\tilde{\varepsilon} > 0$ such that $\forall t_1^* < t \leq t_1^* + \tilde{\varepsilon}, A(t) < \frac{s_L}{d_m}K_L$ which is a contradiction. As a result $\forall t \in [t_0, T], A(t) \leq \frac{s_L}{d_m}K_L$. To conclude, Δ is invariant under the flow induced by (2). \square

Proposition 4.4. All non-negative solutions (i.e. solutions initiating in \mathbb{R}_+^3) eventually enter the set Δ .

Proof. Let $(t_0, X_0 = (E_0, L_0, A_0)) \in \mathbb{R}_+ \times \mathbb{R}_+^3$ such that $(E_0, L_0, A_0) \notin \Delta$ (since Δ is invariant) and $([t_0, T], X = (E, L, A))$ be the maximal solution of the Cauchy problem associated to system (2) with the initial condition (t_0, X_0) .

We know that Δ is an invariant region (Lemma 4.3).

It is then sufficient to show that there exists $t \geq t_0$ such that $X(t) \in \Delta$.

- Assume that for all $t \in [t_0, +\infty[, E(t) > K_E$. Then, due to the first equation of system (2), for all $t \in [t_0, +\infty[, E'(t) < -(s+d)K_E$. Then, by comparison, $\forall t \in [t_0, +\infty[, we have,$

$$E(t) \leq E_0 - (s+d)K_E(t - t_0).$$

For $t_1 = t_0 + \frac{E_0 - K_E}{(s+d)K_E}$, we obtain $E(t) \leq K_E$ which is a contradiction. Therefore, for all $t > t_1, E(t) \leq K_E$.

- If $L(t_1) \leq K_L$, then the solution $L(t)$ belongs to Δ which is invariant. Otherwise, let assume on the contrary that for all $t \in [t_1, +\infty[, t_1$ given above, $L(t) > K_L$. Then $\forall t \in [t_1, +\infty[,$ due to the second equation of system (2), $L'(t) < -(s_L + d_L)K_L$. Then, by comparison $\forall t \in [t_1, +\infty[$ we have,

$$L(t) \leq L(t_1) - (s_L + d_L)K_L(t - t_1).$$

For $t_2 = t_1 + \frac{L(t_1) - K_L}{(s_L + d_L)K_L}$, we obtain $L(t_2) \leq K_L$ which is a contradiction. Thus, there exists $t_2 > t_1$ such that $L(t_2) \leq K_L$.

$$L(t) \leq K_L.$$

- If $A(t_2) \leq \frac{s_L}{d_m}K_L$, the solution $A(t)$ is within Δ which is invariant. Otherwise, let assume on the contrary that for all $t \in [t_2, +\infty[, A(t) > \frac{s_L}{d_m}K_L$. Then, due to the third equation of system (2), $\forall t \in [t_2, +\infty[,$

$$A'(t) < s_L(L(t) - K_L) < 0.$$

Then, there exists $c > 0$ such that $A'(t) \leq c$, since $L(t)$ is now bounded. By comparison, we have $\forall t \in [t_2, T],$

$$A(t) \leq A(t_2) - c(t - t_2).$$

For $t_3 = t_2 + \frac{A(t_2) - \frac{s_L}{d_m}K_L}{c}$, we have $A(t) \leq \frac{s_L}{d_m}K_L$ which is a contradiction. To conclude, for $t \geq \max(t_1, t_2, t_3), (E(t), L(t), A(t)) \in \Delta$. \square

4.2. Stability of the equilibria

Proposition 4.5. The mosquito-free equilibrium $X_0^* = (0, 0, 0)$ is locally asymptotically stable iff $r < 1$.

Proof. The local stability of the mosquito-free equilibrium X_0^* is given by the Jacobian matrix of the system (2) evaluated at this point, $D_F(X_0^*)$,

$$D_F(X_0^*) = \begin{pmatrix} -(s+d) & 0 & b \\ s & -(s_L + d_L) & 0 \\ 0 & s_L & -d_m \end{pmatrix}. \quad (12)$$

The characteristic equation of (12) is given by,

$$\lambda^3 + \alpha_1\lambda^2 + \alpha_2\lambda + \alpha_3,$$

where,

$$\alpha_1 = (s+d) + (s_L + d_L) + d_m,$$

$$\alpha_2 = (s+d)(s_L + d_L) + (s+d)d_m + (s_L + d_L)d_m,$$

$$\alpha_3 = d_m(s+d)(s_L + d_L)(1-r).$$

We apply the Routh-Hurwitz criterion. Clearly $\alpha_1 > 0$, $\alpha_2 > 0$ and $D_1 = \alpha_1\alpha_2 - \alpha_3 > 0$ since,

$$\begin{aligned} D_1 &= \alpha_1\alpha_2 - \alpha_3 \\ &= ((s+d) + (s_L + d_L) + d_m)(s+d)((s_L + d_L) + d_m) \\ &\quad + d_m(s_L + d_L)(r(s+d) + (s_L + d_L) + d_m) > 0. \end{aligned}$$

If $r < 1$ then $\alpha_3 > 0$, thus using the Routh-Hurwitz criterion all eigenvalues of $D_F(X_0^*)$ have negative real part, thus X_0^* is locally asymptotically stable for (2). If $r \geq 1$ then $\alpha_3 < 0$ and we show that $D_F(X_0^*)$ has at least one eigenvalue with non-negative real part consequently X_0^* is not asymptotically stable. \square

Remark 2. Moreover, we can easily prove that X_0^* is globally asymptotically stable for $r \leq 1$ using quadratic Lyapunov function (the proof is similar to the one given below in Proposition 4.7 for X^* , see also Fig. 3).

Proposition 4.6. If $r > 1, X^*$ is locally asymptotically stable.

Proof. The local stability of the endemic equilibrium X^* is given by the Jacobian matrix of the system (2) evaluated at this point,

$$D_F(X^*) = \begin{pmatrix} -d_1 & 0 & d_2 \\ d_3 & -d_4 & 0 \\ 0 & d_5 & -d_6 \end{pmatrix} \quad (13)$$

with

$$d_1 = \frac{bs_L}{d_m \gamma_L} \frac{K_L}{K_E} \left(1 - \frac{1}{r} \right) + (s + d),$$

$$d_2 = (s + d) \frac{d_m \gamma_L K_E}{s_L \gamma_E K_L},$$

$$d_3 = \frac{(s_L + d_L) \gamma_E K_L}{\gamma_L K_E},$$

$$d_4 = \frac{s K_E}{\gamma_E K_L} \left(1 - \frac{1}{r} \right) + (s_L + d_L),$$

$$d_5 = s_L,$$

$$d_6 = d_m.$$

The characteristic equation of (12) is given by,

$$\chi_{X^*}(\lambda) = \lambda^3 + \alpha_1 \lambda^2 + \alpha_2 \lambda + \alpha_3,$$

where

$$\alpha_1 = d_1 + d_4 + d_6,$$

$$\alpha_2 = d_1 d_4 + d_1 d_6 + d_6 d_4,$$

$$\alpha_3 = d_1 d_4 d_6 - d_2 d_3 d_5$$

$$\begin{aligned} &= d_m \left(1 - \frac{1}{r} \right) \left(\frac{bs_L}{d_m \gamma_L \gamma_E} \left(1 - \frac{1}{r} \right) + (s + d) \frac{s K_E}{\gamma_E K_L} \right. \\ &\quad \left. + (s_L + d_L) \frac{bs_L}{d_m \gamma_L K_E} \right). \end{aligned}$$

If $r > 1$, then $\alpha_1 > 0, \alpha_2 > 0$ and $\alpha_3 > 0$ and,

$$D_1 = \alpha_1 \alpha_2 - \alpha_3$$

$$\begin{aligned} &= \alpha_1 \times \left(\frac{bs_L}{d_m \gamma_L} \frac{K_L}{K_E} \left(1 - \frac{1}{r} \right) + (s + d) \right) \times \left(\frac{s K_E}{\gamma_E K_L} \left(1 - \frac{1}{r} \right) \right. \\ &\quad \left. + (s_L + d_L) + d_m \left(\frac{s K_E}{\gamma_E K_L} \left(1 - \frac{1}{r} \right) \right) \left(\frac{s K_E}{\gamma_E K_L} \left(1 - \frac{1}{r} \right) \right. \right. \\ &\quad \left. \left. + (s_L + d_L) + d_m (s_L + d_L) \left(\frac{s K_E}{\gamma_E K_L} \left(1 - \frac{1}{r} \right) \right. \right. \right. \\ &\quad \left. \left. \left. + (s + d) + (s_L + d_L) + d_m \right) \right) > 0. \end{aligned}$$

Then, thanks to the Routh-Hurwitz criterion all eigenvalues of $D_F(X^*)$ have negative real part. Consequently X^* is locally asymptotically stable (see also Fig. 4). \square

Proposition 4.7. If $r > 1$ the endemic equilibrium X^* is globally asymptotically stable in $\text{int}(\Delta)$ (Δ is given by Lemma 4.3).

Proof. Assume $r > 1$. Let $X^*(E^*, L^*, A^*) = (x^*, y^*, z^*)$. To prove the global stability of X^* , we use the Lyapunov function $V_1 : \mathbb{R}^3 \rightarrow \mathbb{R}$ defined by,

$$V_1(x, y, z) = \frac{1}{2} \left(a_1(x - x^*)^2 + a_2(y - y^*)^2 + a_3(z - z^*)^2 \right),$$

where $a = (a_1, a_2, a_3)^T \in (\mathbb{R}_+^*)^3$ is a positive constant vector. Note that since $r > 1$, then x^*, y^* and z^* are positive. We have,

$$V_1(X^*) = 0 \quad \text{and} \quad \forall (x, y, z) \in \mathbb{R}_3 \setminus \{X^*\}, V_1(x, y, z) > 0.$$

Hence, V_1 is well defined. The orbital derivative, that is the derivative of V_1 along solutions of system (2) is,

$$\begin{aligned} \dot{V}_1(x, y, z) &= a_1(x - x^*) \left(bz \left(1 - \frac{x}{K_E} \right) - (s + d)x \right) \\ &\quad + a_2(y - y^*) \left(sx \left(1 - \frac{y}{K_L} \right) - (s_L + d_L)y \right) \\ &\quad + a_3(z - z^*)(s_L y - d_m z). \end{aligned} \tag{14}$$

Let $\tilde{x} = x - x^*, \tilde{y} = y - y^*, \tilde{z} = z - z^*$ and $\tilde{X} = (\tilde{x}, \tilde{y}, \tilde{z})^T$.

Then

$$\begin{aligned} \dot{V}_1(x, y, z) &= \tilde{X}^T \begin{pmatrix} -a_1(s + d) & 0 & a_1 b \left(1 - \frac{x^*}{K_E} \right) \\ a_2 s \left(1 - \frac{y^*}{K_L} \right) & -a_2(s_L + d_L) & 0 \\ 0 & a_3 s_L & -a_3 d_m \end{pmatrix} \tilde{X} \\ &\quad - \frac{a_1 b}{K_E} \tilde{x}^2 z - \frac{a_2 s}{K_L} \tilde{y}^2 x. \end{aligned}$$

Let $A_1 = -D + R_1$ with,

$$D = \begin{pmatrix} a_1(s + d) & 0 & 0 \\ 0 & a_2(s_L + d_L) & 0 \\ 0 & 0 & a_3 d_m \end{pmatrix}$$

and

$$R_1 = \begin{pmatrix} 0 & 0 & a_1 b \left(1 - \frac{x^*}{K_E} \right) \\ a_2 s \left(1 - \frac{y^*}{K_L} \right) & 0 & 0 \\ 0 & a_3 s_L & 0 \end{pmatrix}.$$

Let us denote by $\langle \cdot, \cdot \rangle$ the scalar product in \mathbb{R}^3 . Then the orbital derivative reads as,

$$\dot{V}_1(x, y, z) = \langle A_1 \tilde{X}, \tilde{X} \rangle - \frac{a_1 b}{K_E} \tilde{x}^2 z - \frac{a_2 s}{K_L} \tilde{y}^2 x.$$

The symmetric matrix S_1 defined by,

$$S_1 = -D + \frac{1}{2}(R_1^T + R_1)$$

is given using simple algebraic computations by

$$S_1 = \begin{pmatrix} -a_1(s + d) & \frac{a_2}{2} (s_L + d_L) \frac{y^*}{x^*} & \frac{a_1}{2} (s + d) \frac{x^*}{z^*} \\ \frac{a_2}{2} (s_L + d_L) \frac{y^*}{x^*} & -a_2(s_L + d_L) & \frac{a_3 s_L}{2} \\ \frac{a_1}{2} (s + d) \frac{x^*}{z^*} & \frac{a_3 s_L}{2} & -a_3 d_m \end{pmatrix}.$$

Therefore, we have,

$$\langle A_1 \tilde{X}, \tilde{X} \rangle = \langle S_1 \tilde{X}, \tilde{X} \rangle.$$

The characteristic polynomial of S_1 is,

$$\chi_{S_1}(\lambda) = \lambda^3 + \alpha_1 \lambda^2 + \alpha_2 \lambda + \alpha_3,$$

where,

$$\alpha_1 = a_1(s + d) + a_2(s_L + d_L) + a_3 d_m,$$

$$\begin{aligned} \alpha_2 &= \frac{1}{4} a_1(s + d) \beta_1 + \frac{1}{4} a_2(s_L + d_L) \beta_2 + \frac{1}{4} a_3 \beta_3 + \frac{3}{4} (a_1 a_3 d_m (s + d) \\ &\quad + a_1 a_2 (s + d) (s_L + d_L) + a_2 a_3 d_m (s_L + d_L)) \end{aligned}$$

with

$$\beta_1 = \left(a_3 d_m - a_1(s + d) \left(\frac{x^*}{z^*} \right)^2 \right),$$

$$\beta_2 = \left(a_1(s + d) - a_2(s_L + d_L) \left(\frac{y^*}{x^*} \right)^2 \right),$$

$$\beta_3 = (a_2 d_m (s_L + d_L) - a_3 s_L^2)$$

and

$$\alpha_3 = \frac{1}{4} (a_1 a_2 (s + d) (s_L + d_L) \beta_1 + a_2 a_3 d_m (s_L + d_L) \beta_2 + a_1 a_3 (s + d) \beta_3).$$

Let us choose a_1, a_2 , and a_3 satisfying,

$$\begin{aligned} a_1 &= \frac{1}{s+d} \left(\frac{y^*}{x^*} \right)^2 > 0, \\ a_2 &= \frac{s+d}{s_L + d_L} \left(\frac{x^*}{y^*} \right)^2 a_1, \\ a_3 &= \frac{d_m(s+d)}{s_L^2} \left(\frac{x^*}{y^*} \right)^2 a_1 = a_1 \frac{s+d}{d_m} \left(\frac{x^*}{z^*} \right)^2 \end{aligned}$$

with such a choice, one can easily verify that $\beta_1 = \beta_2 = \beta_3 = 0$. Thus $\alpha_1 > 0$, $\alpha_2 > 0$ and $\alpha_3 = 0$, therefore the characteristic polynomial reads as,

$$\chi_{S_1}(\lambda) = \lambda(\lambda^2 + \alpha_1\lambda + \alpha_2).$$

Then,

$$S_1 = \begin{pmatrix} -\left(\frac{y^*}{x^*}\right)^2 & \frac{y^*}{2x^*} & \frac{d_m y^*}{2s_L x^*} \\ \frac{y^*}{2x^*} & -1 & \frac{d_m}{2s_L} \\ \frac{d_m y^*}{2s_L x^*} & \frac{d_m}{2s_L} & -\frac{d_m^2}{s_L^2}, \end{pmatrix}$$

since S_1 has one zero eigenvalue and two negatives eigenvalues. The matrix S_1 satisfies $\forall \tilde{X} \in \mathbb{R}_{+}^3$,

$$\langle S_1 \tilde{X}, \tilde{X} \rangle \leq 0.$$

Note that if $\tilde{X} \notin \text{Ker}(S_1)$ then $\langle S_1 \tilde{X}, \tilde{X} \rangle < 0$.

Then $\forall (x, y, z) \in \Delta \setminus \{X^*\}$,

$$\begin{aligned} \tilde{X} \notin \text{Ker}(S_1) \Rightarrow \dot{V}_1(x, y, z) &= \langle A_1 \tilde{X}, \tilde{X} \rangle - \left(\frac{a_1 b}{K_E} \tilde{x}^2 z + \frac{a_2 s}{K_L} \tilde{y}^2 x \right) \\ &\leq \langle A_1 \tilde{X}, \tilde{X} \rangle < 0. \end{aligned}$$

If $\tilde{X} \in \text{Ker}(S_1)$, it is sufficient to verify that

$$\left(\frac{a_1 b}{K_E} \tilde{x}^2 z + \frac{a_2 s}{K_L} \tilde{y}^2 x \right) > 0.$$

Note that

$$\begin{aligned} \left(\frac{a_1 b}{K_E} \tilde{x}^2 z + \frac{a_2 s}{K_L} \tilde{y}^2 x \right) &= 0 \\ \iff &\begin{cases} x = 0 \text{ and } z = 0 \\ \text{or } x = x^* \text{ and } y = y^* \\ \text{or } z = 0 \text{ and } y = y^* \end{cases} \\ \iff &\begin{cases} \tilde{x} = -x^* \text{ and } \tilde{z} = -z^* \\ \text{or } \tilde{x} = 0 \text{ and } \tilde{y} = 0 \\ \text{or } \tilde{z} = -z^* \text{ and } \tilde{y} = 0. \end{cases} \end{aligned}$$

Let

$$\begin{aligned} a_1 &= \frac{(s_L + d_L)^2}{s+d} \left(\frac{y^*}{x^*} \right)^2, \\ a_2 &= s_L + d_L, \\ a_3 &= \left(\frac{s_L + d_L}{s_L} \right)^2 d_m, \end{aligned}$$

we have

$$S_1 = (s_L + d_L)^2 \begin{pmatrix} -\left(\frac{y^*}{x^*}\right)^2 & \frac{y^*}{2x^*} & \frac{d_m y^*}{2s_L x^*} \\ \frac{y^*}{2x^*} & -1 & \frac{d_m}{2s_L} \\ \frac{d_m y^*}{2s_L x^*} & \frac{d_m}{2s_L} & -\frac{d_m^2}{s_L^2} \end{pmatrix}$$

and then

$$\text{Ker}(S_1) = \left\{ z \begin{pmatrix} \frac{x^*}{z^*} \\ \frac{y^*}{z^*} \\ 1 \end{pmatrix}, z \in \mathbb{R} \right\}.$$

Finally, we easily see that

$$\left\{ (x, y, z) \in \mathbb{R}^3 \middle/ (\tilde{x}, \tilde{y}, \tilde{z}) \in \text{Ker}(S_1) \text{ and } \left(\frac{a_1 b}{K_E} \tilde{x}^2 z + \frac{a_2 s}{K_L} \tilde{y}^2 x \right) = 0 \right\} = \{X_0^*, X^*\}.$$

Consequently $\forall (x, y, z) \in \Delta \setminus \{X^*\}$,

$$\dot{V}_1(x, y, z) < 0,$$

i.e. V_1 is a strict Lyapunov function and X^* is globally asymptotically stable in Δ . \square

5. Dynamics analysis of the virus transmission model

This section addresses the existence and global stability of equilibrium points of (7) by showing the persistence of the system and using the theory of competitive systems. We will focus on the case $r > 1, r$ given by (10) which is the condition of survival of all populations as we studied in the previous section.

For this aim, we shall use the following reproduction number [7,8], which is defined as the average number of secondary infections produced by an infected individual in a completely susceptible population

$$R_0 = \frac{\beta_m \beta_H}{d_m(\gamma + b_H)} = \frac{\beta_m \beta_H}{s_L \frac{L^*}{A^*} (\gamma + b_H)}, \quad (15)$$

which arises by computing the steady state.

5.1. Existence of equilibria

Proposition 5.1. *We assume that $r > 1$. System (7) always has the disease free equilibrium $N_0^* = (E^*, L^*, A^*, 1, 0, 0)$. Moreover, if $R_0 > 1$, it has an unique endemic equilibrium with disease $N^* = (E^*, L^*, A^*, S_H^*, I_H^*, I_m^*)$ defined on $\Delta \times \Omega$, the last are done by (3) and (8), where*

$$\begin{aligned} S_H^* &= \frac{b_H}{\beta_H + b_H} + \frac{\beta_H}{(\beta_H + b_H) R_0}, \\ I_H^* &= \frac{d_m b_H}{\beta_m (\beta_H + b_H)} (R_0 - 1), \\ I_m^* &= \frac{b_H}{\beta_H + b_H R_0} (R_0 - 1) \end{aligned} \quad (16)$$

and (E^*, L^*, A^*) is the endemic equilibrium of the independent system (2) given by Proposition 4.1.

Proof. Obviously, as $R_0 > 1$, both equilibria are non-negative. Besides, one can easily see that $(1, 0, 0)$ is an equilibrium of the subsystem of (7) given by the three last equations, then it is clear that N_0^* is an equilibrium of (7), belonging to $\Delta \times \Omega$.

It is also easy to check that N^* is an equilibrium of (7), thus we only have to show that (S_H^*, I_H^*, I_m^*) belongs to Ω , since we know that (E^*, L^*, A^*) is in Δ .

Since $R_0 > 1$, then,

$$I_m^* = \frac{R_0 - 1}{R_0 + \frac{\beta_H}{b_H}} \leq 1$$

and

$$I_H^* = \frac{R_0 - 1}{R_0} \frac{1}{\left(1 + \frac{\gamma}{b_H}\right) \left(1 + \frac{b_H}{\beta_H}\right)} \leq 1.$$

Moreover,

$$\begin{aligned} S_H^* + I_H^* &= \frac{b_H}{\beta_H + b_H} + \frac{\beta_H}{(\beta_H + b_H)R_0} + \frac{R_0 - 1}{R_0} \frac{1}{\left(1 + \frac{\gamma}{b_H}\right)\left(1 + \frac{b_H}{\beta_H}\right)} \\ &= \frac{1}{\beta_H + b_H} \left(b_H \left(1 + \frac{\beta_H}{b_H + \gamma}\right) + \frac{\beta_H}{R_0} \left(1 - \frac{b_H}{b_H + \gamma}\right) \right), \end{aligned}$$

which is less than 1, since $R_0 > 1$ and hence,

$$\begin{aligned} b_H + \frac{\gamma}{R_0} < b_H + \gamma &\iff \frac{b_H}{b_H + \gamma} + \frac{1}{R_0} \left(1 - \frac{b_H}{b_H + \gamma}\right) < 1 \\ &\iff \frac{b_H \beta_H}{b_H + \gamma} + \frac{\beta_H}{R_0} \left(1 - \frac{b_H}{b_H + \gamma}\right) < \beta_H \\ &\iff b_H \left(1 + \frac{\beta_H}{b_H + \gamma}\right) + \frac{\beta_H}{R_0} \left(1 - \frac{b_H}{b_H + \gamma}\right) < \beta_H + b_H \\ &\iff \frac{1}{\beta_H + b_H} \left(b_H \left(1 + \frac{\beta_H}{b_H + \gamma}\right) + \frac{\beta_H}{R_0} \left(1 - \frac{b_H}{b_H + \gamma}\right) \right) < 1. \quad \square \end{aligned}$$

Proposition 5.2. The equilibrium $N_0^* = (E^*, L^*, A^*, 1, 0, 0)$ is globally asymptotically stable in Ω iff $R_0 \leq 1$.

Proof. Similar to proof of Proposition 4.7, using the Lyapunov function $V_1 : \mathbb{R}^6 \rightarrow \mathbb{R}$ defined by,

$$\begin{aligned} V_1(x_1, x_2, x_3, x_4, x_5, x_6) &= \frac{1}{2} \left(a_1(x - E^*)^2 + a_2(y - L^*)^2 + a_3(z - A^*)^2 \right) \\ &\quad + \frac{1}{2} (a_4(x_4 - 1)^2 + a_5x_5^2 + a_6x_6^2), \end{aligned}$$

where,

$$\begin{aligned} a_1 &= \frac{(s_L + d_L)^2}{s + d} \left(\frac{L^*}{E^*} \right)^2, \quad a_2 = s_L + d_L, \\ a_3 &= \left(\frac{s_L + d_L}{s_L} \right)^2 d_m, \quad a_4 = \frac{b_H}{(\gamma + b_H)}, \\ a_5 &= \frac{\beta_H^2}{d_m(\gamma + b_H)}, \quad a_6 = R_0^2. \quad \square \end{aligned}$$

System (7) is the coupling of the two subsystems (7a) and (7b), for which the coupling term is the function $s_L \frac{L(t)}{A(t)} I_m(t)$, that is system (7a) drives system (7b). Therefore, since the previous section was devoted to the study of the subsystem (7a) corresponding to the population dynamics we only have to analyze the subsystem (7b),

$$\begin{cases} S'_H(t) = -(b_H + \beta_H I_m(t))S_H(t) + b_H, \\ I'_H(t) = \beta_H I_m(t)S_H(t) - (\gamma + b_H)I_H(t), \\ I'_m(t) = -\left(s_L \frac{L(t)}{A(t)} + \beta_m I_H(t)\right)I_m(t) + \beta_m I_H(t). \end{cases}$$

5.2. Global stability of the endemic equilibrium with disease

First of all, for the reader convenience, let us recall some useful preliminaries, see [36] and [37] in which a similar analysis has been done.

Definition 5.3. Consider the following systems,

$$x' = f(t, x), \quad (17)$$

$$y' = g(y), \quad (18)$$

where f and g are continuous and locally Lipschitz in $x \in \mathbb{R}^n$, thus the solutions exist for all positive time. System (17) is called asymptotically autonomous with limit system (18) if $f(t, x) \rightarrow g(x)$ as $t \rightarrow \infty$ uniformly for $x \in \mathbb{R}^n$.

Lemma 5.4 [36]. Let e be a locally asymptotically stable equilibrium of (18) and ω be the ω -limit set of a forward bounded solution $x(t)$ of (17). If ω contains a point y_0 such that the solution of (18), with $y(0) = y_0$ converges to e as $t \rightarrow \infty$, then $\omega = e$, i.e., $x(t) \rightarrow e$ as $t \rightarrow \infty$.

Corollary 1 [36]. If the solutions of system (17) are bounded and the equilibrium e of the limit system (18) is globally asymptotically stable, then every solution $x(t)$ of the system (17) satisfies $x(t) \rightarrow e$ as $t \rightarrow \infty$.

Let us apply this result to our subsystem (7b).

Since $X^* = (E^*, L^*, A^*)$, the endemic equilibrium of subsystem (7a), is globally asymptotically stable for $r > 1$ (Proposition 4.7), then $\frac{L(t)}{A(t)} \rightarrow \frac{L^*}{A^*}$ as $t \rightarrow +\infty$ uniformly. Therefore, thanks to the results above, system (7b) is a three-dimensional asymptotically autonomous differential system with limit system,

$$\begin{cases} S'_H(t) = -(b_H + \beta_H I_m(t))S_H(t) + b_H, \\ I'_H(t) = \beta_H I_m(t)S_H(t) - (\gamma + b_H)I_H(t), \\ I'_m(t) = -\left(s_L \frac{L^*}{A^*} + \beta_m I_H(t)\right)I_m(t) + \beta_m I_H(t). \end{cases} \quad (19)$$

The equilibrium of which are $\mathcal{L}_0^* = (1, 0, 0)$ and $\mathcal{L}^* = (S_H^*, I_H^*, I_m^*)$ if $R_0 > 1$.

First of all, note that the region of biological interest Ω given by (8) is positively invariant under the flow induced by (19), as the vector field on the boundary does not point to the outside of Ω which is obvious (similar proof is done for Lemma 4.3).

Theorem 5.5. If $R_0 > 1$, the endemic equilibrium with disease \mathcal{L}^* of system (19) is globally asymptotically stable in $\text{int}(\Omega)$.

To prove this theorem we shall use some preliminary results about competitive systems, see [38–40] and stability of periodic orbits, which we recall here for the reader convenience.

Let $D \subset \mathbb{R}^n$ be an open set, and $x \mapsto f(x) \in \mathbb{R}^n$ be a C^1 function defined in D . We consider the autonomous system in \mathbb{R}^n given by,

$$x' = f(x). \quad (20)$$

System (20) is *competitive* in D , if, for some diagonal matrix $H = \text{diag}(\varepsilon_1, \dots, \varepsilon_n)$, where ε_i , ($i = 1 \dots, n$), is either 1 or -1 , the matrix $H(Df(x))H$ has non-positive off-diagonal elements for $x \in D$, where $DF(x)$ is the Jacobian matrix of (20), see [39,40]. It is shown in [39] that, if D is convex, the flow of such a system preserves, for $t < 0$, the partial order in \mathbb{R}^n defined by the orthant

$$K = \{(x_1, \dots, x_n) \in \mathbb{R}^n : \varepsilon_i x_i \geq 0\}.$$

Looking at the Jacobian matrix of system (19) and choosing the matrix H such as

$$H = \begin{pmatrix} -1 & 0 & 0 \\ 0 & 1 & 0 \\ 0 & 0 & -1 \end{pmatrix},$$

we can see that system (19) is competitive in Ω , with respect to the partial order defined by the orthant

$$K = \{(S_H, I_H, I_m) \in \mathbb{R}^3 : S_H \leq 0, I_H \geq 0, I_m \leq 0\}.$$

We recall additional definitions that we will use later [41] and also [38,13,15]. Suppose that (20) has a periodic solution $x = p(t)$ with minimal period $\omega > 0$ and orbit $\gamma = \{p(t) : 0 \leq t \leq \omega\}$. This orbit is *orbitally stable* iff, for each $\varepsilon > 0$, there exists a $\delta > 0$ such that any solution $x(t)$, for which the distance of $x(0)$ from γ is less than δ , remains at a distance less than ε from γ , for all $t \geq 0$. It is *asymptotically orbitally stable*, if the distance of $x(t)$ from γ also tends to zero as t goes to infinity. This orbit γ is *asymptotically orbitally stable with asymptotic phase* if it is asymptotically orbitally stable and there is $b > 0$ such that, any solution $x(t)$, for which the distance of $x(0)$ from γ is less than b , satisfies $|x(t) - p(t - \tau)| \rightarrow 0$ as $t \rightarrow +\infty$ for some τ which may depend on $x(0)$ [41].

System (20) is persistent in the sense described in [42], i.e. iff each solution $x(t)$ starting in $\text{int}(\Omega)$, has the property that $\liminf_{t \rightarrow +\infty} x(t)$ is at a positive distance from the boundary of Ω .

Definition 5.6. We say that system (20) has the *property of stability of periodic orbits*, iff the orbit of any periodic solution $\gamma(t)$, if it exists, is asymptotically orbitally stable.

The following theorem is the main tool to prove the global stability of the endemic equilibrium with disease.

Theorem 5.7 ([13,41]). Assume that $n = 3$, D convex and bounded. Suppose that (20) is competitive, persistent and has the property of stability of periodic orbits. If x_0 is the only equilibrium in $\text{int}(D)$, and if it is locally asymptotically stable, then it is globally asymptotically stable in $\text{int}(D)$.

Now, let us go back and apply those results to the global asymptotic stability study of (S_H^*, I_H^*, I_m^*) . The proof of this theorem is similar to the one in [38]. In order to prove the persistence of system (19), we shall prove the following proposition.

Proposition 5.8. On the boundary of Ω , system (19) has only one ω -limit point which is the equilibrium \mathcal{L}_0^* . Moreover for $R_0 > 1$, \mathcal{L}_0^* cannot be the ω -limit of any orbit in $\text{int}(\Omega)$.

Proof. The vector field is transversal to the boundary of Ω , except in the S_H -axis which is invariant with respect to (19). On the S_H -axis we have

$$S'_H = b_H(1 - S_H).$$

which implies that $S_H(t) \rightarrow 1$ as $t \rightarrow \infty$. Therefore, \mathcal{L}_0^* is the only ω -limit point on the boundary of Ω .

To prove the second part of the proposition, we consider the functional

$$V = I_m + d_m \frac{1+R_0}{2} \frac{1}{\beta_H} I_H, \quad (21)$$

the derivative of which along solutions is given by,

$$\begin{aligned} \dot{V} &= I'_m + d_m \left(\frac{1+R_0}{2} \right) \frac{1}{\beta_H} I'_H \\ &= -s_L \frac{L^*}{A^*} I_m + \beta_m (1 - I_m) I_H \\ &\quad + d_m \left(\frac{1+R_0}{2} \right) \frac{1}{\beta_H} [\beta_H I_m(t) S_H(t) - (\gamma + b_H) I_H(t)] \\ &= -d_m I_m + \beta_m (1 - I_m) I_H + d_m \left(\frac{1+R_0}{2} \right) I_m S_H \\ &\quad - d_m \left(\frac{1+R_0}{2} \right) \frac{(\gamma + b_H)}{\beta_H} I_H \\ &= \left[\beta_m (1 - I_m) - d_m \frac{1+R_0}{2} \frac{(\gamma + b_H)}{\beta_H} \right] I_H + \left[d_m \frac{1+R_0}{2} S_H - d_m \right] I_m \\ &= \left[(1 - I_m) - \left(\frac{1+R_0}{2} \right) \frac{d_m (\gamma + b_H)}{\beta_H \beta_m} \right] \beta_m I_H \\ &\quad + \left[\left(\frac{1+R_0}{2} \right) S_H - 1 \right] d_m I_m \\ &= \left[(1 - I_m) - \left(\frac{1+R_0}{2} \right) \frac{1}{R_0} \right] \beta_m I_H + \left[\left(\frac{1+R_0}{2} \right) S_H - 1 \right] d_m I_m \\ &= \left[(1 - I_m) - \frac{1}{2} \left(\frac{1}{R_0} + 1 \right) \right] \beta_m I_H \\ &\quad + \left[S_H - \left(\frac{2}{1+R_0} \right) \right] d_m \left(\frac{1+R_0}{2} \right) I_m. \end{aligned}$$

Since $R_0 > 1$, then $\frac{1}{2}(1/R_0 + 1) < 1$ and $2/(1+R_0) < 1$. Therefore, there exists a neighborhood U of \mathcal{L}_0^* such that for $(S_H, I_H, I_m) \in U \cup \text{int}(\Omega)$ the expression inside of the brackets are positives. In this neighborhood, we have $\dot{V} > 0$ unless $I_H = I_m = 0$. Moreover, the level sets of V are the planes

$$I_m + d_m \left(\frac{1+R_0}{2} \right) \frac{1}{\beta_H} I_H = c,$$

which go away from the S_H -axis as c increases. Since V increases along the orbits starting in $U \cup \text{int}(\Omega)$, we conclude that they go away from \mathcal{L}_0^* .

This proves the proposition, and therefore, the persistence of system, (19) when $R_0 > 1$. \square

Theorem 5.9. The trajectory of any nonconstant periodic solution to (19), if it exists, is asymptotically orbitally stable with asymptotic phase.

To prove this we used the following results.

Theorem 5.10 [43]. A sufficient condition for a periodic orbit $\gamma = \{p(t): 0 \leq t \leq \omega\}$ of (20) to be asymptotically orbitally stable with asymptotic phase is that the linear non-autonomous system,

$$y'(t) = \frac{\partial f^{[2]}}{\partial x}(p(t))y(t) \text{ is asymptotically stable.} \quad (22)$$

Eq. (22) is called the *second compound equation* of (20) and $\partial f^{[2]}/\partial x$ is the *second compound matrix* [38,43] of the Jacobian matrix $\partial f^{[2]}/\partial x$ of f . Generally speaking, for a $n \times n$ matrix A and an integer $1 \leq k \leq n$, the k th additive compound matrix of A is denoted by $A^{[k]}$. This is a $N \times N$ matrix, $N = \binom{n}{k}$, defined by

$$A^{[k]} = D_+(I + hA)^{(k)}|_{h=0},$$

where $B^{(k)}$ is the k th exterior power of a $n \times n$ matrix B and D_+ denotes the right-hand derivative. For example, if $n = 3$ with the notations,

$$A = \begin{pmatrix} a_{1,1} & a_{1,2} & a_{1,3} \\ a_{2,1} & a_{2,2} & a_{2,3} \\ a_{3,1} & a_{3,2} & a_{3,3} \end{pmatrix}.$$

We have,

$$A^{[1]} = A,$$

$$A^{[2]} = \begin{pmatrix} a_{1,1} + a_{2,2} & a_{2,3} & -a_{1,3} \\ a_{3,2} & a_{1,1} + a_{3,3} & a_{1,2} \\ -a_{3,1} & a_{2,1} & a_{2,2} + a_{3,3} \end{pmatrix},$$

$$A^{[3]} = \text{tr}(A).$$

Proof. of Theorem 5.10 The Jacobian matrix of (19) is given by

$$DF = \begin{pmatrix} -(b_H + \beta_H I_m) & 0 & -\beta_H S_H \\ \beta_H I_m & -(\gamma + b_H) & \beta_H S_H \\ 0 & \beta_m (1 - I_m) & -(s_L \frac{L^*}{A^*} + \beta_m I_H) \end{pmatrix}.$$

For the solution $\gamma(t)$, (22) becomes

$$\begin{cases} X' = -(2b_H + \beta_H I_m + \gamma)X + \beta_H S_H Y + \beta_H S_H Z, \\ Y' = \beta_m (1 - I_m)X - (b_H + \beta_H I_m + s_L \frac{L^*}{A^*} + \beta_m I_H)Y, \\ Z' = \beta_H I_m Y - (s_L \frac{L^*}{A^*} + \beta_m I_H + \gamma + b_H)Z. \end{cases} \quad (23)$$

In order to prove that (23) is asymptotically stable, we consider the following Lyapunov function, where $\|\cdot\|$ is the norm in \mathbb{R}^3 by

$$\|(X, Y, Z)\| = \sup\{|X|, |Y| + |Z|\}$$

with

$$\begin{aligned} V(t) &= V(X(t), Y(t), Z(t); S_H(t), I_H(t), I_m(t)) \\ &= \left\| \begin{pmatrix} 1 & 0 & 0 \\ 0 & \frac{I_H(t)}{I_m(t)} & 0 \\ 0 & 0 & \frac{I_H(t)}{I_m(t)} \end{pmatrix} \begin{pmatrix} X \\ Y \\ Z \end{pmatrix} \right\| = \sup \left(|X|, \frac{I_H}{I_m} (|Y| + |Z|) \right). \end{aligned}$$

Suppose that the solution $p(t) = (S_H(t), I_H(t), I_m(t))$ is periodic of minimal period ω . Then [Proposition 5.8](#) implies that the orbit γ of $p(t)$ remains at a positive distance of the boundary of Ω . Therefore

$I_H(t) \geq \varepsilon$ and $I_m(t) \geq \varepsilon$ with $0 \leq \varepsilon \leq 1$.

Hence, the function V is well defined along $p(t)$ and there exists a constant $c > 0$ such that,

$$V(X, Y, Z; S_H, I_H, I_m) \geq c|(X, Y, Z)| \quad (24)$$

for all $(X, Y, Z) \in \mathbb{R}^3$ and $(S_H, I_H, I_m) \in \gamma$.

The right-hand derivative of $V(t)$ exists and its calculation is described in [\[44\]](#) and [\[45\]](#). In fact direct computation yields,

$$\begin{aligned} D_+|X(t)| &\leq -(2b_H + \beta_H I_m + \gamma)|X(t)| + \beta_H S_H(|Y(t)| + |Z(t)|) \\ &\leq -(2b_H + \beta_H I_m + \gamma)|X(t)| + \beta_H S_H \frac{I_m}{I_H} \left(\frac{I_H}{I_m} (|Y(t)| + |Z(t)|) \right) \end{aligned}$$

and

$$D_+|Y(t)| \leq \beta_m(1 - I_m)|X(t)| - \left(b_H + \beta_H I_m + s_L \frac{L^*}{A^*} + \beta_m I_H \right) |Y(t)|, \quad (25)$$

$$D_+|Z(t)| \leq \beta_H I_m |Y(t)| - \left(s_L \frac{L^*}{A^*} + \beta_m I_H + \gamma + b_H \right) |Z(t)|. \quad (26)$$

Thus,

$$\begin{aligned} D_+ \left[\frac{I_H}{I_m} (|Y(t)| + |Z(t)|) \right] &= \left(\frac{I'_H}{I_H} - \frac{I'_m}{I_m} \right) \frac{I_H}{I_m} (|Y(t)| + |Z(t)|) + \frac{I_H}{I_m} D_+ (|Y(t)| \\ &\quad + |Z(t)|) \leq \left(\frac{I'_H}{I_H} - \frac{I'_m}{I_m} \right) \frac{I_H}{I_m} (|Y(t)| + |Z(t)|) \\ &\quad + \frac{I_H}{I_m} \left[\beta_m(1 - I_m)|X(t)| - (b_H + s_L \frac{L^*}{A^*} + \beta_m I_H) (|Y(t)| + |Z(t)|) \right] \\ &\leq \left(\frac{I'_H}{I_H} - \frac{I'_m}{I_m} - b_H - s_L \frac{L^*}{A^*} - \beta_m I_H \right) (|Y(t)| \\ &\quad + |Z(t)|) + \frac{I_H}{I_m} \beta_m(1 - I_m)|X(t)|. \end{aligned}$$

Then we can obtain

$$D_+V(t) \leq \sup\{g_1(t), g_2(t)\}V(t), \quad (27)$$

where

$$\begin{aligned} g_1(t) &= -(2b_H + \beta_H I_m + \gamma) + \beta_H S_H(t) \frac{I_m(t)}{I_H(t)}, \\ g_2(t) &= \frac{I_H}{I_m} \beta_m(1 - I_m) + \frac{I'_H}{I_H} - \frac{I'_m}{I_m} - b_H - s_L \frac{L^*}{A^*} - \beta_m I_H. \end{aligned}$$

Rewriting the last two equations of [\(19\)](#) as:

$$\frac{I'_H}{I_H} + (\gamma + b_H) = \beta_H \frac{I_m}{I_H} S_H,$$

$$\frac{I'_m}{I_m} + s_L \frac{L^*}{A^*} = \beta_m \frac{I_H}{I_m} (1 - I_m),$$

then

$$g_1(t) = -(2b_H + \beta_H I_m + \gamma) + \frac{I'_H}{I_H} + (\gamma + b_H) = \frac{I'_H}{I_H} - (b_H + \beta_H I_m),$$

$$\begin{aligned} g_2(t) &= \frac{I_H}{I_m} \beta_m(1 - I_m) + \frac{I'_H}{I_H} - \frac{I'_m}{I_m} - b_H - \beta_m \frac{I_H}{I_m} (1 - I_m) - \beta_m I_H \\ &= \frac{I'_H}{I_H} - b_H - \beta_m I_H, \end{aligned}$$

we obtain

$$\begin{aligned} \sup\{g_1(t), g_2(t)\} &= \sup \left\{ \frac{I'_H}{I_H} - (b_H + \beta_H I_m), \frac{I'_H}{I_H} - b_H - \beta_m I_H \right\} \\ &\leq -b_H + \frac{I'_H}{I_H} \end{aligned}$$

and thus, from Eq. [\(27\)](#) and Gronwall's inequality, we obtain

$$V(t) \leq V(0)I_H(t)e^{-b_H t} \leq V(0)e^{-b_H t},$$

since $0 < I_H < 1$ in $\text{int}(\Omega)$, which implies that $V(t) \rightarrow 0$ as $t \rightarrow \infty$. By [\(24\)](#), it turns out that

$$(X(t), Y(t), Z(t)) \rightarrow 0 \text{ as } t \rightarrow \infty.$$

Therefore, system [\(23\)](#) is asymptotically stable and [Theorem 5.9](#) holds. \square

Theorem 5.11. Consider system [\(19\)](#). If $R_0 > 1$, then $\Omega - \{(S_H, 0, 0): 0 \leq S_H \leq 1\}$ is an asymptotic stability region for the endemic equilibrium with disease \mathcal{L}^* . Moreover all trajectories starting in the S_H -axis approach the disease-free equilibrium \mathcal{L}_0^* .

Proof. The first part of the theorem follows from the transversality of the vector field of [\(19\)](#) on $\Omega - \{(S_H, 0, 0): 0 \leq S_H \leq 1\}$ and theorem [\(5.5\)](#). The second part is proved by [Proposition 5.8](#). \square

The graphs shown, [Fig. 5\(a\)-\(b\)](#)–[Fig. 6\(a\)-\(b\)](#), were obtained after the numerical integration of system [\(7\)](#). In the numerical simulations b_H happen to be very small with respect to the other parameters, since the average expected life in humans is about 60 years, whereas the length of the infected period is a few days and the vector life expectancy is about 4–10 weeks.

Theorem 5.12. Assume $R_0 > 1$ and $b_H \ll 1$, then the solutions of system [\(19\)](#) oscillate to the endemic equilibrium with disease.

Proof. The existence of oscillations around the equilibrium \mathcal{L}^* depends on whether the characteristic equation, defined by the Jacobian matrix [\(5.2\)](#),

$$P(\lambda) = \lambda^3 + A\lambda^2 + B\lambda + C,$$

where

$$A = (b_H + \beta_H I_m^*) + (\gamma + b_H) + (d_m + \beta_m I_H^*),$$

$$B = (b_H + \beta_H I_m^*)(\gamma + b_H) + (b_H + \beta_H I_m^*)(d_m + \beta_m I_H^*)$$

$$+ (\gamma + b_H)(d_m + \beta_m I_H^*) - \beta_H S_H^* \beta_m (1 - I_m^*),$$

$$= (b_H + \beta_H I_m^*)(\gamma + b_H) + (b_H + \beta_H I_m^*)(d_m + \beta_m I_H^*)$$

$$+ (\gamma + b_H)\beta_m I_H^*,$$

$$C = (b_H + \beta_H I_m^*)(\gamma + b_H)(d_m + \beta_m I_H^*) + \beta_H S_H^* \beta_H I_m^* \beta_m (1 - I_m^*)$$

$$- (b_H + \beta_H I_m^*)\beta_H S_H^* \beta_m (1 - I_m^*)$$

$$= (\gamma + b_H)((b_H + \beta_H I_m^*)\beta_m I_H^* + \beta_H d_m I_m^*).$$

has eigenvalues with imaginary part different from zero. Recall that a polynomial of degree three has eigenvalues with imaginary part different from zero if the discriminant

$$\Delta = \frac{1}{4}q^2 + \frac{1}{27}p^3 \quad (28)$$

is bigger than zero, where

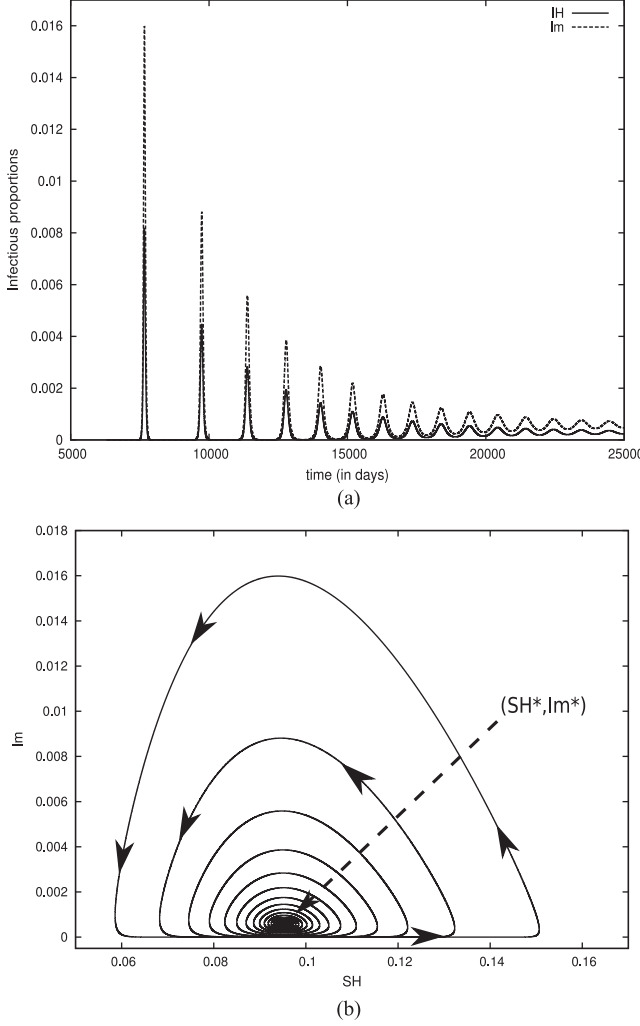


Fig. 5. Numerical solutions of model (7) (b)). The graphs (a) and (b) show the proportion of infective humans and infective vectors versus time and the phase portrait in the (S_H, I_m) plan. The parameters in the simulation are: $d_m = 0.25$, $b_H = 0.0000457$, $\beta_M = 0.5$, $\beta_H = 0.75$, $\gamma_H = 0.1428$ and then $R_0 = 10.500841$.

$$q = \frac{2}{27} A^3 - \frac{AB}{3} + C, \quad p = B - \frac{A^2}{3}.$$

We substitute I_H^* , I_m^* and R_0 in the coefficients A , B and C and expand them in Taylor series around $b_H = 0$. After some computations we obtain the following approximations,

$$\begin{aligned} A &= \gamma + d_m + \left(1 + \frac{\beta_m \beta_H}{d_m \gamma} + \frac{\beta_m}{\gamma} - \frac{d_m}{\beta_H}\right) b_H + \mathcal{O}(b_H^2), \\ B &= \left(\left(\gamma + d_m\right) \frac{\beta_m \beta_H}{d_m \gamma} + \beta_m - \frac{d_m \gamma}{\beta_H}\right) b_H + \mathcal{O}(b_H^2), \\ C &= (\beta_H \beta_m - d_m \gamma) b_H + \mathcal{O}(b_H^2). \end{aligned}$$

On the other hand, in terms of the coefficients A , B and C in Eq. (28), and collecting terms $\mathcal{O}(b_H^2)$, we get,

$$\Delta = \frac{1}{27} (\gamma + d_m)^3 (\beta_H \beta_m - \gamma d_m) b_H + \mathcal{O}(b_H^2).$$

The term $\beta_H \beta_m - \gamma d_m$ is positive since $R_0 > 1$, therefore

$$\lim_{b_H \rightarrow 0} \frac{\Delta}{b_H} > 0,$$

which implies that for b_H sufficiently small and positive, $\Delta > 0$. This prove the theorem (this result is similar to that one given in [13]). \square

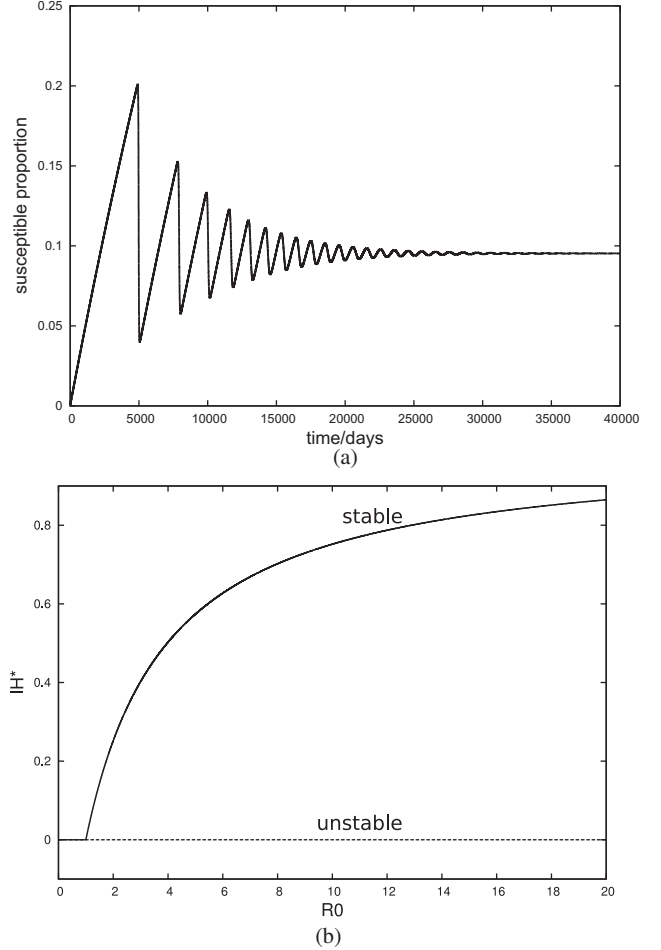


Fig. 6. (a) proportion of susceptible humans versus time (in days). (b) bifurcation diagram for equilibria of model (19) with respect to R_0 . For $R_0 > 1$ we plot the proportion of infective humans I_H^* given in Eq. (16), and we fix the parameters $b_H = 0.0000457$, $\beta_M = 0.9$, $\beta_H = 0.9$, $\gamma_H = 0.1428$, $d_m = 0.25$.

Next, we analyze the asymptotic behavior of the total population $N_H(t)$, and the total number of individuals in the epidemiological classes \bar{S}_H , \bar{I}_H and \bar{R}_H . For this we introduce the following parameters

$$R = \frac{\beta_H \beta_m}{d_m (\gamma + d_H)}$$

and

$$R_1 = R.S_H^*(1 - I_m^*) = \begin{cases} R, & \text{if } R_0 \leq 1, \\ \frac{\gamma + b_H}{\gamma + d_H}, & \text{if } R_0 > 1. \end{cases}$$

First we study the dynamics of solutions whose initial conditions are outside the subspace $\bar{I}_H = \bar{I}_m = 0$. For $R_0 \neq 1$ we have the following results.

Proposition 5.13. For $b_H > d_H$, $(\bar{S}_H(t), \bar{I}_H(t), \bar{R}_H(t))$ tend, as $t \rightarrow \infty$, to $(\infty, 0, 0)$ if $R < 1$ and to (∞, ∞, ∞) if $(R_0 \leq 1 \text{ and } R > 1) \text{ or } (R_0 > 1)$.

Proof. Since $I_m^* \rightarrow 0$ and $s_L \frac{L}{A} \rightarrow d_m$ as $t \rightarrow \infty$, in the limit, the proportion of infectious mosquitoes is related to the proportion of infected humans as

$$I_m = \frac{\beta_m}{d_m} I_H (1 - I_m),$$

thus, the limit form of the equation for $\bar{I}_H(t)$ is given in system (6) by

$$\bar{I}'_H = \left(\frac{\beta_m \beta_H}{d_m} S_H (1 - I_m) - (\gamma + d_H) \right) \bar{I}_H = (\gamma + d_H)(R_1 - 1)\bar{I}_H,$$

which implies that $\bar{I}_H(t)$ declines exponentially if $R_1 < 1$, and grows exponentially if $R_1 > 1$. Moreover,

$$R_1 < 1 \iff R < 1$$

and

$$R_1 > 1 \iff (R_0 \leq 1 \text{ and } R > 1) \text{ or } (R_0 > 1).$$

The solution $\bar{R}_H(t)$ is given by

$$\bar{R}_H(t) = \bar{R}_{H_0}(t)e^{-d_H t} + e^{-d_H t} \gamma \int_0^t \bar{I}_H(s) e^{d_H s} ds.$$

From the exponential nature of $\bar{I}_H(t)$, it follows that $\bar{R}_H(t)$ declines exponentially if $R < 1$, and grows exponentially if $R_1 > 1$. \square

6. Conclusion

We have proposed models to describe the vector (*Aedes albopictus* mosquito) population dynamics and the chikungunya virus transmission to human population.

First of all, we have proposed model (2) to describe the vector population dynamics which takes into account auto-regulation phenomena of eggs and larvae stages. We have shown that this model is well defined. For this model we found that,

$$r = \left(\frac{b}{s+d} \right) \left(\frac{s}{s_L + d_L} \right) \left(\frac{s_L}{d_m} \right)$$

is the threshold condition for the existence of the endemic state, where $(\frac{b}{s+d})$, $(\frac{s}{s_L + d_L})$ and $(\frac{s_L}{d_m})$ are respectively eggs, larvae and adults growth rates. For $r > 1$, we proved, using a Lyapunov functional, that the endemic equilibrium is globally asymptotically stable.

Moreover, following [15], we have proposed model (7) to describe the virus transmission to the human population. This is a model with variable human population and the contact rate among humans depends on the vector population.

In the case $r > 1$ (the biological interesting case) we found the following threshold parameters:

$$R_0 = \frac{\beta_m \beta_H}{d_m(\gamma + b_H)},$$

$$R = \frac{\beta_m \beta_H}{d_m(\gamma + d_H)}$$

and

$$R_1 = \begin{cases} R, & \text{if } R_0 \leq 1, \\ \frac{\gamma + b_H}{\gamma + d_H}, & \text{if } R_0 > 1. \end{cases}$$

On the one hand, parameter R_0 is the threshold condition for the existence of endemic proportions of infected humans and infected mosquitoes. On the other hand, the basic reproduction number R_1 controls the asymptotic behavior of the number of infected humans.

For $b_H = d_H$, we have $R_0 = R$ and hence, $(\bar{S}_H(t), \bar{I}_H(t), \bar{R}_H(t))$ tend, as $t \rightarrow +\infty$, to $(N_H(0), 0, 0)$ if $R < 1$ and to $N_H(S_H^*, I_H^*, R_H^*)$ if $R > 1$, and this work complete [17] (global stability of the disease-free equilibrium and the endemic equilibrium with disease).

For $b_H > d_H$, $(\bar{S}_H(t), \bar{I}_H(t), \bar{R}_H(t))$ tend, as $t \rightarrow +\infty$, to $(+\infty, 0, 0)$ if $R < 1$ and to (∞, ∞, ∞) if $R_1 > 1$.

Before concluding about the possible actions to take to eradicate the disease, we formulate some remarks about proposed models.

- The infective proportion I_H and the total number of infective humans \bar{I}_H may have different behaviors. Thus, I_H may tend to zero and \bar{I}_H would grow exponentially (case $R_0 < 1 < R$).
- For proposed models, the dynamics of the vector does not depend directly on parameters K_E and K_L . We have already pointed out that drying the breeding sites, and then reducing the carrying capacity K_L , has an impact on the parameters d_L and s . However, the size of the vector population depends on the carrying capacity, but the threshold parameter r does not and the proportion $\frac{L}{A}$ (whose expression is reduced to d_m) does not either. Otherwise, it would be the same for threshold parameters R_0 and R_1 .
- The use of the non classical incidence rate among humans leads to some simplifications on the threshold parameter R_0 (we obtain $\frac{A^*}{A^*}$ instead of $\frac{A}{N_H}$). That is another reason of its non-dependence on r, K_L and K_E .
- Our proposed models include models considering classical incidence rate with a constant human population. More precisely, for $b_H = d_H$, the model with a classical incidence rate among human population $(\frac{\beta_H \bar{S}_H \bar{I}_m}{N_H})$ leads to the system (7) where β_H have to be replaced by $\beta_H \frac{A(t)}{N_H}$. As $A(t)$ tends to A^* for $t \rightarrow +\infty$, exactly the same calculations can be made (by substituting β_H by $\beta_H \frac{A^*}{N_H}$) and we obtain the following threshold parameter

$$R_0 = \frac{\beta_m \beta_H}{d_m(\gamma + b_H)} \frac{A^*}{N_H} (= R) \\ = \frac{\beta_m \beta_H}{d_m(\gamma + b_H)} \frac{1}{N_H} \left(1 - \frac{1}{r} \right) \frac{s K_E s_L K_L}{d_m(s K_E + (s_L + d_L) K_L)},$$

which controls the global stability of equilibria. The same approach can be applied to show the global stability of the endemic equilibrium with disease for models in [18] if we consider no influence of the disease on the death rate for vector population.

Following these models and the previous remarks, the eradication of the disease can be achieved if the mosquito population is eradicated or if parameter R is lowered below unity.

Threshold parameter r may provide conditions in order to control the proliferation of the mosquito population. Indeed, even if there is no chikungunya epidemic, we need to be vigilant since in less than 20 years *Aedes albopictus* has developed capabilities to adapt to non tropical regions. That is why several measures have been applied in Europe in order to control the mosquito proliferation. One of the possible interventions to reduce the impact of the epidemic would be to reduce the number of mosquitoes. In this aim we have to focus on some parameters that human intervention can easily control. For instance chemical intervention can reduce the threshold parameter r : chemical aldicarb increases the mortality rate of mosquitoes d_m and chemical larvicide increases the death rate of the larvae d_L . Nevertheless, such intervention has fatal consequences, in particular on the environment. Moreover, the vector can develop a resistance to some insecticides that reduce the impact of chemical interventions. That is why, other method of control must be considered. For instance, the reduction of the number of breeding sites, by drying them, has a double impact. First, it reduces the transfer rate s between the eggs compartment and the immature stage: if there is no water, eggs cannot hatch. Second, it increases the death rate d_L of the immature stage: water is necessary for the development of the immature stage. Note that drying the breeding sites has little impact on d , the death rate of eggs, because they are resistant to desiccation. Another example is the introduction of sterile male mosquitoes in the population (see [46]) that has an incidence on the egg-laying. These interventions allow reducing the birth rate b and then the threshold r , and thus control the mosquitoes proliferation.

In case of an epidemic, we have to reduce the parameter R . Clearly, chemical adulticide can be used to increase the death rate d_m of the vector with its bad consequences on the environment. Moreover, all efforts made by the human population, like the use of mosquito nets or repulsive against mosquitoes bites, wearing appropriate clothes, or isolating infected patients in hospitals, will reduce the contact rates β_h and β_m without the disadvantages of the chemical adulticide. All these efforts and interventions can be formulated in terms of an optimal control problem [47].

However, if we want to eradicate the disease just by controlling the vector population, models with non-classical incidence rate lead necessary to eradicate the vector population while models with a classical incidence rate require only to reduce it. In the case of a classical incidence rate, all measures cited previously (drying the breeding sites, larvicide) impact on K_E , K_L , s , d_L and hence R .

Acknowledgments

This research is supported by region “Haute-Normandie”, France. The authors would like to thank the editors and the anonymous referees for their careful reading and very valuable comments that improved the presentation of this paper.

References

- [1] W.A. Hawley, The biology of *Aedes albopictus*, *J. Amer. Mosq. Control Assoc. Suppl.* 1 (1988) 1.
- [2] S. Christopher, The Yellow fever mosquito. Its Life History, Bionomics and Structure, 1960.
- [3] J.M. Medlock, D. Avenell, I. Barratt, S. Leach, Analysis of the potential for survival and seasonal activity of *Aedes albopictus* (Diptera: Culicidae) in the United Kingdom, *J. Vector Ecol.* 31 (2) (2006) 292.
- [4] M.C. Robinson, An epidemic of virus disease in Southern province, Tanganyika territory, in 1952–1953. I Clinical features, *Transactions of the Royal Society of Tropical Medicine and Hygiene* 49 (1) (1955) 28.
- [5] W.H.R. Lumsden, An epidemic of virus disease in Southern province, Tanganyika territory, in 1952–1953. II General description and epidemiology, *Transactions of the Royal Society of Tropical Medicine and Hygiene* 49 (1) (1955) 23.
- [6] H. Hethcote, The mathematics of infectious diseases, *SIAM Rev.* 42 (2000) 599.
- [7] O. Diekmann, J.A.P. Heesterbeek, Mathematical Epidemiology of Infectious Diseases: Model Building, Analysis and Interpretation, first ed., Wiley, 2000.
- [8] P. vanden Driessche, J. Watmough, Reproduction numbers and sub-threshold endemic equilibria for compartmental models of disease transmission, *Math. Biosci.* 180 (2002) 29.
- [9] Z. Feng, V. Hernandez, Competitive exclusion in a vector-host model for the dengue fever, *Journal of Mathematical Biology* 35 (1997) 523.
- [10] G. Ngwa, W. Shu, A mathematical model for endemic malaria with variable human and mosquito population, *Mathematical and Computer Modelling* 32 (2000) 747.
- [11] A. Tran, M. Raffy, On the dynamics of dengue epidemics from large-scale information, *Theoretical Population Biology* 69 (2006) 3.
- [12] Y. Dumont, F. Chiroleu, C. Domerg, On a temporal model for the Chikungunya disease: Modeling, theory and numerics, *Mathematical Biosciences* 213 (1) (2008) 80.
- [13] L. Esteva, C. Vargas, Analysis of a dengue disease transmission model, *Math. Biosci.* 150 (2) (1998) 131.
- [14] M. Derouich, A. Boutayeb, E. Twizell, A model of dengue fever, *BioMedical Engineering* 2 (1) (2003) 4.
- [15] L. Esteva, C. Vargas, A model for dengue disease with variable human population, *Journal of Mathematical Biology* 38 (3) (1999) 220.
- [16] M. Derouich, A. Boutayeb, Dengue fever: Mathematical modelling and computer simulation, *Applied Mathematics and Computation* 177 (2) (2006) 528.
- [17] H.M. Yang, C.P. Ferreira, Assessing the effects of vector control on dengue transmission, *Applied Mathematics and Computation* 198 (1) (2008) 401.
- [18] Y. Dumont, F. Chiroleu, Vector control for the Chikungunya disease, *Mathematical Biosciences and Engineering* 7 (2010) 313.
- [19] H. Delatte, G. Gimmonneau, A. Triboire, D. Fontenille, Influence of temperature on immature development, survival, longevity, fecundity, and gonotrophic cycles of *Aedes albopictus*, vector of chikungunya and dengue in the Indian Ocean, *J. Med. Entomol.* 46 (2009) 33–41.
- [20] F. Amerasinghe, T. Alagoda, Mosquito oviposition in bamboo traps, with special reference to *Aedes albopictus*, *Aedes vexans*, and *Armigeres subalbatus*, *Insect Sci. Appl.* 5 (1984) 493.
- [21] F. Pages, V. Corbel, C. Paupy, Chronique d'un vecteur expansionniste, *MTdecine tropicale* 66 (3) (2006) 226.
- [22] <<http://moustiquesinfos.sante.gouv.fr>>, 2010.
- [23] C. Paupy, H. Delatte, L. Bagny, V. Corbel, D. Fontenille, *Aedes albopictus*, an arbovirus vector: from the darkness to the light, *Microbes Infect.* 11 (14–15) (2009) 1177.
- [24] T. Sota, M. Mogi, Survival time and resistance to desiccation of diapause and non-diapause eggs of temperate *Aedes* (*Stegomyia*) mosquitoes, *Entomologia Experimentalis et Applicata* 63 (1992) 155.
- [25] <<http://www.cg06.fr/fr/servir-les-habitants/action-medicaile-sociale/votre-sante/lutte-contre-le-moustique-aedes-albopictus/lutte-contre-l->>.
- [26] R.A. Erickson, S.M. Presley, L.J. Allen, K.R. Long, S.B. Cox, A stage-structured, *Aedes albopictus* population model, *Ecol. Model.* 221 (9) (2010) 1273.
- [27] S. Juliano, Population dynamics, *AMCA Bull.* 7 (2007) 265.
- [28] H. Dieng, R. Saifur, A. Hassan, M. Salmah, M. Boots, T. Satho, Z. Jaal, S. AbuBakar, Indoor-Breeding of *Aedes albopictus* in Northern Peninsular Malaysia and its potential epidemiological implications, *PLoS ONE* 5 (7) (2010) e11790.
- [29] W. Foster, Mosquito sugar feeding and reproductive energetics, *Ann. Rev. Entomol.* 40 (1) (1995) 443.
- [30] R. Novak, The asian tiger mosquito, *Aedes albopictus*, *Wing Beats* 3 (5) (1992) 1.
- [31] R. Eritja, R. Escosa, J. Lucientes, E. Marques, D. Roiz, S. Ruiz, Worldwide invasion of vector mosquitoes: present European distribution and challenges for Spain, *Biol. Invasions* 7 (1) (2005) 87.
- [32] M.H. Reiskind, L.P. Lounibos, Effects of intraspecific larval competition on adult longevity in the mosquitoes *Aedes aegypti* and *Aedes albopictus*, *Med. Vet. Entomol.* 23 (1) (2009) 62.
- [33] M. Dubrulle, L. Mousson, S. Moutailler, M. Vazeille, A. Failloux, Chikungunya virus and *Aedes* mosquitoes: saliva is infectious as soon as two days after oral infection, *PLoS ONE* 4 (6) (2009) e5895.
- [34] J.X. Velasco-Hernández, A model for chagas disease involving transmission by vectors and blood transfusion, *Theor. Popul. Biol.* 46 (1) (1994) 1.
- [35] D. Moulay, M. Aziz-Alaoui, Analysis of a delayed model for the Chikungunya disease, in preparation.
- [36] H. Thieme, Convergence results and a Poincaré Bendixson trichotomy for asymptotically autonomous differential equations, *J. Math. Biol.* 30 (7) (1992) 755.
- [37] J. Zhang, Z. Ma, Global dynamics of an SEIR epidemic model with saturating contact rate, *Math. Biosci.* 185 (1) (2003) 15.
- [38] M.Y. Li, J.S. Muldowney, Global stability for the SEIR model in epidemiology, *Math. Biosci.* 125 (2) (1995) 155.
- [39] H.L. Smith, Systems of ordinary differential equations which generate an order preserving flow. A survey of results, *SIAM Rev.* 30 (1) (1988) 87.
- [40] H.L. Smith, Monotone Dynamical Systems: An Introduction to the Theory of Competitive and Cooperative Systems, American Mathematical Society, 1995.
- [41] J.K. Hale, Ordinary Differential Equations, Wiley Inter-science, 1969.
- [42] G. Butler, H. Freedman, P. Waltman, Uniformly persistent systems, *Proc. Amer. Math. Soc.* 96 (3) (1986).
- [43] J.S. Muldowney, Compound matrices and ordinary differential equations, *Rocky Mount. J. Math.* 20 (4) (1990) 857.
- [44] R. Martin Jr, Logarithmic norms and projections applied to linear differential systems, *J. Math. Anal. Appl.* 45 (1974) 432.
- [45] J.S. Muldowney, Dichotomies and asymptotic behaviour for linear differential systems, *Trans. Amer. Math. Soc.* 283 (1984) 465.
- [46] L. Esteva, H.M. Yang, Mathematical model to assess the control of *Aedes aegypti* mosquitoes by the sterile insect technique, *Math. Biosci.* 198 (2005) 132.
- [47] D. Moulay, M.A. Aziz-Alaoui, H.-D. Kwon, Optimal control of Chikungunya disease: Larvae reduction, treatment and prevention, submitted for publication.

OPTIMAL CONTROL OF CHIKUNGUNYA DISEASE: LARVAE REDUCTION, TREATMENT AND PREVENTION

DJAMILA MOULAY

LMAH, Université du Havre, 25 rue Philippe Lebon
BP540, 76058 Le Havre Cedex, France

M. A. AZIZ-ALAOUI

LMAH, Université du Havre, 25 rue Philippe Lebon
BP540, 76058 Le Havre Cedex, France

HEE-DAE KWON

Departement of Mathematics, Inha University, Incheon
402-751, Republic of Korea

(Communicated by H. T. Banks)

ABSTRACT. Since the 1980s, there has been a worldwide re-emergence of vector-borne diseases including Malaria, Dengue, Yellow fever or, more recently, chikungunya. These viruses are arthropod-borne viruses (arboviruses) transmitted by arthropods like mosquitoes of *Aedes* genus. The nature of these arboviruses is complex since it conjugates human, environmental, biological and geographical factors. Recent researchs have suggested, in particular during the Réunion Island epidemic in 2006, that the transmission by *Aedes albopictus* (an *Aedes* genus specie) has been facilitated by genetic mutations of the virus and the vector capacity to adapt to non tropical regions. In this paper we formulate an optimal control problem, based on biological observations. Three main efforts are considered in order to limit the virus transmission. Indeed, there is no vaccine nor specific treatment against chikungunya, that is why the main measures to limit the impact of such epidemic have to be considered. Therefore, we look at time dependent breeding sites destruction, prevention and treatment efforts, for which optimal control theory is applied. Using analytical and numerical techniques, it is shown that there exist cost effective control efforts.

1. Introduction. The chikungunya virus, is an arthropod-borne virus (arbovirus) transmitted by mosquitoes of *Aedes* genus. The chikungunya term, used for both the virus and the disease comes from the Makonde Plateau language in Tanzania, where the virus was first identified in 1953 [31, 39]. It means "that which bends up" in reference to symptoms observed on affected people, like cardiovascular manifestation and fever [37]. The mosquito responsible of this first epidemic is the *Aedes aegypti* [40]. This mosquito is most known for being the main vector of the dengue

2000 *Mathematics Subject Classification.* Primary: 58F15, 58F17; Secondary: 53C35.

Key words and phrases. Optimal control, vector-borne disease, chikungunya, *Aedes albopictus*.

The work of D. Moulay and M.A. Aziz-Alaoui is supported in part by region *Haute-Normandie*, France.

The work of Hee-Dae Kwon was supported in part by the Korea Research Foundation Grant funded by the Korean Government (KRF-2008-314-C00043) and in part by the Korea Research Foundation Grant funded by the Korean Government (KRF-2008-331-C00053).

fever [25], the most rapidly spreading mosquito-borne viral disease in the world. Indeed, in the last 50 years, the incidence of this virus has increased with increasing geographic expansion to new countries, and in the last decades, from urban to rural settings. Moreover, approximately one billion people live in dengue endemic countries and annually, an estimated 50 million dengue infections occur [47]. Like dengue epidemic, which is a major public health problem in several countries, chikungunya appears also to be one of the most important vector-borne disease.

Many factors have influenced the resurgence of such vector-borne diseases like the increase of travel and exchanges [9] or the development of insecticide and drug resistance [4]. Studies have suggested that human activities help carrying eggs on eventually long distances whereas once hatched a mosquito may not have a perimeter wider than 200 meters. This means that people, rather than mosquitoes, rapidly help the spread of the virus within and between communities. Nevertheless, each of these species has a particular ecological behaviour and geographical distribution.

In the fifties, various outbreaks of chikungunya have been observed like in Thailand (1960s and 1995) [29], or in Senegal (1972 to 1986)[15]. After a break of twenty years, severals epidemics have been reported in India [44, 41], in Europe, or in the Indian Ocean Islands like in Mayotte, Comoros archipelago [42], or in the Réunion Island [43]. In the last one, one third of the total population has been infected by this virus in 2006.

Usually transmitted by *Aedes aegypti*, it has been observed during recent epidemics that the virus is additionally transmitted by *Aedes albopictus* [26], also called Asian tiger mosquito and native from Southeast Asia [27]. Indeed, the *Aedes aegypti* mosquito is a tropical and a subtropical specie widely distributed around the world, while the *Aedes albopictus* has developed capabilities to adapt to non tropical regions. The chikungunya used to be localized in tropical regions but, nowadays, because of climate changes that create suitable conditions for outbreaks of diseases, they slowly start to spread all over the world, Europe included where the *Aedes albopictus* mosquito is also present since a long time. For instance, an outbreak of chikungunya occurred in the Emilia Romagna region, in Italy [14, 38, 46], in 2007, with 254 cases of infection. It was the first case of chikungunya transmission within Europe.

Moreover, recent research [21] suggested that in the case of the Réunion Island epidemic, the transmission by *Aedes albopictus* has been facilitated by genetic mutations of the virus. Indeed, during the recent outbreaks reported in the Indian ocean island, the identified chikungunya virus was characterized by a genetic mutation in the E1 glycoprotein gene (E1-226V). This mutation allowed the virus to be present in the mosquito saliva only two days after the infection, instead of approximately seven days [18]. This greatly helped the transmission by *Aedes albopictus*. Moreover this mosquito is present in several parts of the world, like in Albania [3], Spain [10], USA and Australia [7].

Unfortunately, this disease has no specific treatment nor vaccine, that is why preventing or reducing chikungunya virus transmission depends mainly on control of the mosquito vectors or interruption of human-vector contact. Actions focus on individual protection against mosquito bites, symptomatic treatment of patients and mosquito proliferation control. For instance, the number of breeding sites are reduced by eliminating container habitats that are favorable oviposition sites and that permit the development of aquatic stages. Indeed, the *Aedes albopictus* female

lays its eggs in wet places adjacent to the surface of water in all sorts of receptacles: vases, rainwater barrels, used tyres, *etc.* Moreover, as winter approaches, eggs may enter a diapause, that is to say the progression from egg to adult is interrupted by a period of dormancy [24]. In this stage, eggs are resistant to cold climates and droughts, and can wait until next spring to hatch. This diapause may explain the adaptation of the mosquito to temperate climate [34, 32].

Recently, a number of studies have been conducted to explore optimal control theory in some mathematical models for infectious diseases including HIV diseases [2, 1], tuberculosis [28] and vector-borne diseases [8]. Authors in [8] derive the optimal control efforts for treatment and prevention in order to prevent the spread of a vector-borne disease using a system of ordinary differential equations (ODEs) for the host and vector populations. In our effort, we investigate such optimal strategies for prevention, treatment and vector control using two systems of ODEs which consist of a stage structure model for the vector and a SI/SIR type model for the vector/host population.

In this paper, using models described in [33] for the mosquito population dynamics and the transmission virus, we formulate the associated control model in order to derive optimal prevention and treatment strategies with minimal implementation cost. Controls used here are based on three main actions applied in the recent epidemics.

The paper is organized as follows. In section 2, we present the compartmental model used in [33] to describe the *Aedes albopictus* population dynamics and the chikungunya virus transmission to the human population.

In section 3, we formulate an optimal control problem; first, we investigate the existence of an optimal control, then we derive the optimality system which characterizes the optimal control using Pontryagin's Maximum Principle [36]. In section 4 numerical results illustrate our theoretical results.

2. The basic model. We have proposed two models [33] to describe the population dynamics of the *Aedes albopictus* mosquito population and the transmission of the virus to human population. For the reader convenience, we briefly recall here main results which are developed in this work.

i. The vector population is described by a stage-structured model based on the biological life cycle. It consists in four main stages described by the following compartment: egg (E), larvae and pupae (L) which are biologically very closed stages, and the adult stage (A) which contains only females because they are responsible for the transmission. The density variation of each stage is easily done by making the input-output balance in each evolution stage. The *per capita* mortality rate of eggs, larvae and adults are denoted by d , d_L and d_m respectively. The net oviposition rate per female insect is proportional to their density, but it is also regulated by a carrying capacity effect depending on the occupation of the available breeder sites. Moreover, it has been observed that females are able to detect the best breeding sites for the egg development, that is to say breeding sites where eggs and then larvae will be able to develop easily. Thus, in this model, we assume that the *per capita* oviposition rate is also proportional to the number of females and given by $bA(t)(1 - E(t)/K_E)$, where K_E is the carrying capacity related to the amount of available nutrients and space, and b is the intrinsic oviposition rate. The egg population becomes larvae at a *per capita* transfer rate s and the larvae population becomes mosquito female at a *per capita* rate s_L . In addition to the transfer rate

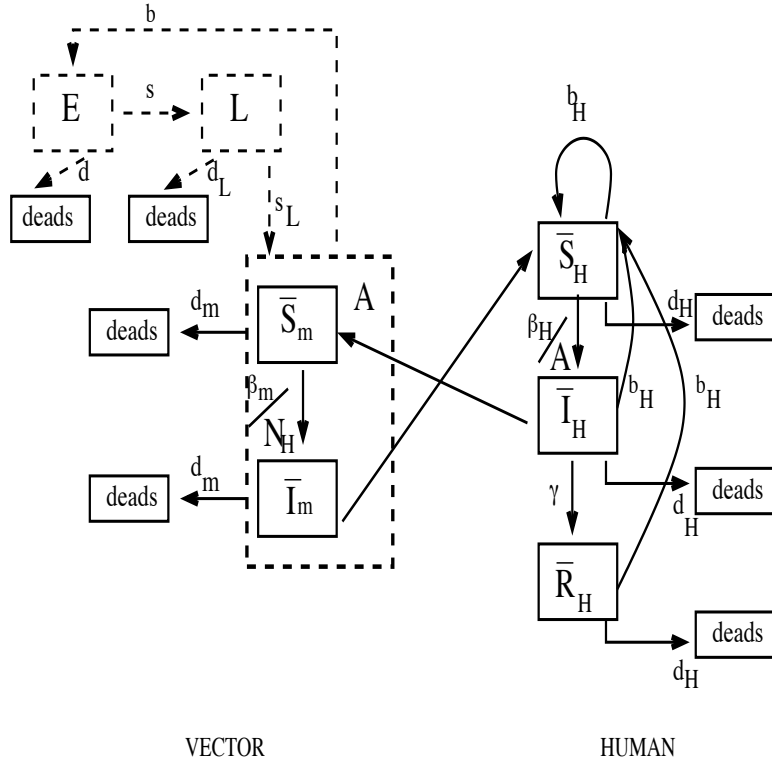


FIGURE 1. Transmission diagram. Coupling of a stage structured model for *Aedes albopictus* population dynamics (dashed line) and a compartmental model describing the transmission of the virus between adult mosquito and human population.

s , the flows from eggs to larvae is regulated by a carrying capacity K_L due to the intra-specific competition with young larvae. Thus the number of new larvae is given by $sE(t)(1 - L(t)/K_L)$. All this hypothesis may be summarize in figure (1) (dashed line) which describes the input-output of each mosquito stages. Therefore, the mosquito population dynamics is described by:

$$\begin{cases} \frac{dE}{dt}(t) = bA(t) \left(1 - \frac{E(t)}{K_E}\right) - (s + d)E(t) \\ \frac{dL}{dt}(t) = sE(t) \left(1 - \frac{L(t)}{K_L}\right) - (s_L + d_L)L(t) \\ \frac{dA}{dt}(t) = s_L L(t) - d_m A(t) \end{cases} \quad (1)$$

This system is defined on the bounded subset of \mathbb{R}^3 ,

$$\Delta = \left\{ (E, L, A) \mid \begin{array}{l} 0 \leq E \leq K_E \\ 0 \leq L \leq K_L \\ 0 \leq A \leq \frac{s_L}{d_m} K_L \end{array} \right\} \quad (2)$$

Let us introduce the following threshold parameter:

$$r = \frac{b}{s + d} \frac{s}{s_L + d_L} \frac{s_L}{d_m}$$

which, as we will see, governs the asymptotic behavior of the mosquito population.

Theorem 2.1.

- System (1) always has the mosquito free equilibrium $X_0^* = (0, 0, 0)$ which is globally asymptotically stable iff $r \leq 1$.
- If $r > 1$, there is a unique non-trivial equilibrium, which is globally asymptotically stable and given by

$$X^* = \left(1 - \frac{1}{r}\right) \left(\frac{K_E}{\gamma_E}; \frac{K_L}{\gamma_L}; \frac{s_L}{d_m} \frac{K_L}{\gamma_L}\right)^T = (E^*; L^*; A^*),$$

where

$$\gamma_E = 1 + \frac{(s+d)d_m K_E}{bs_L K_L} \quad \text{and} \quad \gamma_L = 1 + \frac{(s_L+d_L)K_L}{s K_E}.$$

Proof. The global stability of both equilibrium points is given using Lyapunov function theory. This function is obtained by the construction of a symmetric matrix. The detailed proof is given in [33]. \square

Then, by the previous theorem, we observe that the mosquito population may have two different behaviors. All populations may die out if the threshold parameter r is less than one or tends to an endemic equilibrium which corresponds to the coexistence of species.

ii. The second model uses SI and SIR schemes, which are ordinary differential equations describing the numbers of susceptible, infective and recovered individuals during an epidemic. Indeed, the adult mosquito population (A) is described thanks to a SI model, because an infected vector remains infective until its death, whereas human population is described by an SIR model.

With respect to the circulation of chikungunya virus among adults mosquitoes, they are sub-divided into susceptible (\bar{S}_m) and infectious (\bar{I}_m). The total size of the population is $A = \bar{S}_m + \bar{I}_m$, where A is given previously in system (1). The chikungunya infection occurs when susceptible mosquitoes (\bar{S}_m) are infected during the blood meal from infectious humans (\bar{I}_H). The *per capita* incidence rate among mosquitoes $\beta_m \frac{\bar{I}_H}{N_H}$ depends on the fraction of infectious humans $\frac{\bar{I}_H}{N_H}$, where N_H is the total human population size. This rate takes into account the encounters between susceptible mosquitoes and infectious humans, given by the contact rate β_m , which is related to the frequency of bites. We assume that the mortality rates related to susceptible and infectious mosquitoes are equals and given by d_m . Biological observations allow us to assume that there is no vertical transmission, *i.e.* all new births are susceptible and after recovering, humans become immune.

The chikungunya infection among humans occurs when susceptible individuals \bar{S}_H are bitten by infectious mosquitoes \bar{I}_m during the blood meal. The *per capita* incidence rate among susceptible humans depends on the fraction of infectious mosquitoes $\frac{\bar{I}_m}{A}$ and takes into account the encounters between susceptible humans and infectious mosquitoes, designed by β_H . These infected individuals enter in the recovered class (\bar{R}_H) at a constant rate γ_H . Moreover we assume that N_H is constant, *i.e.* $b_H = d_H$. Then the hypothesis leads to the following virus transmission model:

$$\left\{ \begin{array}{l} \frac{d\bar{S}_H}{dt}(t) = b_H N_H - \beta_H \frac{\bar{I}_m(t)}{A(t)} \bar{S}_H(t) - d_H \bar{S}_H(t) \\ \frac{d\bar{I}_H}{dt}(t) = \beta_H \frac{\bar{I}_m(t)}{A(t)} \bar{S}_H(t) - \gamma \bar{I}_H(t) - d_H \bar{I}_H(t) \\ \frac{d\bar{R}_H}{dt}(t) = \gamma \bar{I}_H(t) - d_H \bar{R}_H(t) \\ \frac{d\bar{S}_m}{dt}(t) = s_L L(t) - d_m \bar{S}_m(t) - \beta_m \frac{\bar{I}_H(t)}{N_H} \bar{S}_m(t) \\ \frac{d\bar{I}_m}{dt}(t) = \beta_m \frac{\bar{I}_H(t)}{N_H} \bar{S}_m(t) - d_m \bar{I}_m(t). \end{array} \right. \quad (3)$$

System (3) is defined on the bounded subset of \mathbb{R}^5 ,

$$\left\{ (\bar{S}_H, \bar{I}_H, \bar{R}_H, \bar{S}_m, \bar{I}_m) \mid \begin{array}{l} \bar{S}_H + \bar{I}_H + \bar{R}_H = N_H, \\ \bar{S}_m + \bar{I}_m = A \end{array} \right\},$$

where A corresponds to the female adult mosquito stage of system (1) and is bounded by $\frac{s_L}{d_m} K_L$.

Introducing proportions $S_H = \bar{S}_H/N_H$, $I_H = \bar{I}_H/N_H$, $R_H = \bar{R}_H/N_H$, $S_m = \bar{S}_m/A$, $I_m = \bar{I}_m/A$ in system (3) by using relations $\bar{S}_H + \bar{I}_H + \bar{R}_H = N_H$ and $\bar{S}_m + \bar{I}_m = A$ and the derivative $dS_H/dt = (d\bar{S}_H/dt)(1/N_H)$, $dI_H/dt = (d\bar{I}_H/dt)(1/N_H)$ and $dI_m/dt = (1/A^2)((d\bar{I}_m/dt)A - \bar{I}_m(dA/dt))$, we obtain the following system,

$$\left\{ \begin{array}{l} \frac{dS_H}{dt}(t) = -(b_H + \beta_H I_m(t)) S_H(t) + b_H \\ \frac{dI_H}{dt}(t) = \beta_H I_m(t) S_H(t) - (\gamma + b_H) I_H(t) \\ \frac{dI_m}{dt}(t) = - \left(s_L \frac{L(t)}{A(t)} + \beta_m I_H(t) \right) I_m(t) + \beta_m I_H(t). \end{array} \right. \quad (4)$$

Remark 1. Due to this classical variable changes, mathematical study of system (3) may reduce to the study of (4).

Our transmission virus model including mosquito population dynamic is then given by:

$$\left\{ \begin{array}{l} \left\{ \begin{array}{l} \frac{dE}{dt}(t) = bA(t) \left(1 - \frac{E(t)}{K_E}\right) - (s + d)E(t) \\ \frac{dL}{dt}(t) = sE(t) \left(1 - \frac{L(t)}{K_L}\right) - (s_L + d_L)L(t) \\ \frac{dA}{dt}(t) = s_L L(t) - d_m A(t) \end{array} \right. \quad (a) \\ \left\{ \begin{array}{l} \frac{dS_H}{dt}(t) = -(b_H + \beta_H I_m(t)) S_H(t) + b_H \\ \frac{dI_H}{dt}(t) = \beta_H I_m(t) S_H(t) - (\gamma + b_H) I_H(t) \\ \frac{dI_m}{dt}(t) = -\left(s_L \frac{L(t)}{A(t)} + \beta_m I_H(t)\right) I_m(t) + \beta_m I_H(t). \end{array} \right. \quad (b) \end{array} \right. \quad (5)$$

defined on $\Delta \times \Omega$, where Δ is given by (2) and

$$\Omega = \left\{ (S_H, I_H, I_m) \in \mathbb{R}_+^3 \mid \begin{array}{l} 0 \leq S_H + I_H \leq 1 \\ 0 \leq I_m \leq 1 \end{array} \right\}. \quad (6)$$

Remark 2. Note that this system has two different time scales, since the subsystem (5a) describes the dynamics of our different mosquito stages, while the subsystem (5b) describes the dynamics of the proportion of susceptible and infected populations. In this paper we consider proportions rather than quantities in the proposed model. We believe it is more convenient for the reader since it refers more easily to the study proposed in [33]. A switch back to a system without densities is straightforward, thanks to the variable change proposed earlier. Besides, considering proportions allows us to use mathematical results on competitive theory for 3-dimensional systems and second compound matrix to study the global stability of the endemic equilibrium of subsystem (5b).

Let us introduce the following reproduction number [16, 17], which is defined as the average number of secondary infections produced by an infected individual in a completely susceptible population

$$R_0 = \frac{\beta_m \beta_H}{d_m(\gamma + b_H)}. \quad (7)$$

Theorem 2.2. Assume that $r > 1$.

- System (4) always has the disease free equilibrium $N_0^* = (1, 0, 0)$ which is globally asymptotically stable iff $R_0 \leq 1$.
- If $R_0 > 1$, there is a unique globally asymptotically stable endemic equilibrium given by

$$N^* = \begin{pmatrix} \frac{b_H}{\beta_H + b_H} + \frac{\beta_H}{(\beta_H + b_H)R_0} \\ \frac{d_m b_H}{\beta_m (\beta_H + b_H)} (R_0 - 1) \\ \frac{b_H}{\beta_H + b_H R_0} (R_0 - 1) \end{pmatrix} = \begin{pmatrix} S_H^* \\ I_H^* \\ I_m^* \end{pmatrix}.$$

Proof. We use Lyapunov function and competitive system theory. The detailed proof is given in [33]. \square

Remark 3. Note that in this model we have considered a non classical incidence rate among humans depending on the total vector population (as in [22, 48]). A simple variable change allows us to consider a classical incidence rate substituting β_H by $\beta_H \frac{A(t)}{N_H}$ in system (3). The second reproduction number is then given by:

$$\begin{aligned} R_0 &= \frac{\beta_m \beta_H}{d_m(\gamma + b_H)} \frac{A^*}{N_H} \\ &= \frac{\beta_m \beta_H}{d_m(\gamma + b_H)} \frac{1}{N_h} \left(1 - \frac{1}{r}\right) \frac{s K_E s_L K_L}{d_m(s K_E + (s_L + d_L) K_L)}. \end{aligned}$$

Biological and modeling details of the previous model and a study of the asymptotic dynamics are given in [33].

3. A model for optimal control. There are several possible interventions in order to reduce or limit the proliferation of mosquitoes and the explosion of the number of infected people.

Using previous models (1) and (4), we formulate the associated control model in order to derive optimal prevention and treatment strategies with minimal implementation cost. Controls used here are based on effective actions applied in the recent epidemics.

- The first control u_1 represents efforts made for prevention on a time interval $[0, T]$. It mainly consists in reducing the number of vector-host contacts due to the use of repulsive against adult mosquitoes and protection with mosquito nets or wearing appropriate clothing. Indeed *Aedes albopictus* has a peak of activity during fresh temperatures, early in the morning and late in the afternoon.
- The second control u_2 represents efforts made for treatment on a time interval $[0, T]$. It mainly consists in isolating infected patients in hospitals, installing an anti-mosquito electric diffuser in the hospital room, or symptomatic treatments. Because, there are no vaccine nor completely satisfying drug to treat all symptoms [11], which can persist several months after the infection [35], the vector control remains a major tool to prevent and control the illness.

More precisely, only symptomatic treatments are used in order to alleviate the symptoms. Their efficacy varies from one person to another, using for instance corticosteroids, paracetamol and non-steroidal anti-inflammatory drugs.

- Finally the third control u_3 represents the effect of interventions used for the vector control. It mainly consists in the reduction of breeding sites with chemical application methods, for instance using larvicides like BTI (*Bacillus Thuringiensis Israensis*) which is a biological larvicide, or by introducing larvivore fish. This control focuses on the reduction of the number of larvae, and thus eggs, of any natural or artificial water-filled container. Moreover, in France, one other type of intervention is the use of traps. This consists in using simple black buckets (black colour is recognized as being attractive), with a capacity of one liter of water, three-quarters full with tannic water (water macerated for 3 days with dead branches and leaves). This traps contain laying sites (little plates of square extruded polystyrene placed on the surface of the water [5]. Finally tablets of bio-insecticide (Dimilin) are introduced in the traps in order to neutralise the potential development of larvae.

We will not consider the use of Deltamethrin, a chemical adulticide, because it has a negative effect on the environment. Moreover the sensitiveness to this adulticide depends on the area, for instance in Martinique Island, a French department, 60% of *Aedes* population have rapidly developed a resistance to Deltamethrin. Let us remark that we have not converted this control by a reduction of eggs and larvae carrying capacity. Indeed, while it is possible to reduce the number of artificial breeding sites, the only possibility to reduce natural ones is to dry them rather than to destroy them. This solution is of course not realistic. Moreover, even if artificial breeding sites are man-made, it is impossible to inventory them all because they are often temporary or random.

Another approach using a biological control consists in the introduction of sterile insects [45]. This method allows to reduce the number of mosquitoes thanks to a decrease of the oviposition rate.

Therefore, our transmission and optimal control model of chikungunya disease reads as

$$\left\{ \begin{array}{l} \frac{dE}{dt}(t) = bA(t) \left(1 - \frac{E(t)}{K_E} \right) - (s + d + \varepsilon u_3(t))E(t) \\ \frac{dL}{dt}(t) = sE(t) \left(1 - \frac{L(t)}{K_L} \right) - (s_L + d_L)L(t) - d_c u_3(t)L(t) \\ \frac{dA}{dt}(t) = s_L L(t) - d_m A(t) \\ \frac{dS_H}{dt}(t) = -(b_H + \beta_H(1 - u_1(t))I_m(t))S_H(t) + b_H \\ \frac{dI_H}{dt}(t) = \beta_H(1 - u_1(t))I_m(t)S_H(t) - (\gamma + \gamma_0 u_2(t) + b_H)I_H(t) \\ \frac{dI_m}{dt}(t) = -s_L \frac{L(t)}{A(t)} I_m(t) + \beta_m(1 - u_1(t))I_H(t)(1 - I_m(t)). \end{array} \right. \quad (8)$$

where $u_1 \in [0, 1]$ corresponds to prevention effort, thus if $u_1 = 1$ there is no contact between humans and mosquitoes and if $u_1 = 0$ the infection rate is maximal and equal to β_H or β_m ; $u_2 \in [0, 1]$ corresponds to the treatment effort and γ_0 is the proportion of effective treatment (thus $\gamma_0 u_2(t)$ is the *per capita* recovery rate induced by treatment); $u_3 \in [0, 1]$ corresponds to the reduction of the mosquito proliferation effort, and ε and d_c are eggs and larvae mortality rates induced by chemical intervention respectively.

Theorem 3.1. $\Delta \times \Omega$ is positively invariant under system (8).

Proof. On the one hand, one can easily see that it is possible to get,

$$\left\{ \begin{array}{l} \frac{dE}{dt} \geq -\left(\frac{b}{K_E} + s + d + \varepsilon\right)E \\ \frac{dL}{dt} \geq -\left(\frac{s}{K_L} + s_L + d_L + d_c\right)L \\ \frac{dA}{dt} \geq -d_mA \\ \frac{dS_H}{dt} \geq -(b_H + \beta_H)S_H \\ \frac{dI_H}{dt} \geq -(\gamma + \gamma_0 + b_H)I_H \\ \frac{dI_m}{dt} \geq -(s_L + \beta_m)I_m, \end{array} \right. \quad (9)$$

for $E_i(0), L_i(0), A_i(0), S_H(0), I_H(0), I_m(0) \geq (0)$. Thus, solutions with initial value in $\Delta \times \Omega$ remain nonnegative for all $t \geq 0$. On the other hand, we have

$$\left\{ \begin{array}{l} \frac{dE}{dt} \leq bA\left(1 - \frac{E}{K_E}\right) - (s + d)E \\ \frac{dL}{dt} \leq sE\left(1 - \frac{L}{K_L}\right) - (s_L + d_L)L \\ \frac{dA}{dt} \leq s_L L - d_mA \\ \frac{dS_H}{dt} \leq (b_H + \beta_H I_m)S_H + b_H \\ \frac{dI_H}{dt} \leq \beta_H I_m S_H - (\gamma + b_H)I_H \\ \frac{dI_m}{dt} \leq \left(s_L \frac{L}{A} + \beta_m I_H\right) I_m + \beta_m I_H. \end{array} \right. \quad (10)$$

The right hand side of the inequality corresponds to the transmission model without control (1) and (3) for which we have shown in [33] that solutions remain in $\Delta \times \Omega$. Then using Gronwall's inequality as before, we deduce that solutions of (8) are bounded. \square

Using system (8), we consider an optimal control problem with the objective (cost) functional given by

$$\begin{aligned} J(u_1, u_2, u_3) = & \\ \int_0^T (A_1 I_H(t) + A_2 I_m(t) + A_3 L(t) + B_1 u_1^2 + B_2 u_2^2 + B_3 u_3^2) dt. & \end{aligned} \quad (11)$$

The first three terms represent benefit of I_H , I_m and L populations. Positive constants B_1 , B_2 and B_3 are weight for prevention, treatment and vector control effort respectively, which regularize the optimal control. These costs are given in quadratic form as usually done in the literature. Our goal is to limit the number of I_H and I_m populations and control the proliferation of the vector population by minimizing the number of larvae and pupae L . We look for an optimal control

(u_1^*, u_2^*, u_3^*) such that

$$J(u_1^*, u_2^*, u_3^*) = \min \{J(u_1, u_2, u_3) | (u_1, u_2, u_3) \in \Gamma\}, \quad (12)$$

where

$$\begin{aligned} \Gamma = & \{(u_1, u_2, u_3) | u_i(t) \text{ is piecewise continuous function on} \\ & [0, T] \text{ such that } a_i \leq u_i(t) \leq b_i, i = 1, 2, 3\} \end{aligned}$$

is the control set and a_i, b_i are constants in $[0, 1]$, $i = 1, 2, 3$. The basic framework of this problem is to prove the following:

- the existence of the optimal control;
- the characterization of the optimal control.

3.1. Existence and characterization of an optimal control. The existence of an optimal control can be obtained by using a result of Fleming and Rishel [23].

Theorem 3.2. *Consider the control problem with system (8). There exists $(u_1^*, u_2^*, u_3^*) \in \Gamma$ such that*

$$\min_{(u_1, u_2, u_3) \in \Gamma} J(u_1, u_2, u_3) = J(u_1^*, u_2^*, u_3^*).$$

Proof. To use an existence result, theorem III.4.1 from [23], we must check if the following properties are satisfied:

1. the set of controls and corresponding state variables is non empty;
2. the control set Γ is convex and closed;
3. the right hand side of the state system is bounded by a linear function in the state and control;
4. the integrand of the objective functional is convex;
5. there exist constants $c_1, c_2, c_3 > 0$, and $\beta > 0$ such that the integrand of the objective functional is bounded below by $c_1(|u_1|^2 + |u_2|^2 + |u_3|^2)^{\frac{\beta}{2}} - c_2$.

In order to verify these properties, we use a result from Lukes [30] to give the existence of solutions for the state system (8) with bounded coefficients, which gives condition 1. The control set Γ is bounded by definition, then, condition 2 is satisfied. The right hand side of the state system (8) satisfies condition 3 since the state solutions are bounded. The integrand of our objective functional is clearly convex on Γ , which gives condition 4. Finally, there are $c_1, c_2 > 0$ and $\beta > 1$ satisfying $A_1 I_H(t) + A_2 I_m(t) + A_3 L(t) + B_1 u_1^2 + B_2 u_2^2 + B_3 u_3^2 \geq c_1(|u_1|^2 + |u_2|^2 + |u_3|^2)^{\frac{\beta}{2}} - c_2$, because the states variables are bounded.

We conclude that there exists an optimal control (u_1^*, u_2^*, u_3^*) that minimizes the objective functional $J(u_1, u_2, u_3)$. \square

Now, that we have established, the existence of an optimal control, we focus on the determination of an optimal control.

Let $Z = (E, L, A, S_H, I_H, I_m) \in \Delta \times \Omega$, $U = (u_1, u_2, u_3) \in \Gamma$ and the adjoint variables $\Pi = (\lambda_1, \lambda_2, \lambda_3, \lambda_4, \lambda_5, \lambda_6)$.

Let us define the Lagrangian of our problems as follows:

$$\begin{aligned}
\mathcal{L}(Z, U, \Pi) = & A_1 I_H(t) + A_2 I_m(t) + A_3 L(t) \\
& + B_1 u_1^2 + B_2 u_2^2 + B_3 u_3^2 \\
& + \lambda_1 \left(bA(t) \left(1 - \frac{E(t)}{K_E} \right) - (s + d + \varepsilon u_3(t)) E(t) \right) \\
& + \lambda_2 \left(sE(t) \left(1 - \frac{L(t)}{K_L} \right) - (s_L + d_L + d_c u_3(t)) L(t) \right) \\
& + \lambda_3 (s_L L(t) - d_m A(t)) \\
& + \lambda_4 (- (b_H + \beta_H (1 - u_1(t))) I_m(t)) S_H(t) + b_H) \\
& + \lambda_5 (\beta_H (1 - u_1(t)) I_m(t) S_H(t) - (\gamma + \gamma_0 u_2(t) + b_H) I_H(t)) \\
& + \lambda_6 \left(-s_L \frac{L(t)}{A(t)} I_m(t) + \beta_m I_H(t) (1 - u_1(t)) (1 - I_m(t)) \right) \\
& - w_{11}(u_1 - a_1) - w_{12}(b_1 - u_1) - w_{21}(u_2 - a_2) \\
& - w_{22}(b_2 - u_2) - w_{31}(u_3 - a_3) - w_{32}(b_3 - u_3),
\end{aligned} \tag{13}$$

where $w_{ij}(t) \geq 0$ are the penalty multipliers satisfying

$$w_{11}(t)(u_1(t) - a_1) = w_{12}(t)(b_1 - u_1(t)) = 0 \text{ at optimal control } u_1^*,$$

$$w_{21}(t)(u_2(t) - a_2) = w_{22}(t)(b_2 - u_2(t)) = 0 \text{ at optimal control } u_2^*$$

and

$$w_{31}(t)(u_3(t) - a_3) = w_{32}(t)(b_3 - u_3(t)) = 0 \text{ at optimal control } u_3^*.$$

Theorem 3.3. *Given an optimal control (u_1^*, u_2^*, u_3^*) and solutions E, L, A, S_H, I_H , and I_m of the corresponding state system (8), there exist adjoint variables $\Pi = (\lambda_1, \lambda_2, \lambda_3, \lambda_4, \lambda_5, \lambda_6)$ satisfying,*

$$\begin{aligned}
\dot{\lambda}_1 = & - \left(\lambda_1 \left[-b \frac{A}{K_E} - (s + d + \varepsilon u_3) \right] + \lambda_2 s \left(1 - \frac{L}{K_L} \right) \right) \\
\dot{\lambda}_2 = & - \left(A_3 + \lambda_2 \left[-s \frac{E}{K_L} - (s_L + d_L + d_c u_3) \right] + \lambda_3 s_L - \lambda_6 s_L \frac{I_m}{A} \right) \\
\dot{\lambda}_3 = & - \left(\lambda_1 b \left(1 - \frac{E}{K_E} \right) - \lambda_3 d_m + \lambda_6 s_L \frac{L}{A^2} I_m \right) \\
\dot{\lambda}_4 = & - (-\lambda_4 [(b_H + \beta_H (1 - u_1)) I_m] + \lambda_5 \beta_H (1 - u_1) I_m) \\
\dot{\lambda}_5 = & - (A_1 - \lambda_5 (\gamma + \gamma_0 u_2 + b_H) + \lambda_6 \beta_m (1 - u_1) (1 - I_m)) \\
\dot{\lambda}_6 = & - \left(A_2 - \lambda_4 \beta_H (1 - u_1) S_H + \lambda_5 \beta_H (1 - u_1) S_H \right. \\
& \left. - \lambda_6 \left[s_L \frac{L}{A} + \beta_m I_H (1 - u_1) \right] \right),
\end{aligned} \tag{14}$$

with the terminal condition

$$\lambda_i(T) = 0 \quad \text{for } i = 1, \dots, 6. \tag{15}$$

Furthermore, u_1^* , u_2^* and u_3^* are represented by

$$\begin{aligned} u_1^* &= \max \left\{ a_1, \min \left\{ b_1, \frac{1}{2B_1} [(\lambda_5 - \lambda_4)\beta_H I_m S_H + \lambda_6 \beta_m I_H (1 - I_m)] \right\} \right\} \\ u_2^* &= \max \left\{ a_2, \min \left\{ b_2, \frac{1}{2B_2} (\lambda_5 \gamma_0 I_H) \right\} \right\} \\ u_3^* &= \max \left\{ a_3, \min \left\{ b_3, \frac{1}{2B_3} (\lambda_1 \varepsilon E + \lambda_2 d_c L) \right\} \right\}. \end{aligned} \quad (16)$$

Proof. The form of the adjoint equations and terminal conditions are standard results from Pontryagin's Maximum Principle [36]. We differentiate the Lagrangian (which is the Hamiltonian augmented with penalty terms for the control constraints) with respect to states and then the adjoint system can be written as

$$\begin{aligned} \dot{\lambda}_1 &= -\frac{\partial \mathcal{L}}{\partial E}, & \dot{\lambda}_2 &= -\frac{\partial \mathcal{L}}{\partial L}, & \dot{\lambda}_3 &= -\frac{\partial \mathcal{L}}{\partial A}, \\ \dot{\lambda}_4 &= -\frac{\partial \mathcal{L}}{\partial S_H}, & \dot{\lambda}_5 &= -\frac{\partial \mathcal{L}}{\partial I_H}, & \dot{\lambda}_6 &= -\frac{\partial \mathcal{L}}{\partial I_m}. \end{aligned}$$

To obtain the optimal control given by (16), we also differentiate the Lagrangian \mathcal{L} , with respect to $U = (u_1, u_2, u_3)$ and set it equal to zero.

$$\begin{aligned} \frac{\partial \mathcal{L}}{\partial u_1} &= 2B_1 u_1 + \lambda_4 \beta_H I_m S_H - \lambda_5 \beta_H I_m S_H \\ &\quad - \lambda_6 \beta_m I_H (1 - I_m) - w_{11} + w_{12} = 0, \\ \frac{\partial \mathcal{L}}{\partial u_2} &= 2B_2 u_2 - \lambda_5 \gamma_0 I_H - w_{21} + w_{22} = 0, \\ \frac{\partial \mathcal{L}}{\partial u_3} &= 2B_3 u_3 - \lambda_1 \varepsilon E - \lambda_2 d_c L - w_{31} + w_{32} = 0. \end{aligned}$$

Solving for the optimal control, we obtain

$$\begin{aligned} u_1^* &= \frac{1}{2B_1} [(\lambda_5 - \lambda_4)\beta_H I_m S_H + \lambda_6 \beta_m I_H (1 - I_m) + w_{11} - w_{12}], \\ u_2^* &= \frac{1}{2B_2} [\lambda_5 \gamma_0 I_H + w_{21} - w_{22}], \\ u_3^* &= \frac{1}{2B_3} [(\lambda_2 d_c L) + w_{31} - w_{32}]. \end{aligned}$$

To determine an explicit expression for the optimal control without $w_{11}, w_{12}, w_{21}, w_{22}, w_{31}$ and w_{32} , we use a standard optimality technique involving the bounds of control. We consider the three following cases.

- On the set $\{t \mid a_1 < u_1^* < b_1\}$, we have

$$w_{11}(u_1^* - a_1) = w_{12}(b_1 - u_1^*) = 0 \Rightarrow w_{11} = w_{12} = 0.$$

Hence the optimal control is

$$u_1^* = \frac{1}{2B_1} [(\lambda_5 - \lambda_4)\beta_H I_m S_H + \lambda_6 \beta_m I_H (1 - I_m)].$$

- On the set $\{t \mid u_1^* = b_1\}$, we have

$$w_{11}(u_1^* - a_1) = w_{12}(b_1 - u_1^*) = 0 \Rightarrow w_{11} = 0.$$

Hence,

$$b_1 = u_1^* = \frac{1}{2B_1} [(\lambda_5 - \lambda_4)\beta_H I_m S_H + \lambda_6 \beta_m I_H (1 - I_m) - w_{12}],$$

and then,

$$\frac{1}{2B_1} [(\lambda_5 - \lambda_4)\beta_H I_m S_H + \lambda_6 \beta_m I_H (1 - I_m)] \geq b_1 \text{ since } w_{12}(t) > 0.$$

- On the set $\{t \mid u_1^* = a_1\}$, we have

$$w_{11}(u_1^* - a_1) = w_{12}(b_1 - u_1^*) = 0 \Rightarrow w_{12} = 0.$$

Hence,

$$a_1 = u_1^* = \frac{1}{2B_1} [(\lambda_5 - \lambda_4)\beta_H I_m S_H + \lambda_6 \beta_m I_H (1 - I_m) - w_{11}],$$

and then,

$$\frac{1}{2B_1} [(\lambda_5 - \lambda_4)\beta_H I_m S_H + \lambda_6 \beta_m I_H (1 - I_m)] \leq a_1 \text{ since } w_{11}(t) > 0,$$

which, in compact notation, reads as

$$u_1^* = \max \left\{ a_1, \min \left\{ b_1, \frac{1}{2B_1} [(\lambda_5 - \lambda_4)\beta_H I_m S_H + \lambda_6 \beta_m I_H (1 - I_m)] \right\} \right\}.$$

- On the set $\{t \mid a_2 < u_2^* < b_2\}$, we have

$$w_{21}(u_2^* - a_2) = w_{22}(b_2 - u_2^*) = 0 \Rightarrow w_{21} = w_{22} = 0.$$

Hence the optimal control is

$$u_2^* = \frac{1}{2B_2} [\lambda_5 \gamma_0 I_H].$$

- On the set $\{t \mid u_2^* = b_2\}$, we have

$$w_{21}(u_2^* - a_2) = w_{22}(b_2 - u_2^*) = 0 \Rightarrow w_{21} = 0.$$

Hence,

$$b_2 = u_2^* = \frac{1}{2B_2} [\lambda_5 \gamma_0 I_H + w_{22}],$$

and then,

$$\frac{1}{2B_2} [\lambda_5 \gamma_0 I_H] \geq b_2 \text{ since } w_{22}(t) \geq 0.$$

- On the set $\{t \mid u_2^* = a_2\}$, we have

$$w_{21}(u_2^* - a_2) = w_{22}(b_2 - u_2^*) = 0 \Rightarrow w_{22} = 0.$$

Hence,

$$a_2 = u_2^* = \frac{1}{2B_2} [\lambda_5 \gamma_0 I_H - w_{21}],$$

and then,

$$\frac{1}{2B_2} [\lambda_5 \gamma_0 I_H] \leq a_2 \text{ since } w_{21}(t) \geq 0,$$

which, in compact notation, reads as

$$u_2^* = \max \left\{ a_2, \min \left\{ b_2, \frac{1}{2B_2} (\lambda_5 \gamma_0 I_H) \right\} \right\}.$$

- On the set $\{t \mid a_3 < u_3^* < b_3\}$, we have

$$w_{31}(u_3^* - a_3) = w_{32}(b_3 - u_3^*) = 0 \Rightarrow w_{31} = w_{32} = 0.$$

Hence the optimal control is

$$u_3^* = \frac{1}{2B_3}(\lambda_1 \varepsilon E + \lambda_2 d_c L).$$

- On the set $\{t \mid u_3^* = b_3\}$, we have

$$w_{31}(u_3^* - a_3) = w_{32}(b_3 - u_3^*) = 0 \Rightarrow w_{31} = 0.$$

Hence

$$b_3 = u_3^* = \frac{1}{2B_3}[\lambda_1 \varepsilon E + \lambda_2 d_c L + w_{32}],$$

and then,

$$\frac{1}{2B_3}(\lambda_2 d_c L) \geq b_3 \text{ since } w_{32}(t) \geq 0.$$

- On the set $\{t \mid u_3^* = a_3\}$, we have

$$w_{31}(u_3^* - a_3) = w_{32}(b_3 - u_3^*) = 0 \Rightarrow w_{32} = 0.$$

Hence,

$$a_3 = u_3^* = \frac{1}{2B_3}[\lambda_1 \varepsilon E + \lambda_2 d_c L - w_{31}],$$

and then,

$$\frac{1}{2B_3}(\lambda_1 \varepsilon E + \lambda_2 d_c L) \leq a_3 \text{ since } w_{31}(t) \geq 0,$$

which, in compact notation, reads as

$$u_3^* = \max \left\{ a_3, \min \left\{ b_3, \frac{1}{2B_3}(\lambda_1 \varepsilon E + \lambda_2 d_c L) \right\} \right\}.$$

□

The optimality system contains the state system (8) with initial condition $Z(0)$, the adjoint system (14) with terminal condition (15), and the optimality condition (16).

4. Numerical results. First of all, note that the optimality system is a two-point boundary problem. Indeed the state (8) is solved forward in time with initial conditions $Z(0) = (100, 40, 10, 0.9, 0.1, 0.2)$ while the adjoint (or costate) system (14) is solved backward in time with terminal conditions $\Pi(T) = (0, 0, 0, 0, 0, 0)$, where $T = 100$ days. We implemented a gradient method, using standard Matlab routines, to solve numerically the optimality system. First of all, we solve the state system and the costate system with an initial guess control $(u_1(t), u_2(t), u_3(t)) = (0, 0, 0)$. The state system is solved forward in time while the costate system is solved backward in time. Then, we update control functions using the optimality condition given by (16) in each iteration. Iterations continue until convergence is achieved.

In the objective functional (11) weight constant values are chosen as follows:

$$A1 = A2 = 10000, A3 = 1, B1 = B2 = B3 = 10,$$

since the mosquito population dynamic and the virus transmission dynamics and control functions are on different scales. The other parameters are given in table 1.

Parameter	Description	Value
b	<i>per capita</i> oviposition rate	1 or 6
K_E	carrying capacity for eggs	1000
ε	chemical eggs mortality rate	0.001
K_L	carrying capacity for larvae	500
s	transfer rate from eggs to larvae	0.7
s_L	transfer rate from larvae to mosquitoes	0.5
d	eggs death rate	0.2 or 0.4
d_L	larvae natural mortality rate	0.2 or 0.4
d_c	chemical larvae mortality rate	0.3
d_m	adult mosquitoes mortality rate	0.25 or 0.5
b_H	human birth rate	0.0000457
β_H	effective contact rate human \rightarrow vector	0.2 or 0.75
β_m	effective contact rate vector \rightarrow human	0.1 or 0.5
γ_H	natural recovery rate	0.1428
γ_0	recovery rate induced by treatment	0.3

TABLE 1. Values of parameters in the chikungunya model. Most of the values were obtained from entomologists and given for instance in [6, 13, 20, 12, 19].

At first, we look for three optimal control functions u_1 , u_2 and u_3 for prevention, treatment and proliferation mosquito control respectively. Numerical results are obtained for different values of b (oviposition rate), d_E , d_L , d_m (mortality rates), β_H and β_m (effective contact rates), while keeping the remaining parameters unchanged in each simulation.

By performing numerical simulations with different parameter sets, we investigate effects of the threshold parameter, r , and the basic reproduction, R_0 , governing the dynamics of the mosquito stage population and the proportion of individuals in each class, respectively.

- Data 1 : $b = 1$, $d = 0.4$, $d_L = 0.4$, $d_m = 0.5$, $\beta_H = 0.2$,
 $\beta_m = 0.1$. In this case $r = 0.7071$, $R_0 = 0.2800$.
- Data 2 : $b = 1$, $d = 0.4$, $d_L = 0.4$, $d_m = 0.5$, $\beta_H = 0.75$,
 $\beta_m = 0.5$. In this case $r = 0.7071$, $R_0 = 5.2504$
- Data 3 : $b = 6$, $d = 0.2$, $d_L = 0.2$, $d_m = 0.25$, $\beta_H = 0.2$,
 $\beta_m = 0.1$. In this case $r = 13.3333$, $R_0 = 0.5600$.
- Data 4 : $b = 6$, $d = 0.2$, $d_L = 0.2$, $d_m = 0.25$, $\beta_H = 0.75$,
 $\beta_m = 0.5$. In this case $r = 13.3333$, $R_0 = 10.5008$.

Optimal strategies, optimal solutions, the threshold parameter, r and the basic reproduction, R_0 suggested by Data 1, Data 2, Data 3 and Data 4, are illustrated in Figs. 2–Fig. 5, respectively. These optimal solutions (solid line), together with non-optimal solutions (dashed line) corresponding to no control functions (that is, $u_1 = u_2 = u_3 = 0$) are presented in (b) and (c) for comparison. In Data 1 and 2, all stages of the vector population without any control become extinct. By contrast, in Data 3 and 4, a certain level of all stages of the vector population is maintained, as we expect in Theorem 2.1 (see (c) in all figures). From (a) in all figures, we observe

that, in the case of Data 1 and Data 2, that is for $r < 1$, almost no efforts on the vector control u_3 are recommended, while the full efforts on the vector control are needed in the case of Data 3 and Data 4, that is for $r > 1$. Notable features include that the shapes of optimal solutions (solid line) are much better than those of solutions (dashed line) of the system without control (see (b) and (c) in all figures). For example, the number of susceptible human with optimal control keeps staying on high level, and the number of infected human with optimal control keeps staying on low level.

Indeed, in Fig.2 and Fig.3, the adapted threshold parameter including control function, given by $r(t) = \frac{b}{(s + d + \varepsilon u_3(t))} \frac{s}{(s_L + d_L + d_c u_3(t))} \frac{s_L}{d_m}$ remains less than one in both cases, hence, the mosquito population density is described by a rapidly decreasing function on the time interval $[0, T]$.

In the cases of Fig. 4 and Fig. 5, the reduction of the density of all infected populations is due to a reduction of the second reproduction number given by $R_0(t) = \frac{\beta_m \beta_H (1 - u_1(t))^2}{d_m (s_L + d_L + d_c u_2(t))}$ (see Fig. 5(e)) when applying control functions while the threshold parameter $r(t)$ remains larger than 1. In Fig. 4, optimal control allows to reduce the function $R_0(t)$ less than 1 in the interval of high epidemic level, Fig. 4(e). In this case, there is only one trivial equilibrium point which is stable and then all trajectories tend to (1,0,0), Fig. 4(b). Moreover in Fig. 5, at the beginning of the epidemic, we have to apply full efforts for all controls.

Then, effort on prevention u_1 have to be more important than effort for treatment, since the epidemics tends to extinction. Thus, efforts have to focus on the prevention that will stabilize populations in order to prevent the appearance of another epidemic peak. Of course, at the end of control measures time T , $R_0(t)$ returns to its initial value. As said before, in the case of $R_0(t) < 1$, full effort has to be applied at the beginning of the epidemic, until the peak is reached, then unlike the previous case, more effort focus on the treatment of patients, since the epidemic tends to the trivial equilibrium. Thus, numerical results suggest that the optimal strategies should be changed depending on the dynamics of the vector population and the transmission of the virus to human population.

5. Conclusion. In this paper, an optimal control model to assess the effectiveness of three measures to reduce the number of chikungunya infected humans is done. Several governmental plans, like in France, focus in the use of insecticides to eradicate in the areas where the *Aedes albopictus* mosquito is newly established. Moreover, even if in several regions, infection has not been yet observed, recommendations and information to limit the mosquito proliferation to population are done. Of course, all interventions or strategies may not be efficient without human mobilization. For instance, after each rainfall, it is advisable to check around the houses regularly and systematically empty or clean all the water receptacles where mosquitoes could lay eggs.

The first action, consists in the reduction of the number of host-vector contact rate due to human prevention. Time dependent intervention strategies have been implemented, in the present work, to limit the bad effects of vector-borne disease on a finite time interval. This model allows to determine activities to be intensified in appropriate time intervals $[0, T]$ relevant to disease outbreak. Of course, such strategies allow to control the epidemic on a short time interval and not to predict the long term of the disease dynamics. In this paper we analyzed the optimal

control using the functional J in terms of quadratic forms. Minimizing the cost, we obtained the optimal controls u_1, u_2 and u_3 , where I_H , I_m and L are minimized. The main conclusion based on results furnished by all these strategies, when the mosquito is established, is that high application of larvicide or measures to control the proliferation of mosquitoes is needed during all the interval $[0, T]$ even if the peak of epidemic is passed. Then, we observe various scenarios depending on the mosquito population and virus transmission dynamics. Specific strategies may be considered in case of an ongoing epidemic. Moreover strategies depend on the expected objectives (prevention of an epidemic, focus on patients treatment, etc.). If we are only interested in weakening the vector independently of the virus, then our attention will focus on the model describing the vector dynamics. Therefore, we only have to consider the first three equations of system (8). The optimal control consists, in this case, in the control u_3 .

REFERENCES

- [1] B. M. Adams, H. T. Banks, M. Davidian, H.-D. Kwon, H. T. Tran, S. N. Wynne and E. S. Rosenberg, *HIV dynamics: Modeling, data analysis, and optimal treatment protocols*, J. Comput. Appl. Math., **184** (2005), 10–49.
- [2] B. M. Adams, H. T. Banks, H.-D. Kwon and H. T. Tran, *Dynamic multidrug therapies for HIV: Optimal and STI control approaches*, Mathematical Biosciences and Engineering, **1** (2004), 223–241.
- [3] J. Adhami and P. Reiter, *Introduction and establishment of Aedes (Stegomyia) albopictus skuse (diptera : Culicidae) in Albania*, American Mosquito Control Association, **14** (1998), 340–343.
- [4] N. Alphey, M. B. Bonsall and L. Alphey, *Modeling resistance to genetic control of insects*, Journal of Theoretical Biology, **270** (2011), 42–55.
- [5] *Be dry with mosquitoes*, 2011. Available from: <http://www.albopictus.eid-med.org/>.
- [6] N. Bacaër, *Approximation of the basic reproduction number R_0 for vector-borne diseases with a periodic vector population*, Bulletin of Mathematical Biology, **69** (2007), 1067–1091.
- [7] M. Q. Benedict, R. S. Levine, W. A. Hawley and L. P. Lounibos, *Spread of the tiger: Global risk of invasion by the mosquito Aedes albopictus*, Vector Borne and Zoonotic Diseases, **7** (2007), 76–85.
- [8] K. Blayneh, Y. Cao and H.-D. Kwon, *Optimal control of vector-borne disease: Treatment and prevention*, Discrete and Continuous Dynamical Systems Series B, **11** (2009), 587–611.
- [9] C. Cosner, J. Beier, R. Cantrell, D. Impoinvil, L. Kapitanski, M. Potts, A. Troyo and S. Ruan, *The effects of human movement on the persistence of vector-borne diseases*, Journal of Theoretical Biology, **258** (2009), 550–560.
- [10] N. Curcó, N. Giménez, M. Serra, A. Ripoll, M. García and P. Vives, *Asian tiger mosquito bites: Perception of the affected population after Aedes albopictus became established in Spain*, Actas Derm-Sifiliogràficas (English Edition), **99** (2008), 708–713.
- [11] T. Das, M. C. Jaffar-Bandjee, J. J. Hoarau, P. K. Trotot, M. Denizot, G. Lee-Pat-Yuen, R. Sahoo, P. Guiraud, D. Ramful, S. Robin, J. L. Alessandri, B. A. Gauzere and P. Gasque, *Chikungunya fever: CNS infection and pathologies of a re-emerging arbovirus*, Progress in Neurobiology, **91** (2010), 121–129.
- [12] H. Delatte, G. Gimmonneau, A. Triboire and D. Fontenille, *Influence of temperature on immature development, survival, longevity, fecundity, and gonotrophic cycles of Aedes albopictus, vector of chikungunya and dengue in the Indian Ocean*, Journal of Medical Entomology, **46** (2009), 33–41.
- [13] H. Delatte, C. Paupy, J. S. Dehecq, J. Thiria, A. B. Failloux and D. Fontenille, *Aedes albopictus, vector of chikungunya and dengue viruses in reunion island: Biology and control*, Parasite, **15** (2008), 3–13.
- [14] E. Depoortere, S. Salmaso, M. Pompa, P. Guglielmetti and D. Coulombier, *Chikungunya in Europe*, The Lancet, **371** (2008), 723–723.
- [15] M. Diallo, J. Thonnon, M. Traore-Lamizana and D. Fontenille, *Vectors of chikungunya virus in Senegal: Current data and transmission cycles*, The American Journal of Tropical Medicine and Hygiene, **60** (1999), 281–286.

- [16] O. Diekmann and J. A. P. Heesterbeek, "Mathematical Epidemiology of Infectious Diseases. Model Building, Analysis and Interpretation," Wiley Series in Mathematical and Computational Biology, John Wiley & Sons, Ltd., Chichester, 2000.
- [17] P. van den Driessche and J. Watmough, *Reproduction numbers and sub-threshold endemic equilibria for compartmental models of disease transmission*, Mathematical Biosciences, **180** (2002), 29–48.
- [18] M. Dubrulle, L. Mousson, S. Moutailler, M. Vazeille and A. B. Failloux, *Chikungunya virus and Aedes mosquitoes: Saliva is infectious as soon as two days after oral infection*, PLoS ONE, **4** (2009), e5895.
- [19] Y. Dumont and F. Chiroleu, *Vector control for the chikungunya disease*, Mathematical Biosciences and Engineering, **7** (2010), 313–345.
- [20] Y. Dumont, F. Chiroleu and C. Domerg, *On a temporal model for the chikungunya disease: Modeling, theory and numerics*, Mathematical Biosciences, **213** (2008), 80–91.
- [21] M. Enserink, *Epidemiology: Tropical disease follows mosquitoes to Europe*, Science, **317** (2007), 1485a.
- [22] L. Esteva and C. Vargas, *A model for dengue disease with variable human population*, Journal of Mathematical Biology, **38** (1999), 220–240.
- [23] W. H. Fleming and R. W. Rishel, "Deterministic and Stochastic Optimal Control," Applications of Mathematics, No. 1, Springer-Verlag, Berlin-New York, 1975.
- [24] P. J. Gullan and P. Cranston, "The Insects: An Outline of Entomology," 4th edition, Wiley-Blackwell, 2010.
- [25] M. G. Guzman and G. Kouri, *Dengue and dengue hemorrhagic fever in the Americas: Lessons and challenges*, Journal of Clinical Virology, **27** (2003), 1–13.
- [26] W. A. Hawley, *The biology of Aedes albopictus*, J. Am. Mosq. Control Assoc. Suppl., **1** (1988), 1–39.
- [27] H. Hethcote, *The mathematics of infectious diseases*, SIAM Review, **42** (2000), 599–653.
- [28] E. Jung, S. Lenhart and Z. Feng, *Optimal control of treatments in a two-strain tuberculosis model*, Discrete and Continuous Dynamical Systems Series B, **2** (2002), 473–482.
- [29] K. Laras, N. C. Sukri, R. P. Larasati, M. J. Bangs, R. Kosim, Djauzi, T. Wandra, J. Master, H. Kosasih, S. Hartati, C. Beckett, E. R. Sedyaningsih, H. J. Beecham III and A. L. Corwin, *Tracking the re-emergence of epidemic chikungunya virus in Indonesia*, Transactions of the Royal Society of Tropical Medicine and Hygiene, **99** (2005), 128–141.
- [30] D. L. Lukes, "Differential Equations. Classical to Controlled," Mathematics in Science and Engineering, **162**, Academic Press, Inc. [Harcourt Brace Jovanovich, Publishers], London-New York, 1982.
- [31] W. H. R. Lumdsen, *An epidemic of virus disease in Southern Province, Tanganyika territory, in 1952–1953. II. General description and epidemiology*, Transactions of the Royal Society of Tropical Medicine and Hygiene, **49** (1955), 23–57.
- [32] C. J. Mitchell, *Geographic spread of Aedes albopictus and potential for involvement in arbovirus cycles in the Mediterranean basin*, Journal of Vector Ecology, **20** (1995), 44–58.
- [33] D. Moulay, M. A. Aziz-Alaoui and M. Cadivel, *The chikungunya disease: Modeling, vector and transmission global dynamics*, Mathematical Biosciences, **229** (2011), 50–63.
- [34] C. Paupy, H. Delatte, L. Bagny, V. Corbel and D. Fontenille, *Aedes albopictus, an arbovirus vector: From the darkness to the light*, Microbes and Infection, **11** (2009), 1177–1185.
- [35] G. Pialoux, B. A. Gaüzère and M. Strobel, *Infection à virus chikungunya: Revue générale par temps d'épidémie*, Médecine et Maladies Infectieuses, **36** (2006), 253–263.
- [36] L. Pontryagin, V. Boltyanskii, R. Gamkrelidze and E. Mishchenko, "The Mathematical Theory of Optimal Processes," A Pergamon Press Book, The Macmillan Co., New York, 1964.
- [37] S. Rajapakse, C. Rodrigo and A. Rajapakse, *Atypical manifestations of chikungunya infection*, Transactions of the Royal Society of Tropical Medicine and Hygiene, **104** (2010), 89–96.
- [38] G. Rezza, L. Nicoletti, R. Angelini, R. Romi, A. Finarelli, M. Panning, P. Cordioli, C. Fortuna, S. Boros, F. Magurano, G. Silvi, P. Angelini, M. Dottori, M. Ciufolini, G. Majori and A. Cassone, *Infection with chikungunya virus in Italy: An outbreak in a temperate region*, The Lancet, **370** (2007), 1840–1846.
- [39] M. C. Robinson, *An epidemic of virus disease in Southern Province, Tanganyika territory, in 1952–53. I. Clinical features*, Transactions of the Royal Society of Tropical Medicine and Hygiene, **49** (1955), 28–32.
- [40] R. W. Ross, *The newala epidemic. III. The virus: Isolation, pathogenic properties and relationship to the epidemic*, Epidemiology and Infection, **54** (1956), 177–191.

- [41] T. Seyler, Y. Hutin, V. Ramachandran, R. Ramakrishnan, P. Manickam and M. Murhekar, *Estimating the burden of disease and the economic cost attributable to chikungunya, Andhra Pradesh, India, 2005–2006*, Transactions of the Royal Society of Tropical Medicine and Hygiene, **104** (2010), 133–138.
- [42] D. Sissoko, D. Malvy, C. Giry, G. Delmas, C. Paquet, P. Gabrie, F. Pettinelli, M. A. Sanquer and V. Pierre, *Outbreak of chikungunya fever in Mayotte, Comoros Archipelago, 2005–2006*, Transactions of the Royal Society of Tropical Medicine and Hygiene, **102** (2008), 780–786.
- [43] A. B. Sudeep and D. Parashar, *Chikungunya: An overview*, Journal of Biosciences, **33** (2008), 443–449.
- [44] B. V. Tandale, P. S. Sathe, V. A. Arankalle, R. Wadia, R. Kulkarni, S. V. Shah, S. K. Shah, J. K. Sheth, A. Sudeep, A. S. Tripathy and A. C. Mishra, *Systemic involvements and fatalities during chikungunya epidemic in India, 2006*, Journal of Clinical Virology, **46** (2009), 145–149.
- [45] R. C. Thomé, H. M. Yang and L. Esteva, *Optimal control of Aedes aegypti mosquitoes by the sterile insect technique and insecticide*, Mathematical Biosciences, **223** (2010), 12–23.
- [46] M. Vazeille, C. Jeannin, E. Martin, F. Schaffner and A. B. Failloux, *Chikungunya: A risk for Mediterranean countries*, Acta Tropica, **105** (2008), 200–202.
- [47] World-Health-Organization, *Dengue and severe dengue*, factsheet no. 117, revised may 2008, Geneva, World Health Organization, 2008. Available from: <http://www.who.int/mediacentre/factsheets/fs117/en/>.
- [48] H. M. Yang and C. P. Ferreira, *Assessing the effects of vector control on dengue transmission*, Applied Mathematics and Computation, **198** (2008), 401–413.

Received April 27, 2011; Accepted December 29, 2011.

E-mail address: djamila.moulay@univ-lehavre.fr

E-mail address: aziz.alaoui@univ-lehavre.fr

E-mail address: hdkwon@inha.ac.kr

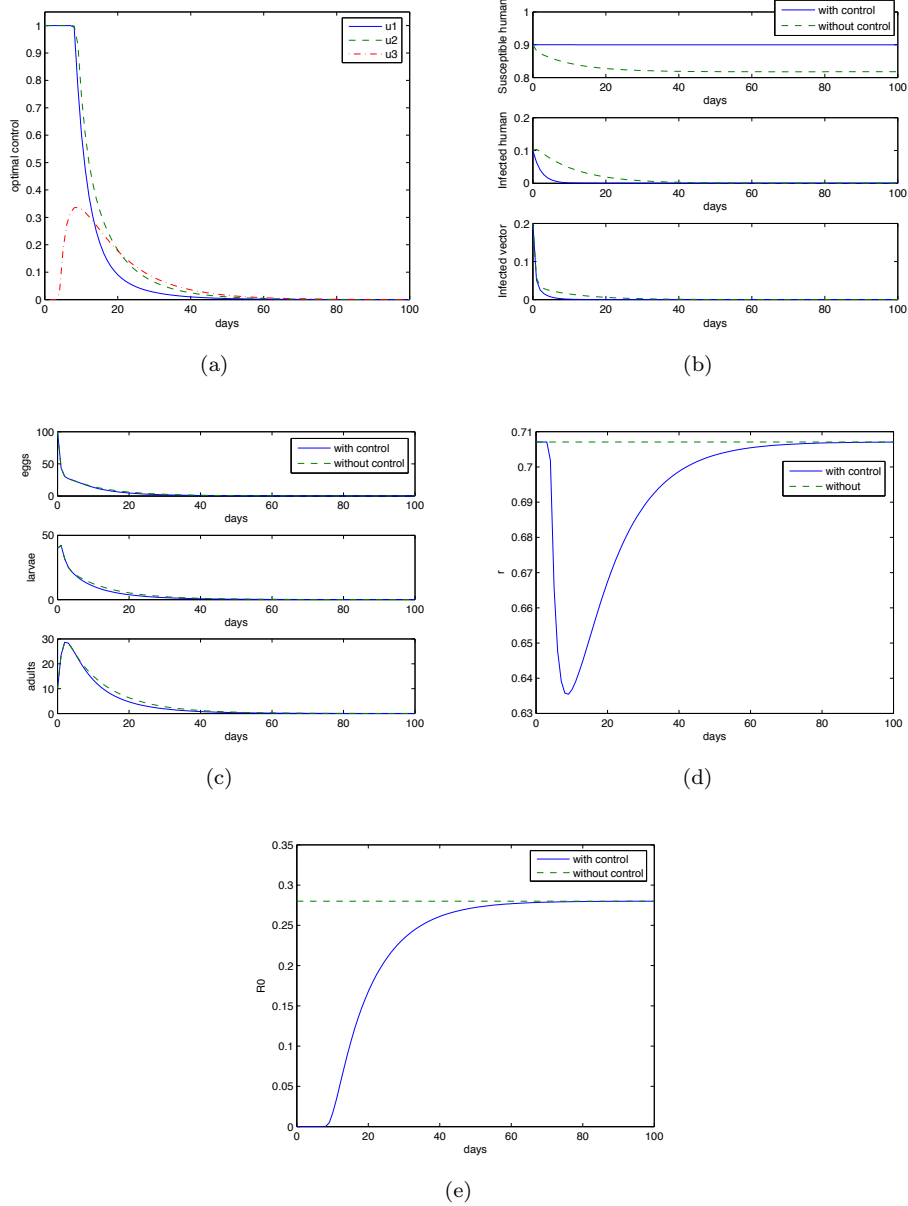


FIGURE 2. Numerical simulations with $b = 1$, $d = 0.4$, $d_L = 0.4$, $d_m = 0.5$, $\beta_H = 0.2$ and $\beta_m = 0.1$. On this case $r = 0.7071 < 1$ and $R_0 = 0.2800 < 1$. (a) Optimal control functions: prevention (—), treatment (---), vector control (·); (b) Solutions for susceptible and infected human and infected vector: optimal solutions (—), solutions without controls (---); (c) Solutions for eggs, larvae and adults of vector: optimal solutions (—), solutions without controls (---); (d) Threshold parameter with the optimal control functions (—) and without the control functions (---); (e) Second reproductive number with the optimal control functions (—) and without the control functions (---).

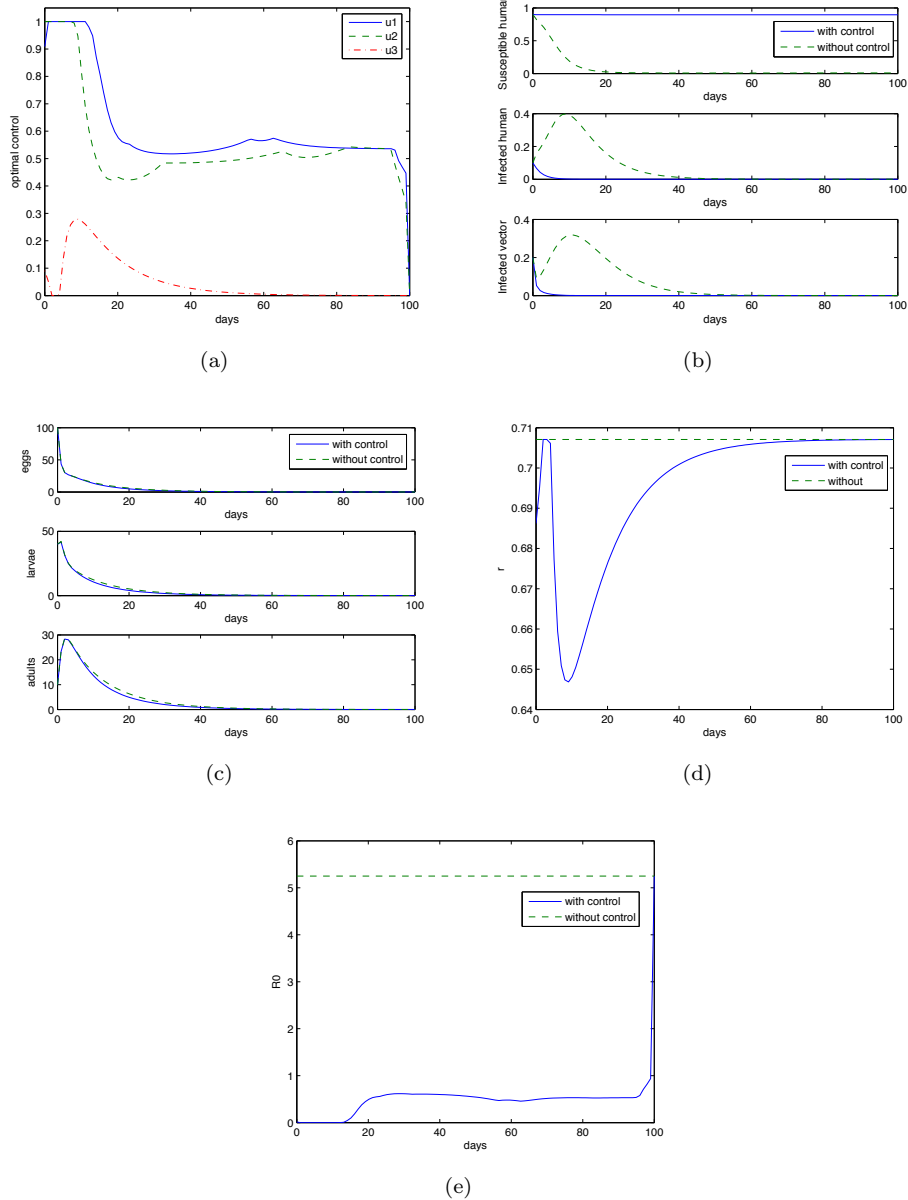


FIGURE 3. Numerical simulations with $b = 1$, $d = 0.4$, $d_L = 0.4$, $d_m = 0.5$, $\beta_H = 0.75$, and $\beta_m = 0.5$. On this case $r = 0.7071 < 1$ and $R_0 = 5.2504 > 1$. (a) Optimal control functions: prevention (—), treatment (---), vector control (···); (b) Solutions for susceptible and infected human and infected vector: optimal solutions (—), solutions without controls (---); (c) Solutions for eggs, larvae and adults of vector: optimal solutions (—), solutions without controls (---); (d) Threshold parameter with the optimal control functions (—) and without the control functions (---); (e) Second reproductive number with the optimal control functions (—) and without the control functions (---).

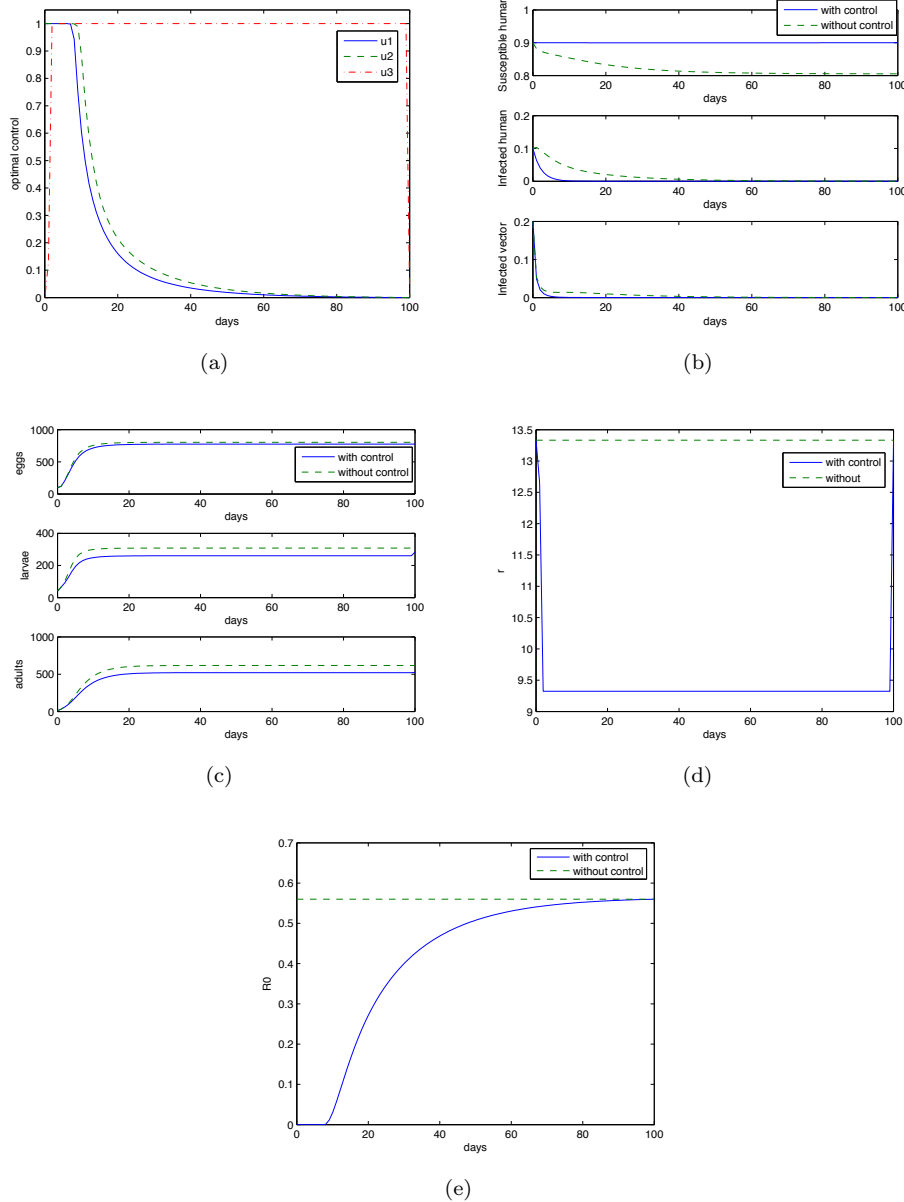


FIGURE 4. Numerical simulations with $b = 6$, $d = 0.2$, $d_L = 0.2$, $d_m = 0.25$, $\beta_H = 0.2$, and $\beta_m = 0.1$. On this case $r = 13.3333 > 1$ and $R_0 = 0.5600 < 1$. (a) Optimal control functions: prevention (—), treatment (---), vector control (···); (b) Solutions for susceptible and infected human and infected vector: optimal solutions (—), solutions without controls (---); (c) Solutions for eggs, larvae and adults of vector: optimal solutions (—), solutions without controls (---); (d) Threshold parameter with the optimal control functions (—) and without the control functions (---); (e) Second reproductive number with the optimal control functions (—) and without the control functions (---).

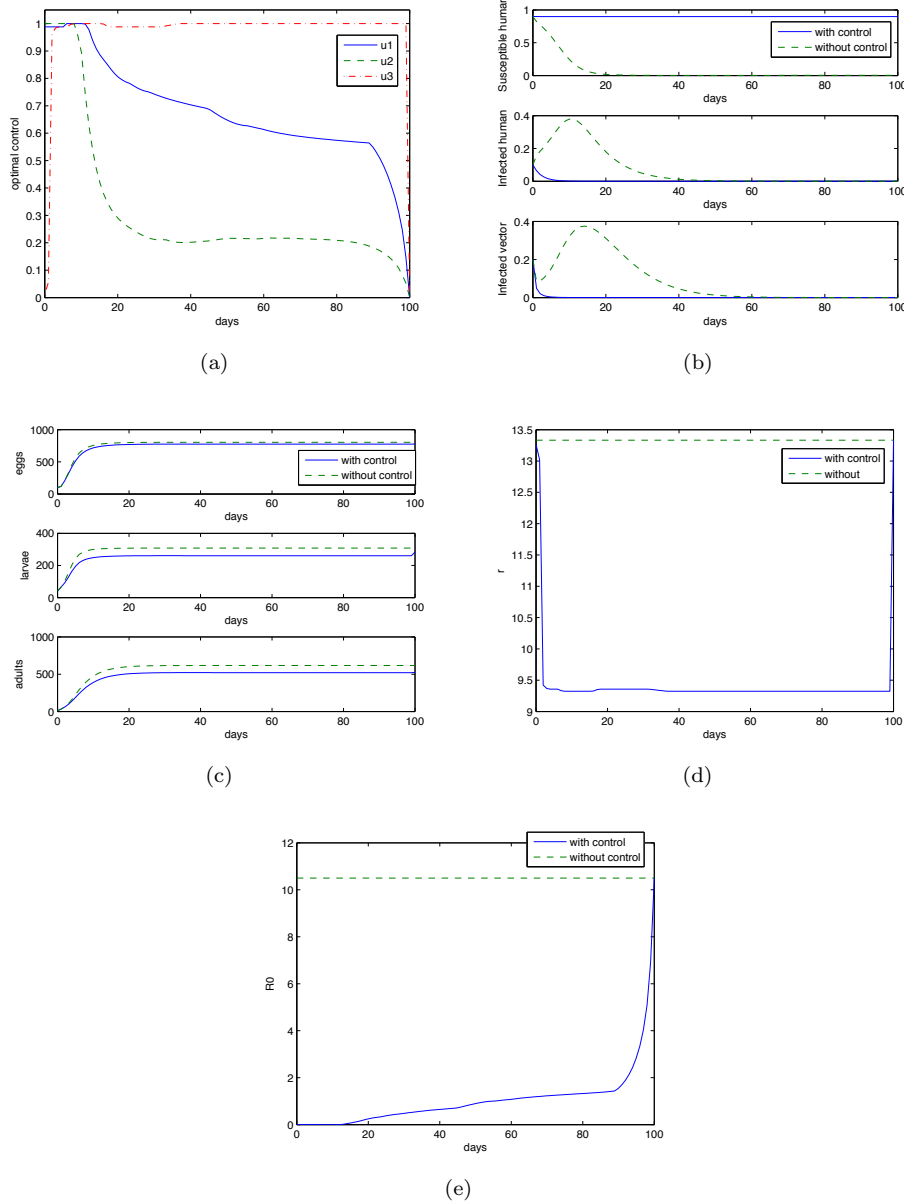


FIGURE 5. Numerical simulations with $b = 6$, $d = 0.2$, $d_L = 0.2$, $d_m = 0.25$, $\beta_H = 0.75$, and $\beta_m = 0.5$. On this case $r = 13.3333 > 1$ and $R_0 = 10.5008 > 1$. (a) Optimal control functions: prevention (—), treatment (---), vector control (···); (b) Solutions for susceptible and infected human and infected vector: optimal solutions (—), solutions without controls (---); (c) Solutions for eggs, larvae and adults of vector: optimal solutions (—), solutions without controls (---); (d) Threshold parameter with the optimal control functions (—) and without the control functions (---); (e) Second reproductive number with the optimal control functions (—) and without the control functions (---).

A Metapopulation Model for Chikungunya Including Populations Mobility on a Large-Scale Network

Djamila Moulay*

LMAH, Le Havre University, France

Yoann Pigné*

LITIS, Le Havre University, France

Abstract

In this work we study the influence of populations mobility on the spread of a vector-borne disease. We focus on the chikungunya epidemic event that occurred in 2005-2006 on the Réunion Island, Indian Ocean, France, and validate our models with real epidemic data from the event. We propose a metapopulation model to represent both a high-resolution patch model of the island with realistic population densities and also mobility models for humans (based on real-motion data) and mosquitoes. In this metapopulation network, two models are coupled: one for the dynamics of the mosquito population and one for the transmission of the disease. A high-resolution numerical model is created out from real geographical, demographical and mobility data. The Island is modeled with an 18 000-nodes metapopulation network. Numerical results show the impact of the geographical environment and populations' mobility on the spread of the disease. The model is finally validated against real epidemic data from the Réunion event.

Keywords: Complex Networks, Epidemiological model, Human mobility models, Metapopulation

*Corresponding author. LMAH, Université du Havre, 25 rue Philippe Lebon, BP540, 76058 Le Havre Cedex

Email addresses: djamila.moulay@univ-lehavre.fr (Djamila Moulay), yoann.pigne@univ-lehavre.fr (Yoann Pigné)

URL: <http://djamila-moulay.org> (Djamila Moulay), <http://pigne.org> (Yoann Pigné)

1. Introduction

Many factors have influence the emergence and re-emergence of vector borne diseases [1, 2]. Brutal changes in natural habitats so as massive or recurrent population migrations tend to speed up the spread of vector-borne diseases. The spatiotemporal evolution of such disease is becoming a key issue for epidemiologists. To this purpose, models that consider the spatial distribution of a natural environment are of great interest. In this paper we are interested in the spatial spread of a vector-borne disease under the effect of human and vector mobility. Indeed, human migration is one of the factor that have influenced the re-emergence of several diseases [3, 4]. The modeling of geographical environments and populations mobilities are becoming mandatory in this context. There are several approaches to describe such spread. One of the typical approaches, introducing spatial spread variation in epidemic models, involves the use of partial differential equations [5, 6, 7, 8, 9]. However, in the case of human mobility these approaches may not be appropriate. The theory of "metapopulation", first introduced in 1969 [10], in the field of ecology, allows such modeling. In this case for instance, the disease is carried from one node to another by human displacements. Several research have been devoted to the study of disease spread in heterogenous environments [11, 12, 13]. In [14, 15], authors study the influence of human dispersal among n patches in the dynamics of disease spread. In [16], authors, to study the spread of seasonal influenza, focus on air displacements and model the environment with a network where the nodes are the airports and the edges represent the flights. In [17] and [18], authors are also interested in the case of influenza and mobility in terms of long journeys. In [19, 20, 21], the authors propose a virus spread model based on this theory. In [22, 23], the mobility of mosquitoes has been modeled to study the spatiotemporal dynamics of malaria. Other studies focus on direct-transmission diseases like [20, 21]. In [16], influenza in the case of long trips (aircraft flights) is tackled. In [24], the authors rely on the Ross-Macdonald model [25, 26], to consider human mobility.

Human mobility is usually considered in epidemic problems. Also, models that consider the dynamics of the vector population are numerous. However, to our knowledge, no model considers to couple population dynamics with populations mobility as we propose here. More over our approach promotes the consideration of vectors's mobility since the resolution of our model is greater than usual models.

In this work we are proposing to couple two models (published in [27]): a mosquito dynamics model (growth and evolution of the population) with a transmission model between two populations (humans and mosquitoes). The dynamics of the mosquito population is a compartment model based on its life cycle. The different compartment states are egg, larvae, pupae and adult. The disease transmission model is, for the human population, a SIR (Susceptible, Infected, Recovered) model, since human may be recovered after being infected. For mosquitoes, the transmission model is a SI (Susceptible, Infected) model, since mosquitoes never recover from the disease.

Those two models are formalized using the metapopulation theory. It considers a network where nodes represent real habitats of the environment. In each of these nodes, transmission and population dynamics models appear and are coupled with neighbor nodes. Links in the network represent both the local neighborhood of a node and farther nodes that code for the mobility of humans.

In order to validate the approach, we focus on a real case of chikungunya epidemic with the 2005-2006 event that occurred on the Reunion Island, a French island in the Indian Ocean. The island is modeled with a network. Since we want that network to reflect the local population's density, we consider the road network of the island as a proxy to the human density, considering that each crossroad is a node of the network. Then the local population on each node is adjusted according to real data given by the INSEE (French Institute for Statistics). Finally the all island is modeled with a 18,000 nodes network.

Human mobility is constructed according to a study of real datasets of cell phone probes. In [28], authors could reconstruct the time-resolved trajectory of 100,000 cell phones owners, based on the analyze of log data that give time and location when phone calls are emitted. These analyses allowed them to propose general mobility distributions for the distances, the number and the frequency of displacements. We rely on these distributions to create human mobility patterns for the population in our model. We assume that individuals only change disease status when they are on a node and not during displacements. See [29] for a model with disease transmission during travel.

Results show the decisive influence of mobilities over the spread of the disease. Not only the human mobility but also the vector local interaction that play an important role at the considered scale. Results are then compared to real data epidemic regarding the 2005-2006 event at the scale of the

all Réunion Island and the model is validated.

The remaining of this paper is organized as follows. Next section recalls original transmission and population dynamics models that this work is inspired of. Section 3 introduces the original metapopulation model that is able to include the previous model in a network of patches couple to represent populations mobility. Then, in Sect. 4, according to the wish to validate the model against a real epidemic, a numerical implementation of the metapopulation model is constructed. This section details the construction of the metapopulation network in terms of environment and populations mobility. Section 5 presents various analysis performed on the model, showing the impact of mobilities. A validation is then proposed with a comparison with real epidemic data. Finally Sect. 6 concludes that paper.

2. Original Model

We first recall the model proposed and studied in [27] describing the vector dynamics. The formulated model is a stage structured model based on the biological mosquito life cycle. The vector population is subdivided into several classes: the aquatic stage consisting in eggs E and larvae/pupae L , and then the adult stage A , representing adult females. We assume first that the number of eggs b , laid by females, is proportional to the number of females itself. Secondly, the number of eggs and larvae is regulated by the effect of a carrying capacity K_E and K_L respectively. Then we formulate a transmission virus model where the female adult stage, is subdivided into two epidemiological states: susceptible, S_m and infectious, I_m . It assumes that there is no vertical transmission of the virus, so that births from susceptible and infectious mosquitos occur into the egg stage with the same rate.

The human population consists in three epidemiological states: susceptible (or non-immune) S_H ; infectious, I_H and removed (or immune) R_H . It is assumed that there is no vertical transmission of the disease, so that all births occur into the susceptible human class, at the rate $b_H > 0$. Moreover we assume that the total human population N_H remains constant, thus birth and death rates are equal. An infected human is infectious during $\frac{1}{\gamma_h}$ days, called the viremic period, and then becomes resistant or immune.

Forces of infections used in the model, which describe the rates of apparition of new infections, are standard and modeled by the mass-action principle normalized by the total population of humans, given by $\beta_m \frac{I_H(t)}{N_H}$

and $\beta_H \frac{I_m(t)}{N_H} S_H(t)$ where β_m and β_H are the transmission parameters.
 This hypothesis are summed up in Fig. 1.

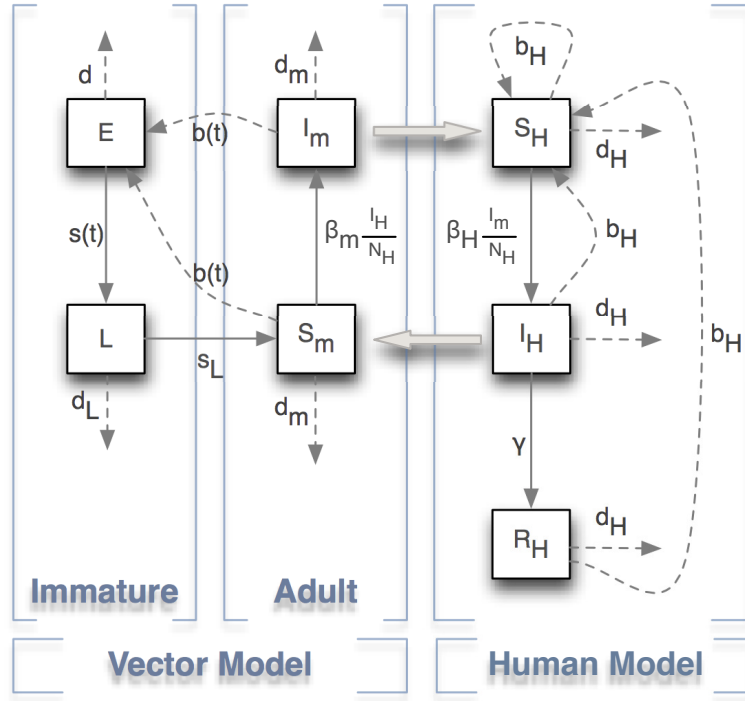


Figure 1: Compartmental model for the dynamics of *Aedes albopictus* mosquitoes and the virus transmission to human population. $b(t) = bA(t) \left(1 - \frac{E(t)}{K_E}\right)$, $s(t) = sE(t) \left(1 - \frac{L(t)}{K_L}\right)$ and the parameters of the model are given in table 1.

Based on our model description (see Fig. 1) and assumptions, we establish the following equations.

Table 1: Parameters of the mosquito and transmission dynamics models

Parameters	Description
b	oviposition rate
K_E	egg carrying capacity
K_L	larva carrying capacity
s	transfer rate from eggs to larvae
s_L	transfer rate from larva to adult female
d	egg mortality rate
d_L	larva mortality rate
d_A	female adult mortality rate
b_H	human birth rate
β_H	infection rate from human to vector
β_m	infection rate from vector to human
γ_H	human recovery rate

$$\left\{ \begin{array}{l} \frac{dE}{dt}(t) = bA(t) \left(1 - \frac{E(t)}{K_E} \right) - (s + d)E(t) \\ \frac{dL}{dt}(t) = sE(t) \left(1 - \frac{L(t)}{K_L} \right) - (s_L + d_L)L(t) \\ \frac{dA}{dt}(t) = s_L L(t) - d_m A(t) \\ \frac{dS_m}{dt}(t) = s_L L(t) - d_m S_m(t) - \beta_m \frac{I_H(t)}{N_H} S_m(t) \\ \frac{dI_m}{dt}(t) = \beta_m \frac{I_H(t)}{N_H} S_m(t) - d_m I_m(t) \\ \frac{dS_H}{dt}(t) = -\beta_H \frac{I_m(t)}{N_H} S_H(t) + b_H(S_H(t) + I_H(t) + R_H(t)) - d_H \bar{S}_H(t) \\ \frac{dI_H}{dt}(t) = \beta_H \frac{I_m(t)}{N_H} S_H(t) - \gamma I_H(t) - d_H I_H(t) \\ \frac{dR_H}{dt}(t) = \gamma I_H(t) - d_H \bar{R}_H(t) \end{array} \right. \quad (1)$$

The study of the model is detailed in [27]. For this model (1), the second basic reproduction number is given by

$$R_0 = \frac{\beta_m \beta_H}{d_m(\gamma + b_H)} \frac{1}{N_H} \left(1 - \frac{1}{r} \right) \frac{s K_E s_L K_L}{d_m(s K_E + (s_L + d_L) K_L)}$$

$$\text{where } r = \left(\frac{b}{s+d} \right) \left(\frac{s}{s_L + d_L} \right) \left(\frac{s_L}{d_m} \right)$$

The threshold r governs the dynamics of mosquitoes. In this article we assume that this threshold is larger than one. This ensures the existence, persistence and global stability of a unique endemic equilibrium, which corresponds to the biological and interesting case. The second reproduction number R_0 , which may be calculated using Metzler matrices or next generation matrices[30, 31] governs the dynamic of the transmission model. If $R_0 \leq 1$ then the disease dies out, since there is only one disease free equilibrium and no other equilibria. We show that this equilibrium is globally asymptotically stable, while there exists an endemic equilibrium which is globally asymptotically stable when $R_0 > 1$.

3. Metapopulation Model

In [19, 20] the authors formulate a general system of differential equations allowing to describe human mobility. In this model, they identify each population by its origin and its present location. We rely on this model and extend it with the definition of a neighborhood in which humans and mosquitoes interact.

3.1. Human mobility

Based on this model we proposed an adaptive model of that given in [27] to describe the spread of a vector-borne disease (such as chikungunya) under human and vector mobility on a large scale network, such as the one proposed here to represent the Réunion Island.

Assume that the number of nodes in the network is n . A human population is identified due to two characteristics: the node from which he is originated, *i.e.* its residence and the node where it is at time t . We assume that the total human population is constant, *i.e.* births and deaths occur with the same rate $b_H = d_H$. Moreover, we suppose that birth occur in the resident node while deaths take place in nodes where human are present.

Let us denote by $S_{Hij}(t), I_{Hij}(t)$ and $R_{Hij}(t)$ the susceptible, infected and removed human population originated from node i and present on node j at time t . We denote by S_{mi} and I_{Hi} the susceptible and infected mosquito respectively, present in node i . In a first assumption mosquitoes mobility is neglected, which looks like realistic compared to the distance of humans

displacements. So, resident mosquitoes from node i are also present on this node.

Then, the total number of susceptible, infected and removed human residents of node i , denoted respectively $S_{H_i}^r$, $I_{H_i}^r$ and $R_{H_i}^r$ is given by

$$S_{H_i}^r = \sum_{j=1}^n S_{H_{ij}}, \quad I_{H_i}^r = \sum_{j=1}^n I_{H_{ij}}, \quad R_{H_i}^r = \sum_{j=1}^n R_{H_{ij}}.$$

Then, the total number of susceptible, infected and removed humans present on node i , denoted respectively $S_{H_i}^p$, $I_{H_i}^p$ and $R_{H_i}^p$ is give by

$$S_{H_i}^p = \sum_{j=1}^n S_{H_{ji}}, \quad I_{H_i}^p = \sum_{j=1}^n I_{H_{ji}}, \quad R_{H_i}^p = \sum_{j=1}^n R_{H_{ji}}.$$

The number of human residents on node i is then equal to $N_{H_i}^r = S_{H_i}^r + I_{H_i}^r + R_{H_i}^r$ and the human population present on node i is $N_{H_i}^p = S_{H_i}^p + I_{H_i}^p + R_{H_i}^p$.

As in [32] and [21], we define the travel rate from node i to node j by $g_i m_{ji}$, where g_i corresponds to the per capita rate at which residents of node i leave this node and a fraction m_{ji} of them go to node j . Residents of node i , present on node j , then return to node i with a per capita rate $r_{ij} \geq 0$, with $r_{ii} = 0$. Displacements between two nodes are represented in Fig. 2.

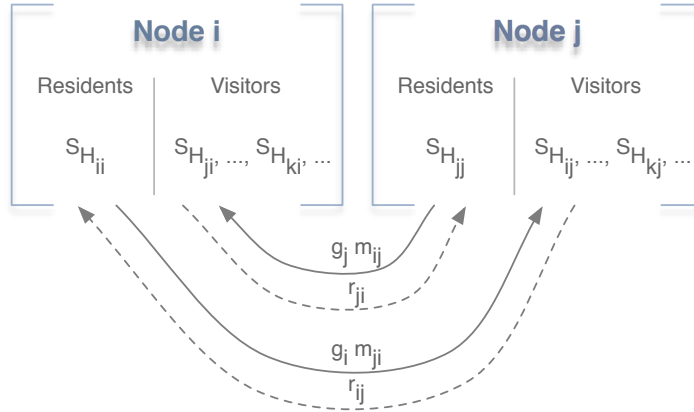


Figure 2: Human population mobility between nodes i and j .

1. The dynamics of human population (susceptible, infected and removed)

resident and present on node i is given by:

$$\begin{aligned}\frac{dS_{Hii}}{dt} &= d_H(N_{Hi}^r - S_{Hii}) - g_i S_{Hii} + \sum_{k=1}^n r_{ik} S_{Hik} - \beta_{Hi} \frac{Im_i}{N_{Hi}^p} S_{Hii} \\ \frac{dI_{Hii}}{dt} &= -d_H I_{Hii} - g_i I_{Hii} + \sum_{k=1}^n r_{ik} I_{Hik} + \beta_{Hi} \frac{Im_i}{N_{Hi}^p} S_{Hii} - \gamma_H I_{Hii} \\ \frac{dR_{Hii}}{dt} &= -d_H R_{Hii} + \gamma_H I_{Hii} - g_i R_{Hii} + \sum_{k=1}^n r_{ik} R_{Hik}\end{aligned}$$

2. The dynamics of human population (susceptible, infected and removed) resident on node i and present on node j is given by:

$$\begin{aligned}\frac{dS_{Hij}}{dt} &= -d_H S_{Hij} + g_i m_{ji} S_{Hii} - r_{ij} S_{Hij} - \beta_{Hj} \frac{Im_j}{N_{Hj}^p} S_{Hij} \\ \frac{dI_{Hij}}{dt} &= -d_H I_{Hij} + g_i m_{ji} I_{Hii} - r_{ij} I_{Hij} + \beta_{Hj} \frac{Im_j}{N_{Hj}^p} S_{Hij} - \gamma_H I_{Hij} \\ \frac{dR_{Hij}}{dt} &= -d_H R_{Hij} + g_i m_{ji} R_{Hii} - r_{ij} R_{Hij} + \gamma_H I_{Hij}.\end{aligned}$$

The dynamic of mosquito population (eggs, larvae an pupae, adult females) given in [27] in each node is :

$$\begin{aligned}\frac{dS_{mi}}{dt} &= s_L L_i - d_m S_{mi} - \beta_{mi} \frac{S_{mi}}{N_{Hi}^p} I_{Hi}^p \\ \frac{dI_{mi}}{dt} &= \beta_{mi} \frac{S_{mi}}{N_{Hi}^p} I_{Hi}^p - d_m I_{mi} \\ \frac{dE_i}{dt} &= b(S_{mi}(t) + I_{mi}(t)) \left(1 - \frac{E_i(t)}{K_{Ei}}\right) - (s + d) E_i(t) \\ \frac{dL_i}{dt} &= s E_i(t) \left(1 - \frac{L_i(t)}{K_{Li}}\right) - (s_L + d_L) L_i(t).\end{aligned}$$

Here we assume that the dynamic of immature stages E and L is described by corresponding equations in system (1)

Remark 1. Note that the infection transmitted in node i between susceptible mosquitoes and infected humans depends now on the human population present on this node N_{Hi}^p

$$\sum_{j=1}^n \beta_{mi} \frac{S_{mi}}{N_{Hi}^p} I_{Hji} = \beta_{mi} \frac{S_{mi}}{N_{Hi}^p} I_{Hi}^p.$$

The distance between nodes is not explicitly taken into account, nevertheless it is implicitly included in the coefficient m_{ji} and r_{ij} .

In the following we focus on daily displacements, humans who leave their resident node, obviously return to their resident node on a daily basis. Displacement matrices $M^T = [g_i m_{ji}]$ and $R = [r_{ij}]$ have the same zero/nonzero pattern.

The human mobility model and the virus transmission dynamics is given by system 2.

$$\frac{dS_{Hii}}{dt} = d_H(N_{Hi}^r - S_{Hii}) - g_i S_{Hii} + \sum_{k=1}^n r_{ik} S_{Hik} - \beta_{Hi} \frac{Im_i}{N_{Hi}^p} S_{Hii} \quad (2a)$$

$$\frac{dS_{Hij}}{dt} = g_i m_{ji} S_{Hii} - d_H S_{Hij} - r_{ij} S_{Hij} - \beta_{Hj} \frac{Im_j}{N_{Hj}^p} S_{Hij} \quad (2b)$$

$$\frac{dI_{Hii}}{dt} = -d_H I_{Hii} - g_i I_{Hii} + \sum_{k=1}^n r_{ik} I_{Hik} + \beta_{Hi} \frac{Im_i}{N_{Hi}^p} S_{Hii} - \gamma_H I_{Hii} \quad (2c)$$

$$\frac{dI_{Hij}}{dt} = g_i m_{ji} I_{Hii} - d_H I_{Hij} - r_{ij} I_{Hij} + \beta_{Hj} \frac{Im_j}{N_{Hj}^p} S_{Hij} - \gamma_H I_{Hij} \quad (2d)$$

$$\frac{dR_{Hii}}{dt} = \gamma_H I_{Hii} - d_H R_{Hii} - g_i R_{Hii} + \sum_{k=1}^n r_{ik} R_{Hik} \quad (2e)$$

$$\frac{dR_{Hij}}{dt} = g_i m_{ji} R_{Hii} + \gamma_H I_{Hij} - d_H R_{Hij} - r_{ij} R_{Hij} \quad (2f)$$

$$\frac{dS_{mi}}{dt} = s_L L_i^* - d_m S_{mi} - \sum_{j=1}^n \beta_{mi} \frac{S_{mi} I_{Hji}}{N_{Hi}^p} \quad (2g)$$

$$\frac{dI_{mi}}{dt} = \sum_{j=1}^n \beta_{mi} \frac{S_{mi} I_{Hji}}{N_{Hi}^p} - d_m I_{mi} \quad (2h)$$

In this model, each node is described by $(3n + 2)n$ equations.

3.1.1. Equilibrium of the model

Proposition 3.1. *The nonnegative orthant $\mathbb{R}_+^{(3n+2)n}$ is positively invariant under the flow of (2) and, for all $t > 0$, $S_{Hii} > 0$ and $S_{Hij} > 0$ provided that $g_i m_{ji} > 0$. Moreover, solutions of (2) are bounded.*

Proof. We easily see that solutions of system (2) remain nonnegative. Indeed, it is sufficient to show that for all nonnegative initial condition, the vector-field, for all initial conditions, points out to the interior of the positive orthant. Assume now that $S_{Hii} = 0$ at $t = 0$, then

$$\frac{dS_{Hii}}{dt}(0) = d_H N_{Hi}^r + \sum_{k=1}^n r_{ik} S_{Hik} > 0,$$

which means that $S_{Hii} > 0$. Equally, if $S_{Hij} = 0$ at time $t = 0$, then

$$dS_{Hij}/dt = g_i m_{ji} S_{Hii} > 0.$$

Finally, the boundedness follows from the positive invariance of $\mathbb{R}_+^{(3n+2)n}$ and the constant population property. Indeed

$$\frac{dN_{Hi}^r}{dt} = \frac{dS_{Hi}^r}{dt} + \frac{dI_{Hi}^r}{dt} + \frac{dR_{Hi}^r}{dt} = 0,$$

which means that, for any node i , the resident population is constant, thus by extension, the whole population is constant. Moreover, solutions of (2) are bounded, since $(\mathbb{R}^+)^{(3n+2)n}$ is invariant, human population is constant and vector population is bounded [27]. \square

Definition 3.2. *The system is at an equilibrium if the time derivatives in (2) are zero.*

A node i is at the disease free equilibrium (DFE) if $I_{Hji} = 0$, $I_{mi} = 0$ for all $j = 1, \dots, n$.

The n -nodes model given by (2) is at the DFE if each node is at the DFE, i.e., $I_{Hji} = 0$ and $I_{mi} = 0$, for all $i, j = 1, \dots, n$.

Proposition 3.3. *System (2) always has the following disease free equilibrium:*

$$\begin{aligned} S_{Hii}^* &= \left(\frac{1}{1 + g_i \sum_{k=1}^n \frac{m_{ki}}{d_H + r_{ik}}} \right) N_{Hi}^r, \\ S_{Hij}^* &= g_i \frac{m_{ji}}{d_H + r_{ij}} S_{Hii}^* \\ I_{Hii}^* &= 0, \quad I_{Hji}^* = 0 \\ S_{mi}^* &= \frac{s_L}{d_m} L_i^*, \quad I_{mi}^* = 0, \end{aligned}$$

for all $i, j = 1, \dots, n$, $i \neq j$.

Proof. It is sufficient to remark that

$$1 - \sum_{k=1}^n \frac{m_{ki} r_{ik}}{d_H + r_{ik}} = \sum_{k=1}^n m_{ki} - \sum_{k=1}^n \frac{m_{ki} r_{ik}}{d_H + r_{ik}} = d_H \sum_{k=1}^n \frac{m_{ki}}{d_H + r_{ik}}$$

□

Theorem 3.4. *Assume that system (2) is at an equilibrium and a node i is at the DFE. Then all nodes that can be accessed from node i and all nodes that have an access to node i are at the DFE. Moreover, if the outgoing matrix M^T is irreducible, then all nodes are at the DFE.*

Proof. Assume that node 1 is at the DFE (without loss of generality), i.e. $I_{Hk1} = 0$ for all $k = 1, \dots, n$ and $I_{m1} = 0$. From equation (2c), we have

$$\frac{dI_{H11}}{dt} = \sum_{k=1}^n r_{1k} I_{H1k}.$$

But node $i = 1$ is at the DFE, i.e. $dI_{H11}/dt = 0$, and since $r_{1v} > 0$, for all $v \in V_{1\rightarrow}$, then, $I_{H1v} = 0$ for all $v \in V_{1\rightarrow}$. Consider now equation (2d) with $i = 1$ and let $v \in V_{1\rightarrow}$, then

$$\frac{dI_{H1v}}{dt} = \beta_{Hv} \frac{I_{mv}}{N_{Hv}^p} S_{H1v}.$$

As the system (2) is at an equilibrium point, thus $dI_{H1v}/dt = 0$. However $\beta_{H1} > 0$ and $S_{H1v} > 0$ from proposition 3.1, then $I_{mv} = 0$ for all $v \in V_{1\rightarrow}$.

Finally, we have to show that for all $v \in V_{1\rightarrow}$ and for all $k = 1, \dots, n$, $I_{Hkv} = 0$ i.e., all humans resident of node k and present at node v are not infected. Consider equation (2h) for a node $v \in V_{1\rightarrow}$, then,

$$\frac{dI_{mv}}{dt} = \sum_{j=1}^n \beta_{mv} \frac{S_{mv} I_{Hjv}}{N_{H_i}^p} - d_m I_{mv} = \beta_{mv} \frac{S_{mv}}{N_{H_i}^p} \sum_{j=1}^n I_{Hjv} = \beta_{mv} \frac{S_{mv}}{N_{H_v}^p} I_{H_v}^p = 0.$$

Since $\beta_{mv} > 0$, and from proposition 3.1, $S_{mv} > 0$ then $I_{H_v}^p = 0$, i.e. $\sum_{k=1}^n I_{Hkv} = 0$. It follows that for all $k = 1, \dots, n$, $I_{Hkv} = 0$, since $I_{Hij} \geq 0$ for all $i, j = 1, \dots, n$. Thus, all adjacent nodes to node $i = 1$ are the DFE equilibrium. Moreover, by induction, we obtain that all nodes $v \in \mathcal{A}_{1\rightarrow}$ are at the DFE.

Assume now that M^T is irreducible. From equation (2d) with $j = 1$, we have,

$$\frac{dI_{Hi1}}{dt} = g_i m_{1i} I_{Hi1}.$$

Since system is at the equilibrium $dI_{Hi1}/dt = 0$, beside $g_i m_{1i} > 0$ for $i \in \mathcal{V}_{\rightarrow 1}$, then $I_{Hi1} = 0$ for all $i \in \mathcal{V}_{\rightarrow 1}$. Let $v \in \mathcal{V}_{\rightarrow 1}$, from equation (2c), we have,

$$\frac{dI_{Hvv}}{dt} = \sum_{k=1}^n r_{vk} I_{Hvk} + \beta_{Hi} \frac{I_{mv}}{N_{H_v}^p} S_{Hvv} = 0$$

then $\sum_{k=1}^n r_{vk} I_{Hvk} = 0$ and $\beta_{Hi} \frac{I_{mv}}{N_{H_v}^p} S_{Hvv} = 0$ and $S_{Hvv} > 0$, from proposition 3.1, thus $I_{mv} = 0$ for all $v \in \mathcal{V}_{\rightarrow 1}$. Finally, consider equation (2h) for $v \in \mathcal{V}_{\rightarrow 1}$, we have,

$$\frac{dI_{mv}}{dt} = \beta_{mv} \frac{S_{mv}}{N_{H_v}^p} I_{H_v}^p = 0$$

then $I_{H_v}^p = 0$, i.e. $\sum_{k=1}^n I_{Hkv} = 0$ for all $k = 1, \dots, n$. Thus all nodes are the DFE. \square

Definition 3.5. *The disease is endemic within the population if the number of infective individuals is positive in this population.*

The disease is endemic on node i if there is a population on node i in which the disease is endemic, i.e., there exists $k \in \{1, \dots, n\}$ such as $I_{Hki} > 0$.

Theorem 3.6. Assume that system (2) is at an equilibrium and the disease is endemic on node i . Then the disease is endemic on all nodes that can be reached from node i . In particular, if the matrix M^T is irreducible, then the disease is endemic in all nodes.

Proof. Assume that the disease is endemic in node $i = 1$, i.e. there exists $q \in 1, \dots, n$ such that $I_{Hq1} > 0$. We have to show that, in this case, $I_{H11} > 0$. If $q = 1$ then we can proceed. Assume that $q \neq 1$. Assume by contradiction that $I_{H11} = 0$. Since the system is at the equilibrium, from (2c), we have:

$$0 = \frac{dI_{H11}}{dt} = + \sum_{k=1}^n r_{1k} I_{H1k} + \beta_{H1} \frac{I_{m1}}{N_{H1}^p} S_{H11}$$

Beside $\beta_{Hi} > 0$ and $S_{H11} > 0$ then $I_{m1} = 0$. Thus, from equation (2h), we have,

$$0 = \frac{dI_{m1}}{dt} = \sum_{j=1}^n \beta_{mj} \frac{I_{Hj1}}{N_{Hj}^p} S_{mj}$$

Beside $\beta_{mi} > 0$ and $S_{mi} > 0$ then $I_{Hj1} = 0$ for all $j = 1, \dots, n$, which is a contradiction. We have $I_{H11} > 0$, if the disease is endemic in node 1, which we now assume.

Consider equation (2d) with $i = 1$ and $j \neq i$. Assume $I_{Hij} = 0$. Since the system is at equilibrium, we have,

$$0 = \frac{dI_{Hij}}{dt} = g_1 m_{j1} I_{H11} + \beta_{Hj} \frac{I_{mj}}{N_{Hj}^p} S_{Hij}.$$

If $j \in \mathcal{V}_{1 \rightarrow}$ then $g_1 m_{j1} > 0$ thus $I_{Hii} = 0$, which is a contradiction. Finally $I_{H1j} > 0$ for all $j \in \mathcal{V}_{1 \rightarrow}$, which means that the disease is endemic. Particularly, we deduce that $I_{Hjj} > 0$ from the first part of the proof. By continuing, we can show that the disease is endemic in all nodes $j \in \mathcal{A}_{1 \rightarrow}$, that is to say, nodes reachable from node 1. \square

3.2. The vector mobility model

Contrary to human displacements, it is unrealistic to identify mosquitoes by their origin and destination. Nevertheless, we know that *Aedes albopictus* mosquitoes have a limited flight range. Most mosquitoes disperse less than two hundred meters away from their original breeding place [33, 34]. Indeed, mosquitoes present in a node i may have an activity in neighboring nodes j ,

depending on their proximity (defined later). Metapopulation models of the spread of vector borne diseases (see for instance [35, 36]) that include human long-distance displacements, do not take into account mosquito mobility. In our case of daily movements and very precise resolution, we cannot neglect the influence of mosquitoes displacements. We propose to model this activity using the biological radius of interaction around their breeding sites. Let us denote by d_{ij} the distance between nodes i and j and by d_{max} the maximum interaction radius of mosquitoes (approximately 200 m). In particular, we have $d_{ii} = 0$ for all $i = 1, \dots, n$. Now we assume that mosquitoes originated from node i interact with population of node j , according to a function of the distance linearly decreasing. This function is given by

$$\psi(d_{ij}) = \begin{cases} \frac{d_{max} - d_{ij}}{d_{max}} & \text{if } d_{ij} < d_{max} \\ 0 & \text{else} \end{cases} \quad (3)$$

Then, model (2) becomes

$$\frac{dS_{Hii}}{dt} = d_H(N_{Hi}^r - S_{Hii}) - g_i S_{Hii} + \sum_{k=1}^n r_{ik} S_{Hik} - \sum_{k=1}^n \beta_{Hi} \psi(d_{ik}) \frac{Im_k}{N_{Hi}^p} S_{Hii} \quad (4a)$$

$$\frac{dS_{Hij}}{dt} = g_i m_{ji} S_{Hii} - d_H S_{Hij} - r_{ij} S_{Hij} - \sum_{k=1}^n \beta_{Hj} \psi(d_{ik}) \frac{Im_k}{N_{Hj}^p} S_{Hij} \quad (4b)$$

$$\frac{dI_{Hii}}{dt} = -d_H I_{Hii} - g_i I_{Hii} + \sum_{k=1}^n r_{ik} I_{Hik} + \sum_{k=1}^n \beta_{Hi} \psi(d_{ik}) \frac{Im_k}{N_{Hi}^p} S_{Hii} - \gamma_H I_{Hii} \quad (4c)$$

$$\frac{dI_{Hij}}{dt} = g_i m_{ji} I_{Hii} - d_H I_{Hij} - r_{ij} I_{Hij} + \sum_{k=1}^n \beta_{Hj} \psi(d_{ik}) \frac{Im_k}{N_{Hj}^p} S_{Hij} - \gamma_H I_{Hij} \quad (4d)$$

$$\frac{dR_{Hii}}{dt} = \gamma_H I_{Hii} - d_H R_{Hii} - g_i R_{Hii} + \sum_{k=1}^n r_{ik} R_{Hik} \quad (4e)$$

$$\frac{dR_{Hij}}{dt} = g_i m_{ji} R_{Hii} + \gamma_H I_{Hij} - d_H R_{Hij} - r_{ij} R_{Hij} \quad (4f)$$

$$\frac{dS_{mi}}{dt} = s_L L_i - d_m S_{mi} - \sum_{k=1}^n \beta_{mi} \psi(d_{ik}) \frac{S_{mi}}{N_{Hk}^p} I_{Hk} \quad (4g)$$

$$\frac{dI_{mi}}{dt} = \sum_{k=1}^n \beta_{mi} \psi(d_{ik}) \frac{S_{mi}}{N_{Hk}^p} I_{Hk} - d_m I_{mi} \quad (4h)$$

$$\frac{dE_i}{dt} = b(S_{mi}(t) + I_{mi}(t)) \left(1 - \frac{E_i(t)}{K_{Ei}}\right) - (s + d) E_i(t) \quad (4i)$$

$$\frac{dL_i}{dt} = s E_i(t) \left(1 - \frac{L_i(t)}{K_{Li}}\right) - (s_L + d_L) L_i(t) \quad (4j)$$

4. Application

Willing to validate this approach, this section proposes a comparison of this model with a real-life example of chikungunya epidemic, namely, the event that occurred in 2005-2006 on the Réunion Island, Indian Ocean. This

validation process makes a strong usage of real and realistic data, to reflect as much as possible the original environment. From the environment point of view, geographical data is used to construct the metapopulation network. From the epidemic point of view, results generated with our model are compared with real logs of the 2005-2006 epidemic.

This section focusses on the modeling of the Réunion Island scenario with our metapopulation approach. The accuracy of the model goes through the construction of a realistic network where considered populations (humans and mosquitoes) are spread. Then the mobility of these populations is also modeled.

4.1. Distribution of the Human Population

The Réunion Island is a mountainous region and the local population is not uniformly spread over the land. The population density is of course higher in cities but also along the shore and in regions at low altitude. To reflect this particular density in the metapopulation model, we need realistic information. We rely here on two sources of information. The first source is of high confidence but has a low granularity while the second source of information is more hypothetic but also has a finer grain.

We first rely on data from the French Institution for Statistics (INSEE) which gives access to an estimated density of the population, based on a mesh zoning of the space [37]. This zoning consists in squares of one kilometer long. In each square, the number of people living in are estimated based on both tax cards and cadastral data. this estimation gives a very precise overview of the distribution of populations, up to one square kilometer. Figure 3 shows these $1km^2$ squares with their associated population.

There is a good confidence in the quality of this data and it could be used as an input to create our metapopulation model. However the limited granularity of one square kilometer is not precise enough for our purpose. Indeed, this model envisions to consider interactions at lower scale, with local interactions between humans and mosquitoes. The range of interaction of a mosquito being in the order of a couple hundreds of meters, the INSEE source of information is not precise enough.

To have a thinner-gain estimation of the population's density, a hypothesis is to consider the road network as a proxy to the population's density. In this idea, the road network is denser where the population is dense and lighter where no one lives. Finally we propose to use the road network and especially crossroads as the set of nodes that constitute the metapopulation

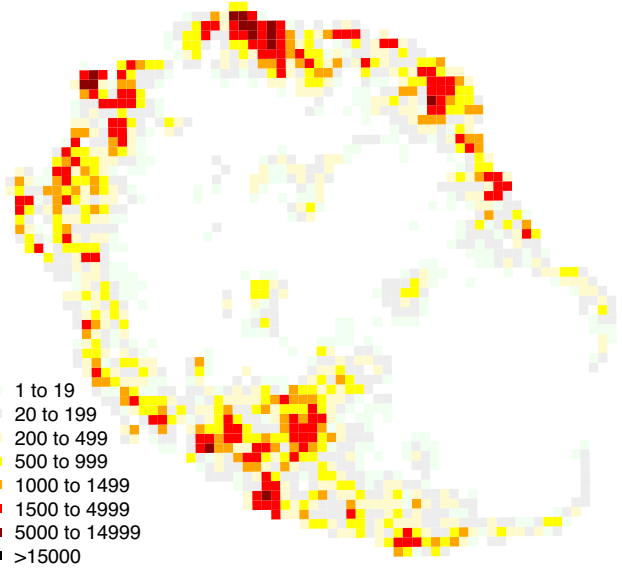


Figure 3: Estimated population distribution of the Réunion in 2007, according to the French Institution for Statistics (INSEE), on a 1km^2 granularity.

model. This network is extracted from the OpenStreetMap (OSM) project [38].

To validate this approach we propose a first version of the metapopulation network with a uniform distribution of the population over the node of this network. The approximatively 750 000 inhabitants of the island are evenly distributed on the approximatively 18 000-nodes network. This distribution is compared using the same method used by the French Institution for Statistics (INSEE), with a 1km -scaled mesh zoning. Figure 4 compares the INSEE real spread with this first model. This first approximation reveals a first global validation of the model. As can be observed on Fig. 4, the general spread looks alike the real data. However, some flaws appear in precise areas.

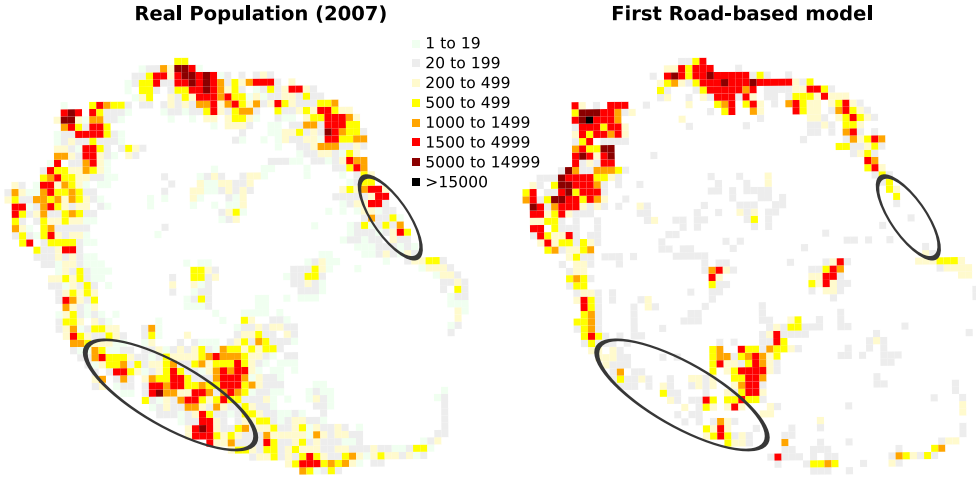


Figure 4: Comparison between the real population spread and a first road-based model where the population is uniformly spread over the nodes of our network. Oval shapes show zones where the density of the road network is not appropriated.

Flaws of this first model can be explained by two phenomenon. First, it is simply possible that the heuristic of using road intersections as a proxy to the human population is inappropriate. The second reason may come from the quality of the road map used. Indeed, some flows appear in the the OSM road network. This is explained by the nature of roads in the Réunion Island that usually are simple trails that are not properly classified by the OSM project.

Those flaws can be adjusted. Indeed, the INSEE's densities can be used at the scale of a square kilometer for the spread of the population on the population nodes. Each node of our model belongs to one of the squares of the INSEE model, so, given such a square, we can select the set of nodes associated to it and distribute, among these nodes, the local population of this square. If a square has no node associated to it (it appears on low density areas) then a node is created for this particular square. This gives a spread for the population that is as good as the real INSEE data at the scale of the square kilometer. Finally our model is at least as precise as the real INSEE data at the 1km scale but the resolution goes below the 1km limit, thanks to the crossroad/node analogy. Figure 5 illustrates the main steps of the construction of the model.

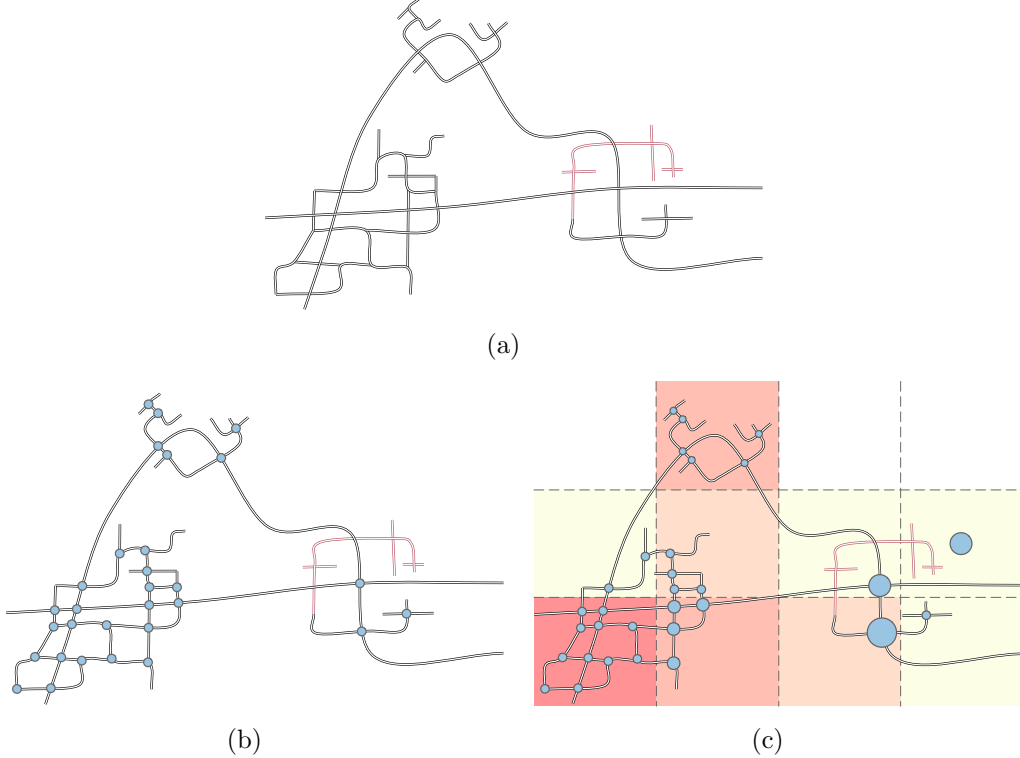


Figure 5: Schematic steps of the construction of the metapopulation network. 5(a), start from the OSM road network and knowing that this network may not be totally accurate (red roads missing in the map). 5(b), network nodes are associated to road crossroads of the known OSM road network. 5(c), Comparison with real data from the INSEE (French Institution for Statistics) and distribution of the population on nodes according to the INSEE data. Empty cells (with no known road network) are given one node (as in Fig. 5(c), rightmost cell, second row).

4.1.1. Distribution of the Mosquito Population

Unlike the human population, no information about the density of mosquito population is available. Moreover, we are not interested in the whole population but rather in the part of it that interacts with humans. Our hypothesis is that the density of mosquitoes is homogeneous. As seen previously, the network's node density reflects the human density which is not homogeneous. Setting an equal quantity of mosquitoes on each node would also lead to a non-homogeneous density.

To retrieve the desired density, each node is given a number of mosquitoes (through the carrying capacities) proportional to the geographical surface

associated with each node. To compute the geographical surface associated with each node, a simple Voronoï tessellation is computed on the nodes of the metapopulation network.

Since we only consider mosquitoes that interact with humans, the surface is upper-bounded with the disk of radius d_{max} that expresses the maximum interaction distance for a mosquito along it's life.

Let S_i be the surface of node i computed thanks to the Voronoï tessellation on the network. Let $S_{max} = \pi d_{max}^2$ be the surface associated with the maximal interaction radius d_{max} . Carrying capacities for each node are then set as follows:

$$\begin{aligned} K_{E_i} &= K_E \varphi(S_i), \\ K_{L_i} &= K_L \varphi(S_i), \end{aligned}$$

with K_E and K_L , constants for the carrying capacities of eggs, respectively larvae and $\varphi(S_i)$ as follows:

$$\varphi(S_i) = \begin{cases} \frac{S_i}{S_{max}} & \text{if } S_i < S_{max} \\ 1 & \text{else} \end{cases}$$

4.1.2. Human Mobility

In our model, humans trips are given by outgoing matrix M^T and incoming matrix R and represent for any pair i and j , the probability for humans living on i to go to j . Non-null values in the matrix define edges between nodes in our metapopulation network.

Our aim in this application of the model is to propose realistic patterns for human mobility on the Réunion Island. To reach realistic motion we need to rely on realistic data or model for human mobility. Unfortunately, we could not rely on real human mobility data from the Island, so we have to rely on a more general human mobility model.

To do so, we consider the analysis work of González, Hidalgo and Barabási [28] where the authors consider real data that can be associated to the real mobility of humans. Indeed they observe the mobile phone communication logs of 100,000 users. These logs register the geographical position of these mobile phones when calls append or when texts are emitted/received. Mobile phones are a good proxy to the human mobility because users always carry their phone.

The authors after studying a huge amount of communication logs were able to produce general laws on observed mobility patterns. These results give general formulas that describe the mobility observed. Our hypothesis is that these formulas can then be used to generate new human mobility patterns. We finally consider the three following measures for the creation of our mobility model.

Trips length. Analyzing the distance between 2 consecutive phone calls for each mobile phone, the authors could approximate the distribution of the length of a human trip Δr in kilometer according to the following power law:

$$P(\Delta r) = (\Delta r + \Delta r_0)^{-\beta} \exp(-\Delta r/\kappa) \quad (5)$$

where $\Delta r_0 = 1,5km$ is the cutoff value of the law and $\kappa = 80km$.

Presence probability. For one given individual (one mobile phone) and a finite number N of destinations, the authors observe the duration spent in each of these destinations. Let X be the random variable describing the duration of a visit by an individual. If destinations are decreasingly sorted according to the time spent on them, and if k is their according rank, then this time spent follows a Zipf law

$$f(k; N) = \frac{1/k}{\sum_{n=1}^N (1/n)}.$$

Finally we obtain an estimation of the time spent in each of these destinations.

Return probability. Given a destination, the authors observe the return probability of individuals. The result is that there is a peak of probability of returning to the same place every 24h hours. In other words González, Hidalgo and Barabási observe that the human mobility mainly follows a daily pattern such as home/work trips.

From these measures carried out by the authors, we are able to propose a mobility model for the human population leaving on the Réunion Island. Indeed, the trips length, the destination distribution and the return probability formulas are used to generate artificial per-individual trips on the island that respect the observed properties in the original data set.

To fit the mobility matrices (M^T and R) and the network approach of our model, human mobility from node i to node j is represented as a weighted

directed edge from i to j . The weight of the edge is a non-null coefficient in matrices. If no edge exists between i and j , the corresponding coefficient is null in matrices M^T and R . Figure 6 illustrates such links showing the mobility of humans.

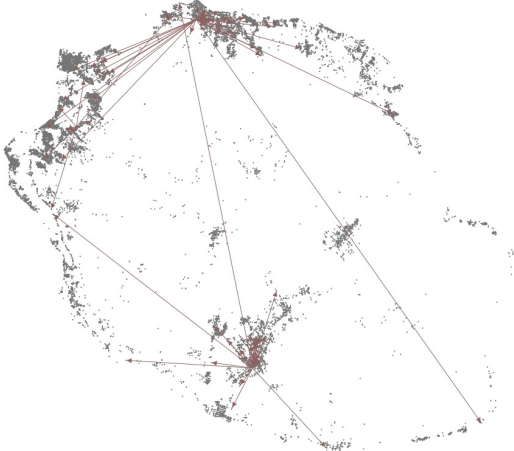


Figure 6: The metapopulation node network with some edges showing human mobility. For sake of readability, only three starting nodes are show on this example.

Remark 2. Our model defines matrices M^T and R as tables indicating respectively departures and returns. The Mobility model we could create out from [28] however does not give departures and returns for each human, but instead gives access to the probability of presence for a human given all of its destinations. Our hypothesis here is that there is a link between first, departures and returns probabilities and second, presence probabilities. Hereafter the values in our coefficients define this human's probability of presence.

4.1.3. Mosquito Mobility

As stated in the model description, it is unrealistic and would be impossible to identify mosquitoes by their origin and destination. Since we are aware of their limited flight range, their mobility is thus defined by a geographical circular area of interaction centered in their origin node. Function (3) defines their interaction with humans.

Back to the metapopulation network, this new mobility pattern is constructed with edges linking nodes that are below the interaction range d_{max} . This leads to very dense connections where node are geographically close one

another, and oppositely, sparse areas where the network is not dense. Figure 7 shows a subset of the metapopulation network with the mosquito mobility edges.

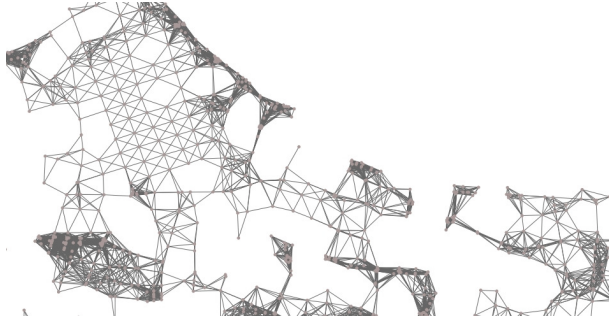


Figure 7: Closeup on a part of the metapopulation network with edges showing mosquito mobility.

5. Results

In this section we show and discuss results of the simulation of our metapopulation model applied to the scenario of the Réunion Island described in the previous section. Our results are then compared with real data from the 2005-2006 epidemic event.

5.1. Analysis of the Metapopulation Network

The metapopulation network can be represented by two graphs sharing the same set of nodes, or in other words it is a graph with 2 subsets of edges, one for human mobility and one for mosquito mobility. The purpose of Table 2 is to give some metrics for those two graphs to give a general overview of theirs dimension. Indeed due to its size no visualization of the all network is proposed since it doesn't give any useful information.

5.2. Spread of the Disease in the Network

The spread of the disease follows some geographical pattern. With the use of a network to model the environment we believe that we can approach the natural spread.

To illustrate this phenomenon we propose a scenario where one infected individual is put on one node of the network. Provided infection parameters

Table 2: Some metric for the two graphs of the metapopulation network

	Mosquitoes	Humans
number of nodes	17988	17988
number of links	151772	744313
average degree	≈ 17	≈ 83
connectivity	no (1729 connected components)	yes
diameter	71 (for the biggest component)	15

(β_H and β_m) are set high enough, the insertion of this individual in a system at disease-free equilibrium may start an epidemic event. Three nodes of the network are then monitored: the first node where the individual has inserted, secondly, a one-hop neighbor node, and third, a farther node located 6km from the insertion node. Four metrics are observed: susceptible humans (S_H), susceptible mosquitoes (S_m), infected humans (I_H), and infected mosquitoes (I_m).

Figure 8 shows the results of this scenario. As expected a shift in the evolution is observed from the closest nodes to the infection to the farther one : the epidemic peak appears first on the local node then on the neighbor node, quickly followed by the third one. It is worth noticing that the shift (and thus the spread of the disease) is not proportional to the distance between nodes. In terms of graph distance, the third observed node is 60 hops far from the insertion node in the mosquito mobility graph. But if the human mobility graph is considered, then this node is only 4 hops away from the first node. In this context, the human mobility greatly speeds up the spread.

5.3. Consequences of the Mosquito Mobility

As stated in the introduction, most of the metapopulation works about the vector-borne viruses focus on long distance and long duration journeys for the human population. In those models the vector mobility can easily be ignored. Here we consider that human mobility is daily based and journeys are shorter. We believe that this shorter scale in time and space brings the new constraint that mosquito mobility cannot be neglected anymore.

The effect produced by local mosquito interaction can be seen as a diffusion phenomenon and may actually be considered with a real diffusion process in the future.

The effect is shown in our model with a scenario where, similarly to the previous scenario, an infected human is inserted into the whole Réunion

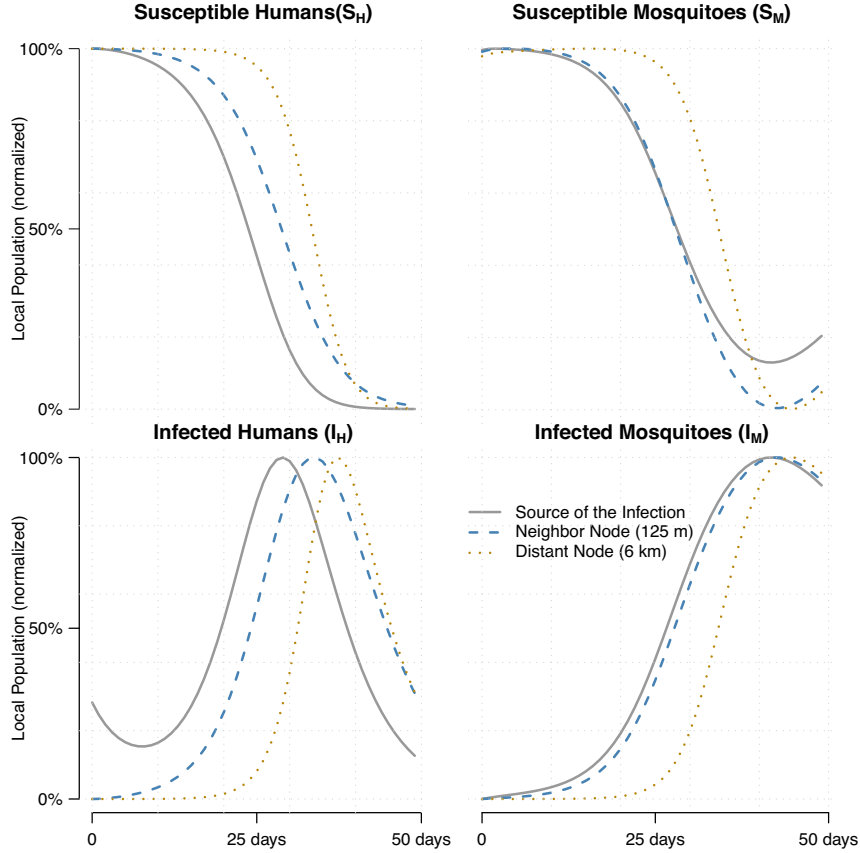


Figure 8: Spread of the disease in the network for three observed nodes. The first node gets the infected human. The second node is an immediate neighbor (125m away from first node). The third node, 6km away from the first node, is 60 hops away in the mosquito mobility graph and 4 hops away in the human mobility graph. Quantities of population (y-axis) are normalized. A wave effect in the spread is observed: the first node is infected then the second, then the third.

Island population. Two experiments are carried out, one with the mobility of humans and mosquitoes enabled, and one where only humans move, not mosquitoes who only interact with humans present on their node and not with the neighboring ones.

Figure 9 shows the results of this experiment on the number of instantaneous infected humans (I_H). Results show that the infection starts rapidly and is concentrated with mosquito mobility enabled. Oppositely, without this mobility, the spread takes more time to start and the peak is less impor-

tant. It is clear with this example that mosquito mobility at this scale has to be considered.

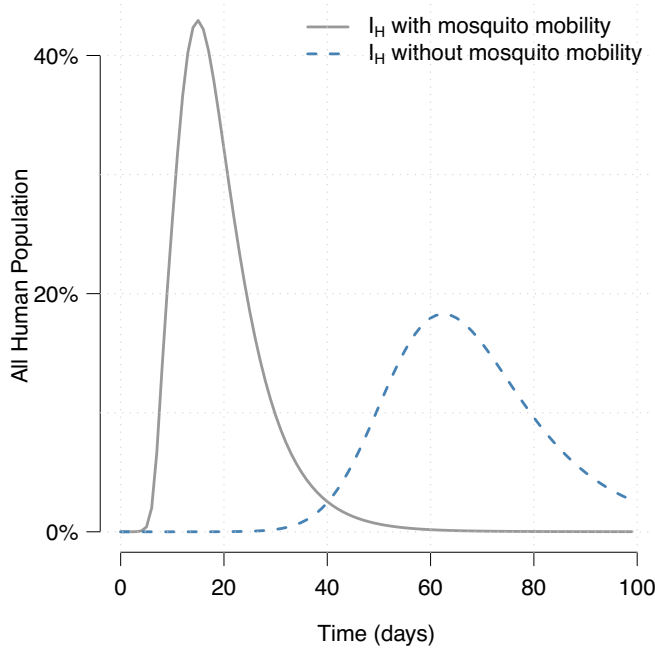


Figure 9: Effect of mosquito mobility of the spread of an epidemic. Evolution of the number of infected humans (I_H) with and without mosquito mobility. In order to obtain comparable results, infection rates as set to a relatively high level: $\beta_H = 0.2$ $\beta_m = 0.15$.

5.4. Consequences of the Human Mobility

Consequences of the human mobility are important on the obtained results. The purpose is not to observe the system with and without the human mobility, which would give obvious results, but rather to analyze more realistic and slight modifications of this mobility. In case of a real life epidemic, one can imagine that authorities would take quarantine measure in order to limit the spread. To imitate this kind of measures, this scenario proposes to stop the human mobility on infected parcels. So quarantine measures will be localized only on nodes where a given threshold of infection is reached. In this hypothesis, only the mobility of human is changed. In quarantined nodes inhabitants are not allowed to move out. Moreover no foreigners are allowed to visit in. Considering vectors, their are not stopped by quarantine

measures and continue to interact whether they come from these nodes or from neighbor ones.

Figure 10 shows global instantaneous and cumulated infections values for humans at the scale of the all population. Simulation results show that it is possible to act on the spread of the disease. This effect depends on the threshold of infection (percentage of local inhabitants that are infected) at which nodes are decided as quarantined. In this scenario, characteristics of the disease would, without any control, reach 35% of the population, just like the chikungunya event of 2005-2006.

The first outcome shown by Fig. 10 is the possibility to rapidly reduce the instantaneous infection rate. For instance, the peak of this rate is almost divided by two when the quarantine threshold is set to 10%. However looking at cumulated infection cases (seroprevalence), we see that such a threshold does not significantly reduces the total amount of people getting infected during the event. To expect a real effect on the total number of infections one have to set the threshold below 1%. In our example, each node on average has less than 50 humans, so any threshold below 2% is technically impossible to achieve.

5.5. Parameters Analysis

The identification of predominant parameters of the system is needed to understand its behavior. We propose here a numerical analysis of the parameters of the system. An in depth statistical sensitivity analysis or a study or the analytical estimation of parameters would be of great interest too, but are out of the scope of this paper.

Among the various parameters that rule the system, some drive the populations dynamics, some drive their mobility and others deal with the transmission model. We focus on the infection rates parameters β_H (mosquitoes to humans) and β_m (humans to mosquitoes) that have a strong impact on the results. Figure 11 shows the effect of those two parameters on the seroprevalence. Depending on the values selected for β_H and β_m , the infection goes from some few isolated cases to an epidemic that contaminates the whole population.

In Fig. 12 another representation shows a scatter plot of values taken by β_H and β_m . For each couple (β_H, β_m) the seroprevalence (after 400 days of epidemic) is observed. Values in percentage represent the ratio of the total human population ever infected depending on the two parameters. Contour

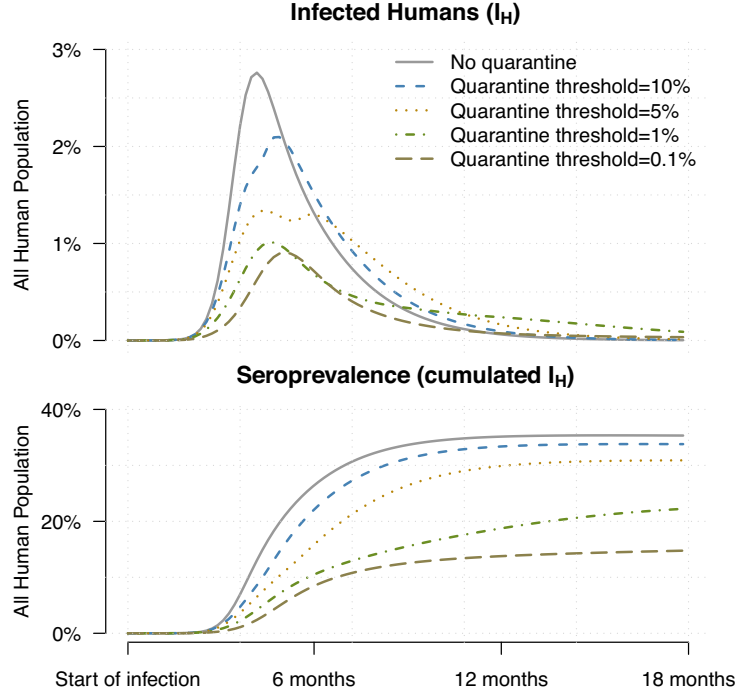


Figure 10: Consequences of the human mobility. The instantaneous number of infected humans and the seroprevalence (or number of people ever infected) are observed during an epidemic. Infection values depend on the quarantine threshold that reduce, node per node, the human mobility, over the time. A threshold of 10% indicates that a node with an infection rate of at least 10% will be quarantined (incoming and outgoing human mobility are blocked).

lines help finding, given a seroprevalence percentage, values for β_H and β_m . These values are used in the next subsection.

5.6. Validation against real data

In the final part of this work a validation of the model with a comparison to real data is investigated. As already stated, the focus is put on the 2005-2006 chikungunya epidemic of the Réunion Island. The two first cases of chikungunya were reported at the beginning of March 2005. The disease propagated during the following weeks and reached a peak at mid of May. The number of new cases then started to decrease until authorities thought the event was over at the end of the year 2005 with a seroprevalence (total number of cases) of 6,000 people. But in the second half of December 2005 the

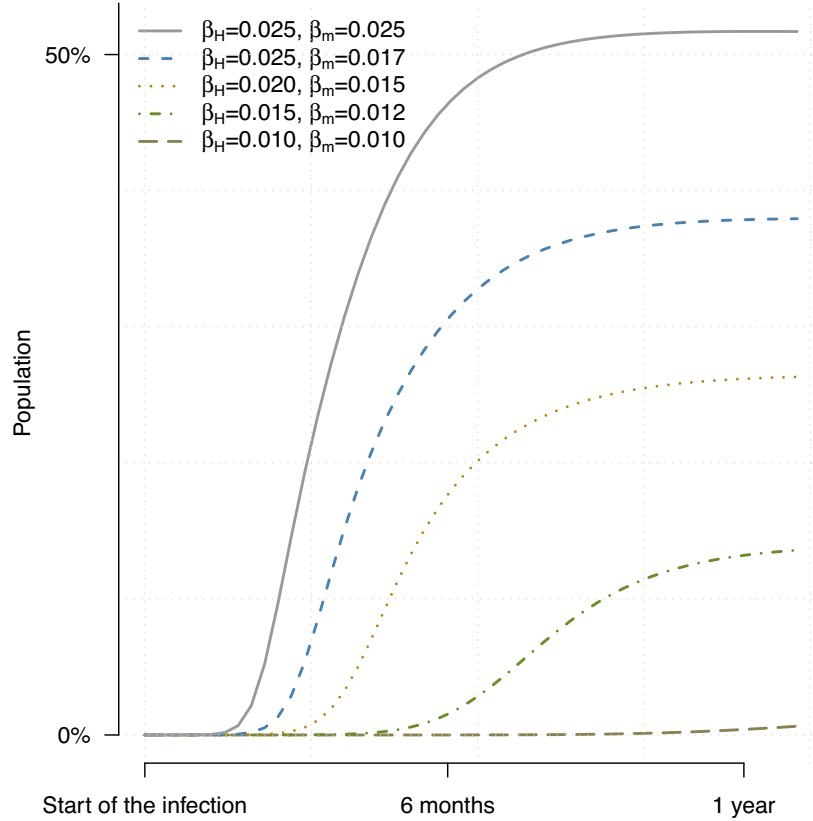


Figure 11: Effect of the β_H and β_m parameters on the seroprevalence. The infection greatly varies from a few cases to a total epidemic, depending on these values.

spread started over with a strength that was not comparable to the previous peak. This second event reached a peak in February 2006 with more than 47,000 cases in a week. This sudden reactivation of the spread was later explained by a genetic mutation of the virus that changed the way it could adapt to the mosquito. This mutation allowed the virus to be redistributed by the host only two days after its infection instead of 7 days before the mutation. After the peak, the number of cases slowly started to decrease. The epidemic was declared over by April 2006. In the end, the INVS (French Institute for Health Care) counted 265,733 cases of chikungunya from March 2005 to April 2006. This represents more than 35% of the total population of the Island.

The following results are compared to real data indicating, week per week,

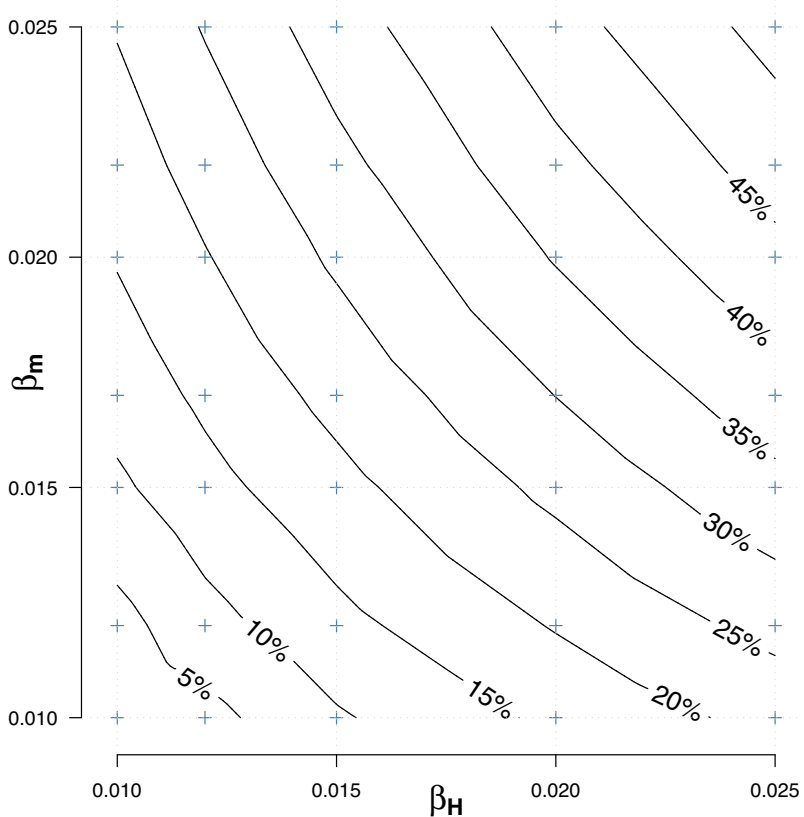


Figure 12: Effect of the β_H and β_m parameters on the seroprevalence. Blue crosses are values obtained by simulation. Contour lines are obtained with a bilinear interpolation of these data points.

new cases of the disease. This information was kindly provided by the INVS.

Back to our model, such a genetic mutation changing the incubation period is expressed thanks to infection rates β_H and β_m . We try to reproduce the all event by starting the simulation of the epidemic with one set of parameters, and then, by changing once only once the values of β_H and β_m at the moment it appears in the real event. The two sets of parameters where selected experimentally with the help of the previous study (see Fig. 12) giving possible values for β_H and β_m for a given seroprevalence.

From the real data, the seroprevalence at the time of the mutation (2006-12) was around 7,000 cases. We refer the results shown in 12 to retrieve a couple of β_H and β_m giving a seroprevalence of 7,000 cases after 300 days.

With the same approach values are found for seroprevalence stabilized at 265,733 cases. We obtain the two sets of parameters for β_H and β_m : 0.0118 and 0.0101 before the mutation and 0.0245 and 0.0161 after the mutation.

Figure 13 compares the evolution of the real seroprevalence of the chikungunya on the Réunion Island from March 2005 to May 2006, with simulation results obtained with our model. Although the two curves do not fit perfectly, it allows a visual overall validation of the model.

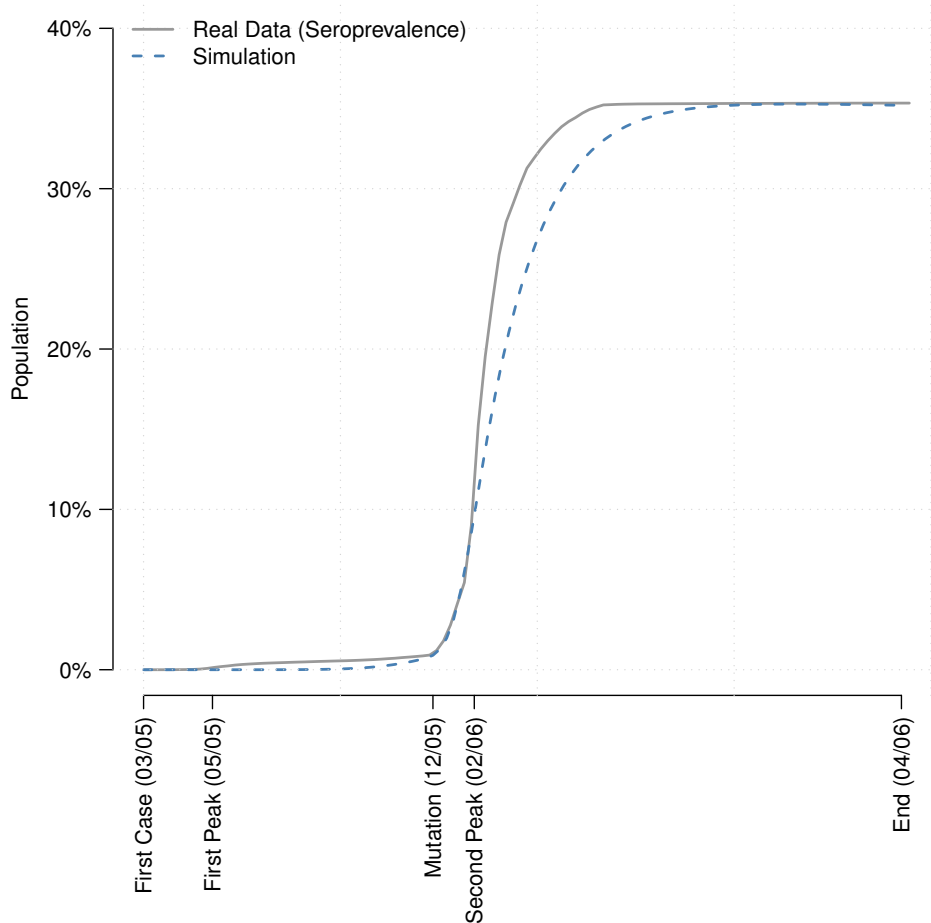


Figure 13: Comparison of the model with real data. The seroprevalence is considered for the duration of the Réunion Island epidemic. Real data provided by the INVS and simulation results from or model visually look alike though do not totally fit. Values of β_H and β_m are 0.0118 and 0.0101, before the mutation event and 0.0245 and 0.0161, after. Those two couples (β_H, β_m) are chosen thanks to the study in section 5.5.

These results are a first step in the validation of this approach. In these experiments, only infection rates were investigated. Of course, other parameters need to be considered. Especially those leading the human mobility. Moreover the metapopulation approach needs to be validated at a lower scale than the scale of the all Island. These last observations form the perspectives of this work.

6. Conclusion

In this work the main concern was to try to validate dynamical systems for the spread of a vectorial disease against a real epidemic scenario. We focused on the Réunion Island's epidemic that occurred in 2005-2006.

Many issues appear when trying to bridge the gap between global models and real life problems. Among them we chose to focus on the modeling of populations' mobilities. This logically implied a realistic modeling of environment, bringing us from temporal modeling to spatio-temporal modeling.

Designed to consider spatial interactions, the theory of metapopulations allows the special geographical environment of the Island to be included into the original model. This metapopulation network was created based on real geographical and demographical data. It could then handle local interactions between nodes and thus allow populations mobilities to become part of the model too.

We proposed two mobility models. The first one, for humans, is based on the analysis of real human mobility data sets (mobile phones probes). The second model, for mosquitoes, is based on local interactions between nodes.

After various studies of the consequences of mobilities on the spread of the disease, and after an analysis of the parameters of the system, a validation of the model against real seroprevalence data from the Réunion epidemic was proposed. Results validate the approach and clearly identify the human mobility as a key parameter in the spread of such an epidemic.

As stated above, the choice in this work was to focus on mobilities. However, other recognized issues play a key role in the all process. For instance, the effect of rain falls and weather seasons are known to directly influence mosquitoes evolution stages (especially aquatic phases). Studying the effect of seasons on the epidemic is definitely a perspective of this work.

Finally, the integration of the metapopulation model and mobilities contributed to increase the complexity of the model. This last model which has only been explored on a numerical bases would need an analytical study.

Acknowledgment

This work would not have been done without the precious help of the French institution for public health (the *Institut de Veille Sanitaire*). The authors are particularly thankful to Ms. Elsa BALLEYDIER epidemiologist at *CIRE Océan Indien, InVS* in Saint Denis, Réunion Island, France, for her help and availability.

- [1] N. G. Gratz, Emerging and resurging vector-borne diseases, Annual Review of Entomology 44 (1) (1999) 51–75. doi:10.1146/annurev.ento.44.1.51.
URL <http://www.annualreviews.org/doi/abs/10.1146/annurev.ento.44.1.51?journalCode=ento>
- [2] R. W. Sutherst, Global change and human vulnerability to vector-borne diseases, Clinical Microbiology Reviews 17 (1) (2004) 136–173. arXiv:<http://cmr.asm.org/content/17/1/136.full.pdf+html>, doi:10.1128/CMR.17.1.136-173.2004.
URL <http://cmr.asm.org/content/17/1/136.abstract>
- [3] S. Knobler, A. Mahmoud, S. Lemon, L. Pray, The Impact of Globalization on Infectious Disease Emergence and Control: Exploring the Consequences and Opportunities, Workshop Summary - Forum on Microbial Threats, The National Academies Press, 2006.
URL http://www.nap.edu/openbook.php?record_id=11588
- [4] P. Martens, L. Hall, Malaria on the move: human population movement and malaria transmission., Emerging Infectious Diseases 6 (2) (2000) 103–109.
URL <http://www.ncbi.nlm.nih.gov/pmc/articles/PMC131013/>
- [5] N. T. J. Bailey, Spatial models in the epidemiology of infectious diseases, in: Biological growth and spread (Proc. Conf., Heidelberg, 1979), Vol. 38 of Lecture Notes in Biomath., Springer, Berlin, 1980, pp. 233–261.
- [6] J. Murray, Mathematical biology: I. An introduction, Springer New York, 2002.
- [7] J. Murray, Mathematical Biology II: Spatial Models and Biomedical Applications, 3rd Edition, Springer-Verlag, 2002.

- [8] W. E. Fitzgibbon, M. Langlais, A diffusive S.I.S. model describing the propagation of F.I.V, *Commun. Appl. Anal.* 7 (2-3) (2003) 387–403.
- [9] W. E. Fitzgibbon, M. Langlais, J. J. Morgan, A reaction-diffusion system modeling direct and indirect transmission of diseases, *Discrete Contin. Dyn. Syst. Ser. B* 4 (4) (2004) 893–910. doi:10.3934/dcdsb.2004.4.893.
URL <http://dx.doi.org/10.3934/dcdsb.2004.4.893>
- [10] R. Levins, Some demographic and genetic consequences of environmental heterogeneity for biological control, *Bull. Entomol. Soc. Am.* (15) (1969) 237–240.
- [11] Dushoff, S. Levin, The effects of population heterogeneity on disease invasion., *Mathematical Biosciences* 128 (1-2) (1995) 25–40.
- [12] W. Wang, X.-Q. Zhao, An epidemic model in a patchy environment, *Mathematical Biosciences* 190 (1) (2004) 97 – 112. doi:10.1016/j.mbs.2002.11.001.
URL <http://www.sciencedirect.com/science/article/pii/S0025556404000719>
- [13] A. L. Lloyd, R. M. May, Spatial heterogeneity in epidemic models, *Journal of Theoretical Biology* 179 (1) (1996) 1–11. doi:10.1006/jtbi.1996.0042.
- [14] V. Colizza, A. Vespignani, Epidemic modeling in metapopulation systems with heterogeneous coupling pattern: Theory and simulations, *Journal of Theoretical Biology* 251 (3) (2008) 450 – 467. doi:10.1016/j.jtbi.2007.11.028.
URL <http://www.sciencedirect.com/science/article/pii/S0022519307005991>
- [15] C. Cosner, J. Beier, R. Cantrell, D. Impoinvil, L. Kapitanski, M. Potts, A. Troyo, S. Ruan, The effects of human movement on the persistence of vector-borne diseases, *Journal of Theoretical Biology* 258 (4) (2009) 550 – 560. doi:10.1016/j.jtbi.2009.02.016.
URL <http://www.sciencedirect.com/science/article/pii/S0022519309000757>

- [16] D. Balcan, B. Gonçalves, H. Hu, J. J. Ramasco, V. Colizza, V. Vespignani, Modeling the spatial spread of infectious diseases: The global epidemic and mobility computational model, *Journal of Computational Science* 1 (3) (2010) 132 – 145. doi:DOI: 10.1016/j.jocs.2010.07.002.
 URL <http://www.sciencedirect.com/science/article/B9HC1-50M1S3K-2/2/d91e1d3f081c30c1f916b27b7a54cfc2>
- [17] I. M. Longini Jr, A mathematical model for predicting the geographic spread of new infectious agents, *Mathematical Biosciences* 90 (1-2) (1988) 367 – 383. doi:DOI: 10.1016/0025-5564(88)90075-2.
 URL <http://www.sciencedirect.com/science/article/B6VHX-45F63KS-7Y/2/1aa65d351e772dd62dc489424e8c7037>
- [18] L. A. Rvachev, I. M. Longini Jr, A mathematical model for the global spread of influenza, *Mathematical Biosciences* 75 (1) (1985) 3 – 22. doi:DOI: 10.1016/0025-5564(85)90064-1.
 URL <http://www.sciencedirect.com/science/article/B6VHX-45FSKW0-7R/2/d91967ba3c72cf5a34f22a96398b9ae1>
- [19] J. Arino, Diseases in metapopulations, in: Z. Ma, Y. Zhou, J. Wu (Eds.), *Modeling and Dynamics of Infectious Diseases*, Vol. 11 of Series in Contemporary Applied Mathematics, World Scientific, 2009, pp. 65–123, also CDM Preprint Series report 2008-04.
- [20] J. Arino, J. Davis, D. Hartley, R. Jordan, J. Miller, J. van den Driessche, A multi-species epidemic model with spatial dynamics, *Mathematical Medicine and Biology* 22 (2) (June 2005) 129–142. arXiv:<http://imammb.oxfordjournals.org/content/22/2/129.full.pdf+html>, doi:10.1093/imammb/dqi003.
 URL <http://imammb.oxfordjournals.org/content/22/2/129.abstract>
- [21] J. Arino, P. van den Driessche, A multi-city epidemic model, *Mathematical Population Studies* 10 (2003) 175–193. doi:10.1080/08898480306720.
- [22] A. Menach, F. E. McKenzie, A. Flahault, D. Smith, The unexpected importance of mosquito oviposition behaviour for malaria: non-productive larval habitats can be sources for malaria transmission, *Malaria Journal* 4 (1) (2005) 23. doi:10.1186/1475-2875-4-23.
 URL <http://www.malariajournal.com/content/4/1/23>

- [23] D. L. Smith, J. Dushoff, F. E. McKenzie, , PLoS Biol 2 (11) (2004) e368. doi:10.1371/journal.pbio.0020368.
URL <http://dx.doi.org/10.1371/journal.pbio.0020368>
- [24] P. Auger, E. Kouokam, G. Sallet, M. Tchuente, B. Tsanou, The ross-macdonald model in a patchy environment, Mathematical Biosciences 216 (2) (2008) 123 – 131. doi:DOI: 10.1016/j.mbs.2008.08.010.
URL <http://www.sciencedirect.com/science/article/B6VHX-4TC353M-1/2/03a39a13b8c555560bf5d88d69e4a687>
- [25] R. Ross, The Prevention of Malaria by Ronald Ross, Murray, London, 1910.
- [26] L. W. Hackett, The epidemiology and control of malaria, Am J Trop Med Hyg 7 (5) (1958) 577–578. arXiv:<http://www.ajtmh.org/cgi/reprint/7/5/577-b.pdf>.
URL <http://www.ajtmh.org/cgi/content/abstract/7/5/577-b>
- [27] D. Moulay, M. Aziz-Alaoui, M. Cadivel, The chikungunya disease: Modeling, vector and transmission global dynamics, Mathematical Biosciences 229 (1) (2011) 50–63.
- [28] M. C. González, C. A. Hidalgo, A. Barabási, Understanding individual human mobility patterns, Nature 453 (7196) (2008) 779–782.
URL <http://dx.doi.org/10.1038/nature06958>
- [29] J. Cui, Y. Takeuchi, Y. Saito, Spreading disease with transport-related infection, Journal of Theoretical Biology 239 (3) (2006) 376–390. doi:10.1016/j.jtbi.2005.08.005.
URL <http://www.sciencedirect.com/science/article/pii/S002251930500336X>
- [30] O. Diekmann, J. A. P. Heesterbeek, J. A. J. Metz, On the definition and the computation of the basic reproduction ratio r_0 in models for infectious diseases in heterogeneous populations, Journal of Mathematical Biology 28 (4) (1990) 365–382. doi:10.1007/BF00178324.
URL <http://dx.doi.org/10.1007/BF00178324>
- [31] P. van den Driessche, J. Watmough, Reproduction numbers and sub-threshold endemic equilibria for compartmental models of disease transmission., Mathematical biosciences 180 (2002) 29–48.

- [32] L. Sattenspiel, C. P. Simon, The spread and persistence of infectious diseases in structured populations, Mathematical Biosciences 90 (1-2) (1988) 341–366. doi:10.1016/0025-5564(88)90074-0.
URL <http://www.sciencedirect.com/science/article/pii/0025556488900740>
- [33] G. Vermillard, Le chikungunya : un virus, une maladie - a propos de l'épidémie 2005-2006 à l'ile de la réunion, Ph.D. thesis, UHP - Université Henri Poincaré (2009).
- [34] G. Nishida, J. Tenorio, What Bit Me? Identifying Hawaii's Stinging and Biting Insects and Their Kin., University of Hawaii Press, 1993.
- [35] P. Zongo, Modélisation mathématique de la dynamique de transmission du paludisme, Phd Thesis, 2008.
- [36] B. Tsanou, Etude de quelques modèles épidémiologiques de métapopulations : Application au paludisme et à la tuberculose, Ph.D. thesis, University Paul Verlaine of Metz and University of Yaoundé (2011).
- [37] INSEE, *Estimations carroyées de population en 2007*, <http://www.insee.fr/fr/ppp/bases-de-donnees/donnees-detaillées/duicq/region.asp?reg=04> (02 2012).
- [38] Openstreetmap, <http://www.openstreetmap.org/> (02 2012).